

1
2
3
4
5 1 Late Ordovician to Early Devonian tectono-magmatic prequel to
6 2 the Acadian Orogeny in northeastern North America and the
7 3 British Isles
8
9
10 4

11
12 5 Pierre Jutras^a and Jaroslav Dostal^a
13

14 6 ^a *Department of Geology, Saint Mary's University, Halifax, Nova Scotia B3H 3C3, Canada*
15
16
17 7
18
19 8
20
21 9
22

23 10 ABSTRACT
24
25
26 11
27

28 12 Geochemical data from Katian to earliest Emsian (~453–405 Ma) igneous rocks in northeastern
29 13 North America and the British Isles were compiled to identify tectono-magmatic events related
30 14 to ocean closure and the formation of the Appalachian–Caledonian Belt. These rocks all have
31 15 geochemical affinities with plate-margin settings, but only a few can be attributed to arc
32 16 magmatism, whereas the others have slab-failure signatures or affinities with anhydrous,
33 17 extensional plate-margin (A2-type) settings. Based on these setting attributions as well as
34 18 constraints from the palaeomagnetic, palaeontologic, structural, stratigraphic and sedimentologic
35 19 records, a model for Iapetus and Rheic ocean closure is proposed, which also involves three
36 20 subordinate ocean plate segments: the Tornquist Sea, Acadian Seaway and Tetagouche–Exploits
37 21 oceanic back-arc basin. The model includes several new perspectives, such as (1) an early
38 22 Silurian rather than late Silurian closure of the Tetagouche–Exploits back-arc basin; (2) Acadian
39 23 Seaway slab failure at the Ludlow–Pridoli boundary due to its interaction at depth with the
40 24 overlying and slowly-sinking Tetagouche–Exploits slab, which generated profuse, extensional,
41 25 A2-type volcanism; and (3) an Early Devonian reactivation of Acadian Seaway slab subduction,
42
43
44
45
46
47
48
49
50
51
52
53
54
55
56
57
58
59
60
61
62
63
64
65

1
2
3
4 26 possibly due to Rheic Ocean closure and the convergence of a Gondwanan promontory against
5
6
7 27 Avalonia, which was attached to oceanic lithosphere of the Acadian Seaway. Furthermore, age
8
9 28 constraints allowed to identify chronological trends in the geochemical signatures of the igneous
10
11 29 rocks under study, which suggest that development of a new tectono-magmatic signature was
12
13
14 30 gradual due to compositional inheritance from the previous setting. These trends also suggest
15
16 31 that, although the transition from active subduction to slab failure generates an increase in Nb/Y
17
18
19 32 and light over heavy rare earth elements, these ratios tend to decrease with time due to a fading
20
21 33 contribution of the sinking slab at the source, whereas high-field-strength element contents tend
22
23
24 34 to increase due to a lack of new water input from subduction.
25

26 35 _____

27
28 36 *Keywords:*

29
30
31 37 Appalachian–Caledonian Belt

32
33 38 Arc magmatism

34
35 39 Continental collisions

36
37 40 Slab failure

38
39 41 A2-type igneous rocks

40
41 42 West Avalonia

42
43 43 Composite East Avalonia

44
45 44 South and North Ganderia

46
47 45 _____

48
49 46

50
51 47

52
53 48

54
55

56
57

58
59

60
61
62
63
64
65

1
2
3
4 49 **1. Introduction**
5
6
7 50
8
9 51

10 The Appalachian–Caledonian Belt of eastern North America and northern Europe was
11 formed by oceanic closure, which was accompanied by the accretion of various types of oceanic
12 terranes and the collision of continental masses. The belt formed the most complex accretionary
13 zone of Pangaea as it recorded collisions between Gondwana, Laurentia, Baltica and associated
14 micro-continents that had detached from them (Nance et al., 2012).
15
16 54
17
18
19 55

20
21 56 In the geology of northeastern North America and the British Isles, the interval separating
22 the Middle to early Late Ordovician Taconic–Grampian orogenies from the late Early to Middle
23 Devonian Acadian Orogeny is problematic (Woodcock, 2012a-c; Strachan, 2012a,b; Dewey et
24 al., 2015; Wilson et al., 2017). Based on palaeomagnetic, palaeontologic and provenance studies,
25 most terranes associated with the peri-Gondwanan and peri-Baltican (*sensu* Landing et al., 2022)
26 Avalonian and Ganderian domains (indicated in Fig. 1) were converging with Laurentia during
27 most of the Ordovician and Silurian, but had already docked with it before the end of the Silurian
28 (eg., Cocks and Torsvik, 2002; Murphy et al., 2004; van Staal et al., 2009, 2012, 2016;
29 Woodcock, 2012a,b). However, the conclusions of these studies still need to be reconciled with
30 the structural and igneous rock records, as the Katian to earliest Emsian interval (~453–405 Ma)
31 in these terranes is characterized by a paucity of igneous rocks with a clear arc signature and by
32 rare and not regionally extensive compressional structures (Dostal et al., 1989, 1993; Strachan,
33 2012a,b; Woodcock, 2012a-c; Wilson et al., 2017). This paper uses geochemical data on 417
34 samples of mafic to intermediate-felsic igneous rocks (45-70% SiO₂ contents on a volatile-free
35 basis) from the problematic ~453–405 Ma interval in Ganderian, Avalonian and northeastern
36 Laurentian domains to help clarify the complex tectono-magmatic history of that interval within
37
38
39
40
41
42
43
44
45
46
47
48
49
50
51
52
53
54
55
56
57
58
59
60
61
62
63
64
65

1
2
3
4 72 the constraints of palaeomagnetic, palaeontologic, structural, stratigraphic and sedimentologic
5
6 73 data.

7
8
9 74

10 11 75 **2. Nomenclature**

12
13
14 76

15
16 77 Waldron et al. (2022) discussed at length nomenclatural issues surrounding the
17
18 78 interchangeable usage in the literature of the Gander, Avalon and Meguma zones of Williams
19
20 79 (1979) as terranes, Late Precambrian to Early Ordovician (Tremadocian) peri-Gondwanan or
21
22 80 peri-Baltican domains (ie., terrane assemblages), and drifting post-Tremadocian micro-
23
24 81 continents. These problems were exacerbated by the identification of terranes that have affinities
25
26 82 with the Ganderian and Megumian domains alongside Avalonian domains in the British Isles
27
28 83 (eg. Waldron et al., 2011, 2019a; Pothier et al., 2015; Schofield et al., 2016), whereas geological
29
30 84 evidence suggests that the three domain components were part of the same drifting micro-
31
32 85 continent in late Early Ordovician (Floian) to Silurian times (Woodcock, 2012a; Waldron et al.,
33
34 86 2014). Another problem stems from profuse evidence (eg. Wilson et al., 2004, 2017; van Staal et
35
36 87 al., 2009, 2016; Zagorevski et al., 2008, 2010, 2012; Wilson, 2017) suggesting that the bulk of
37
38 88 Ganderian domains drifted as two separate segments due to the opening of a wide, intra-
39
40 89 Ganderian back-arc basin that evolved into oceanic lithosphere (the Tetagouche–Exploits back-
41
42 90 arc basin of van Staal, 1994).

43
44
45 91 In this paper, we use the terms Ganderian, Avalonian and Megumian domains in
46
47 92 reference to groupings of geological provinces with strong similarities in their Late Precambrian
48
49 93 to earliest Ordovician histories (ie., preceding the late Tremadocian Monian–Penobscottian
50
51 94 orogeny, *sensu* Waldron et al., 2022) along the Gondwanan and/or Baltican margins.
52
53
54
55
56
57
58
59
60
61
62
63
64
65

1
2
3
4
5
6
7
8
9
10
11
12
13
14
15
16
17
18
19
20
21
22
23
24
25
26
27
28
29
30
31
32
33
34
35
36
37
38
39
40
41
42
43
44
45
46
47
48
49
50
51
52
53
54
55
56
57
58
59
60
61
62
63
64
65

95 Furthermore, we restrict the terms “Ganderia and Avalonia” to inferred post–Tremadocian
96 micro-continents in line with the common usage of the suffixes “a” or “ia” for other palaeo-
97 continents, such as Laurentia, Gondwana and Baltica. In an attempt to minimize deviations from
98 historical usage while avoiding cumbersome or confusing nomenclature, we refer to the
99 “leading” and “trailing edges” of Ganderia (*sensu* van Staal et al., 2009, 2016; Zagorevski et al.,
100 2010; Wilson et al., 2017) as respectively “North Ganderia” and “South Ganderia”. We also
101 maintain the commonly used terms “West Avalonia” (the “Avalon–Brookville terrane
102 assemblage” of Waldron et al., 2022, now part of northeastern North America) and East
103 Avalonia” (the “Gander–Lakesman terrane assemblage” of Waldron et al., 2022, now part of the
104 British Isles) for drifting post–Early Ordovician continental assemblages that are mainly
105 composed of Avalonian domains. However, because East Avalonia is now pictured as having
106 travelled with some terranes that correlate better with the Ganderian and Megumian, we refer to
107 this part of Avalonia as “composite”.

109 **2. Tremadocian to Sandbian precursor setting**

110
111 Along the Laurentian margin of Iapetus, late Early to Middle Ordovician times were
112 characterized by the accretion of terranes associated with the Taconic 2 (*sensu* van Staal et al.,
113 2007, 2009) and Grampian orogenies, which peaked *circa* 463 Ma in both the British Isles
114 (Chew and Strachan, 2014) and northeastern North America (Whitehead et al., 1996) (Fig. 2).
115 Based mostly on palaeomagnetic and palaeontologic data, terranes associated with the Ganderian
116 and Avalonian domains were migrating northward on the same plate towards Laurentia and away
117 from Gondwana in late Early to Middle Ordovician times, closing the Iapetus Ocean to the north,
118 and enlarging the Rheic Ocean to the south (Nance et al., 2010, 2012; van Staal et al., 2012 and

1
2
3
4 119 references therein) (Fig. 3). At that time, Baltica (the Scandinavian craton) was separated from
5
6
7 120 Laurentia by the Iapetus Ocean and from composite East Avalonia by the Tornquist Sea (Cocks
8
9 121 and Torsvik, 2002; Torsvik and Rehnström, 2003) (Fig. 3).

10
11 122 According to Zagorevski et al. (2008), accretion of North Ganderia to the Laurentian
12
13
14 123 margin occurred *circa* 455 Ma through south-dipping subduction in the third and last tectonic
15
16 124 phase attributed to the Taconic Orogeny (Figs. 2 and 4). The collision was preceded by the
17
18
19 125 accretion of the peri-Laurentian Rowe belt (west of the area covered by our palaeo-continental
20
21 126 reconstructions) to the North Ganderian assemblage *circa* 475 Ma (MacDonald et al., 2014;
22
23
24 127 Karabinos et al., 2017; van Staal et al., 2021) and subduction of a Iapetan mid-oceanic ridge
25
26 128 beneath North Ganderia *circa* 459–455 Ma (Rogers and van Staal, 2003; Zagorevski et al. 2010,
27
28
29 129 2012; van Staal et al., 2016). Furthermore, the accretion of North Ganderia to the Laurentian
30
31 130 margin was accompanied by the incomplete subduction of the Iapetan ridge beneath West and
32
33
34 131 composite East Avalonia laterally along the same plate margin, which generated slab-window
35
36 132 volcanism at ~454 Ma (Woodcock, 2012a, Jutras et al., 2020) (Figs. 2 and 4).

37 38 133 39 40 41 134 **3. Late Ordovician to early Silurian tectonic setting**

42
43 135
44
45 136 The shutdown of south-dipping Iapetan slab subduction is penecontemporaneous with the
46
47
48 137 onset of southwest-dipping subduction of the Tornquist slab beneath the northeastern part of
49
50
51 138 composite East Avalonia and the Late Ordovician convergence of the latter with Baltica
52
53 139 (Pharaoh et al., 1993; Noble et al., 1993; Torsvik and Rehnström, 2003) (Fig. 5). Katian times
54
55 140 also saw the development of north-dipping subduction zones beneath composite Laurentia,
56
57
58 141 which produced the Brunswick subduction complex from consumption of the Tetagouche–
59
60 142 Exploits back-arc slab (van Staal et al., 1990, 1998, 2009; van Staal, 1994; Wilson et al., 2004,
61
62
63
64
65

1
2
3
4
5
6
7
8
9
10
11
12
13
14
15
16
17
18
19
20
21
22
23
24
25
26
27
28
29
30
31
32
33
34
35
36
37
38
39
40
41
42
43
44
45
46
47
48
49
50
51
52
53
54
55
56
57
58
59
60
61
62
63
64
65

143 2015, 2017) while the Southern Uplands accretionary wedge was developing from consumption
144 of the Iapetan slab beneath geological terranes now belonging to the British Isles and Greenland
145 (McKerrow et al. 1977; Leggett et al., 1979; Ryan and Dewey, 1991; Strachan, 2012b; Hollocher
146 et al., 2016; Chew and Strachan, 2014; McConnell et al., 2021) (Figs. 2 and 5).

147 In most palaeo-continental reconstructions (eg. van Staal et al. 2009; Piñán-Llamas and
148 Hepburn, 2013; Tremblay and Pinet, 2016; Wilson et al., 2017), early Silurian convergence
149 between composite Laurentia and West Avalonia occurred through northwest-dipping
150 subduction of the Acadian Seaway slab (*sensu* van Staal et al. 2009), a remnant of oceanic crust
151 that was trapped between them. The Silurian volcanic rocks of coastal Maine (Piñán-Llamas and
152 Hepburn, 2013) and southern New Brunswick (Barr et al., 2002) are interpreted as products of
153 this subduction zone. Hence, the Laurentian margin is pictured in some models as having been
154 characterized by two closely spaced subduction zones dipping in the same direction in early
155 Silurian times (van Staal et al. 2009; Tremblay and Pinet, 2016; Wilson et al., 2017). Based on
156 the record of Silurian arc volcanic centres distributed along the southern margin of the British
157 Isles, a north-dipping subduction zone had also developed beneath the East Avalonian–Baltican
158 assemblage by the early Silurian at the latest (Fig. 2), contributing to Rheic Ocean closure
159 (Woodcock et al., 2007).

4. Katian to earliest Emsian (~453–405 Ma) magmatic record in northeastern North America and the British Isles

160
161
162
163
164 In the following sub-sections, geochemical data on igneous rocks from the ~453–405 Ma
165 interval that followed the Taconic and Grampian orogenies and preceded the Acadian Orogeny
166 are subdivided into four sectors:

1
2
3
4
5
6
7
8
9
10
11
12
13
14
15
16
17
18
19
20
21
22
23
24
25
26
27
28
29
30
31
32
33
34
35
36
37
38
39
40
41
42
43
44
45
46
47
48
49
50
51
52
53
54
55
56
57
58
59
60
61
62
63
64
65

- 167 - (1) Mafic to intermediate-felsic rocks (45-70% SiO₂ contents on a volatile-free basis)
168 located in the former micro-continent of South Ganderia to the south of the Dog Bay
169 Line, which separates the two main Ganderian domain components in northeastern
170 North America (Fig. 1). Occurrences are known from southern New Brunswick and
171 coastal Maine (localities a-d in Fig. 1; Seaman et al., 1999; Barr et al., 2002; van
172 Wagoner et al., 2002; Piñán-Llamas and Hepburn, 2013). These rocks have been
173 associated with closure of the Acadian Seaway (Piñán-Llamas and Hepburn, 2013).
- 174 - (2) Mafic to intermediate-felsic rocks located to the north of the Dog Bay Line along
175 the former margin of composite Laurentia (including the former micro-continent of
176 North Ganderia) in northeastern North America (localities e-p in Fig. 1; Murphy,
177 1989; David and Gariépy, 1990; Dostal et al., 1993, 2016, 2021, 2022; Whalen et al.,
178 1996, 2006; Giggie, 1999; Wilson et al., 2005, 2008; Walker, 2010; Wilson, 2017).
179 These occurrences have been associated with closure of the Tetagouche–Exploits
180 back-arc basin (van Staal, 1994; van Staal et al., 1998, 2009; Wilson et al., 2008,
181 2017).
- 182 - (3) Mafic to intermediate-felsic rocks located to the north of the Solway Line (Fig. 1)
183 along the former margin of Laurentia in northwestern sectors of the British Isles
184 (localities r-t in Fig. 1; Tindle and Pearce, 1981; Badenszki et al., 2019; Murphy et
185 al., 2019; Archibald and Murphy, 2021). The latter authors associated these
186 occurrences with Iapetus Ocean closure.
- 187 - (4) Mafic to intermediate-felsic rocks located in the former micro-continent of West
188 Avalonia and composite East Avalonia to the south of the Solway Line, including
189 occurrences from northeast England that have been associated with closure of the

1
2
3
4 190 Tornquist Sea (Thor Suture) (locality y in Fig. 1; Pharaoh et al., 1993), and
5
6 191 occurrences from southeast Newfoundland (locality q in Fig. 1; Greenough, 1984,
7
8
9 192 Greenough et al., 1993) and the southern end of the British Isles (localities u-x and y
10
11 193 in Fig. 1; van de Kamp, 1969; Thorpe et al., 1989; Sloan and Bennett, 1990; Pharaoh
12
13 et al., 1991) that have been associated with Rheic Ocean closure (Woodcock et al.,
14 194
15
16 195 2007; Woodcock, 2012b).
17
18
19 196

21 197 Within those sectors, data from the literature on Katian to earliest Emsian igneous rocks
22
23 198 of mafic to intermediate-felsic compositions were selected when including the right combination
24
25
26 199 of trace elements to be plotted on at least one of four discrimination diagrams used in this paper:
27
28 200 (1) the Hf/3 vs Th vs Ta diagram of Wood (1980) (Figs. 6a–11a), which is one of the most
29
30 201 widely used and understood tectonic discrimination diagrams in the literature, and which is
31
32
33 202 herein used for mafic to intermediate rocks; (2) the Zr/Y vs Th/Yb diagram of Ross and Bédard
34
35 203 (2009) (Figs. 6b–11b), from which tholeiites are perhaps best separated from calc-alkaline
36
37 204 subduction-related magmas, and which is herein used for mafic to intermediate-felsic rocks; and
38
39
40 205 (3) the Nb+Y vs Nb/Y (Figs. 6c–11c) and (4) Ta+Yb vs La/Yb (Figs. 6d–11d) diagrams of
41
42
43 206 Whalen and Hildebrand (2019), which reflect recent advances in the design of discrimination
44
45 207 diagrams to differentiate arc magmas from slab failure and A-type magmas, and which are herein
46
47
48 208 used for intermediate to intermediate-felsic rocks with an aluminium saturation index [molar
49
50 209 $\text{Al}_2\text{O}_3/(\text{CaO} + \text{Na}_2\text{O} + \text{K}_2\text{O})$] lower than 1.1, and SiO_2 contents ranging between 55 and 70 wt.%
51
52 210 on a volatile-free basis. Data points on Figures 6 to 11 represent chemical analyses from
53
54
55 211 individual samples (data compiled in Appendix A).
56
57
58
59
60
61
62
63
64
65

1
2
3
4
5
6
7
8
9
10
11
12
13
14
15
16
17
18
19
20
21
22
23
24
25
26
27
28
29
30
31
32
33
34
35
36
37
38
39
40
41
42
43
44
45
46
47
48
49
50
51
52
53
54
55
56
57
58
59
60
61
62
63
64
65

212 Because the lithospheric mantle components of the Appalachian–Caledonian have all
213 experienced subduction-related metasomatism at some point in late Precambrian to early
214 Palaeozoic times, Katian to earliest Emsian igneous rocks from all above-mentioned localities
215 have trace element ratios that are overall characteristic of calc-alkaline arc environments (Figs.
216 6a–11a and 6b–11b). However, an extensional within-plate environment for these rocks has been
217 inferred in many instances based on the bimodal composition of some suites and a tendency
218 towards high contents in high-field-strength elements (HFSEs) paired with dominantly tholeiitic
219 Si vs Fe/Mg trends (Dostal et al., 1989, 2016; Seaman et al., 1999; van Wagoner et al., 2002;
220 Piñán-Llamas and Hepburn, 2013).

221 To further constrain the plate-margin tectono-magmatic environments, Whalen and
222 Hildebrand (2019) developed diagrams that refined our means to differentiate between hydrous
223 arc or slab failure magmatism and anhydrous extensional magmatism (A-type) with the use of
224 immobile trace element contents and ratios (Figs. 6c,d–11c,d). Diagrams using Nb/Y ratios can
225 also be used to subdivide the A-type range by allowing a differentiation to be made between the
226 A1-type igneous rocks of intra-plate environments and the A2-type igneous rocks of plate
227 margin environments (*sensu* Eby, 1992).

228
229 *4.1. South Ganderian terranes*

230
231 Barr et al. (2002) analysed intrusive and extrusive rocks from the South Ganderian
232 Kingston terrane of southern New Brunswick (locality d on Fig. 1; Table 1), reporting U-Pb
233 zircon ages ranging between 442 ± 6 and 435 ± 1.5 Ma (the younger date is from Doig et al.,
234 1990). Piñán-Llamas and Hepburn (2013) studied other volcanic rocks in coastal Maine (the
235 Dennys Formation; locality b on Fig. 1; Table 1) that are possibly coeval (ie., Llandoverly to

1
2
3
4
5
6
7
8
9
10
11
12
13
14
15
16
17
18
19
20
21
22
23
24
25
26
27
28
29
30
31
32
33
34
35
36
37
38
39
40
41
42
43
44
45
46
47
48
49
50
51
52
53
54
55
56
57
58
59
60
61
62
63
64
65

236 Wenlock) based on biostratigraphic constraints, whereas volcanic rocks of the overlying
237 Edmunds, Leighton and Eastport formations are considered to range from the Ludlow to the
238 Pridoli. However, within the current framework of the International Commission on Stratigraphy
239 (Melchin et al., 2020), studies by Miller and Fyffe (2002), van Wagoner et al (2002), Churchill-
240 Dickson (2004), and Wilson et al. (2008) have shown significant discrepancies between
241 radiometric ages and assigned Siluro-Devonian biostratigraphic ages in the region. Because
242 stratigraphic subdivisions in this paper are mainly based on radiometric ages, the Dennys,
243 Edmunds, Leighton and Eastport formations are here considered as undivided Silurian rocks.

244 The Cranberry Island volcanic series of coastal Maine (locality a on Fig. 1; Table 1) and
245 the Passamaquoddy Bay volcanic sequence of southern New Brunswick (locality c on Fig. 1;
246 Table 1) respectively yielded U-Pb zircon dates of 424 ± 1 Ma (Ludlow; Seaman et al., 1995)
247 and 423 ± 1 Ma (Pridoli; van Wagoner et al., 2001). Although Seaman et al. (1999) and van
248 Wagoner et al. (2002) referred to both successions as bimodal due to the presence of a SiO₂ gap
249 within the intermediate range, the two successions include andesites and dacites.

250

251 *4.1.2. Geochemistry*

252 The Pridoli Passamaquoddy Bay volcanic sequence (~423 Ma) of southern New
253 Brunswick clearly plots in the A2-type range determined by Whalen and Hildebrand (2019) (Fig.
254 6c,d). The limited amount of geochemical data from older Silurian andesites and dacites in South
255 Ganderia does not allow a firm determination of the tectonic environment to be made, but
256 although they straddle the three ranges, these volcanic rocks dominantly plot into the arc range
257 (Fig. 6c,d). Previous authors concluded that the ~424 Ma Cranberry Island volcanic series and
258 the undated Eastport Formation of coastal Maine have affinities with the within-plate

1
2
3
4 259 Passamaquoddy Bay volcanic sequence of southern New Brunswick (Seaman et al., 1999; van
5
6 260 Wagoner et al., 2002; Piñán-Llamas et al., 2013). However, their trace element contents have
7
8
9 261 more in common with older Silurian igneous rocks of the region (the Dennys, Edmunds and
10
11 262 Leighton formations, as well as the Kingston Group volcanic rocks and associated plutons) that
12
13
14 263 have been interpreted as arc related (Barr et al., 2002; Piñán-Llamas and Hepburn, 2013). Hence,
15
16 264 the onset of arc volcanism in South Ganderian terranes of coastal Maine and southern New
17
18
19 265 Brunswick may have occurred near the beginning of the Silurian based on a 442 ± 6 Ma U-Pb
20
21 266 zircon age obtained from a dacitic tuff in the Kingston terrane of southern New Brunswick (Barr
22
23
24 267 et al., 2002), and persisted until the end of the Ludlow Epoch based on the 424 ± 1 Ma U-Pb
25
26 268 zircon age obtained by Seaman et al. (1995) in the Cranberry Island volcanic series of coastal
27
28
29 269 Maine.

30
31 270

32 33 271 *4.2. Laurentian margin and North Ganderian terranes in northeastern North America*

34
35
36 272

37 38 273 *4.2.1. Katian to Pridoli interval (~453–420 Ma)*

39
40 274 The record of Late Ordovician magmatism along the composite Laurentian margin in
41
42
43 275 northeastern North America is very scarce, being limited to a foliated granodiorite sheet in
44
45 276 Newfoundland from which a 445.8 ± 0.6 Ma U-Pb zircon date was obtained (Brem et al., 2007),
46
47
48 277 but which was not analyzed for its major and trace element contents. Furthermore, the Duncans
49
50 278 Brook Formation of northern New Brunswick includes basalt flows intercalated with
51
52
53 279 sedimentary rocks that bear detrital zircons as young as 444 ± 6 Ma (Wilson et al., 2015),
54
55 280 suggesting that it is either uppermost Ordovician or early Llandovery.

56
57 281 Apart from possibly the Duncans Brook Formation of northern New Brunswick, the
58
59
60 282 oldest Silurian igneous rock record along the composite Laurentian margin in northeastern North
61
62
63
64
65

1
2
3
4 283 America is from the granitic Glover Island and granodioritic Burlington plutons of northwest
5
6 284 Newfoundland, which are both dated at 440 ± 2 Ma (early Llandovery) (Cawood and Dunning,
7
8 285 1993; Cawood et al., 1996; Whalen et al., 2006) (locality l on Fig. 1; Table 1). Other Silurian
9
10 286 igneous rocks in northwest Newfoundland include the Boogie Lake and Main Gut complexes at
11
12 287 respectively 435 ± 6 and 431 ± 2 Ma (Dunning et al., 1990), the Rainy Lake and Silver Pond
13
14 288 complexes at respectively 435 ± 1 and 431.6 ± 4 Ma (Whalen et al., 2006), the Puddle Pond
15
16 289 complex at 432.4 ± 1 (Lissenberg et al., 2005), and the Taylor Brook complex at 430.5 ± 2 Ma
17
18 290 (Heaman et al., 2002) (all at locality m on Fig. 1; Table 1), as well as the Topsails and
19
20 291 Springdale volcanic groups (both at locality o on Fig. 1; Table 1) at 429 ± 4 Ma (Whalen et al.,
21
22 292 1987), and the Topsails intrusive suite (locality n on Fig. 1; Table 1) at 427 ± 1 Ma (Whalen et
23
24 293 al., 2006) and 425 ± 4 Ma (van Staal et al., 2014). Moreover, slightly younger Silurian igneous
25
26 294 rocks are found farther to the northeast, just to the north of the Dog Bay Line (locality p on Fig.
27
28 295 1), with U-Pb zircon ages ranging from 424 ± 2 Ma in the Mount Peyton Batholith to 421.2 ± 0.6
29
30 296 Ma in the Brimstone Head Formation of the Botwood Group (Dunning et al., 1990; Hamilton
31
32 297 and Kerr, 2016) (Table 1).

33
34 298 Silurian volcanic rocks are also found along the composite Laurentian margin (including
35
36 299 North Ganderian terranes) in southeastern Quebec (the Lac Raymond and Pointe aux Trembles
37
38 300 formations; David and Gariépy, 1990) and northwest New Brunswick (Weir Formation; Wilson
39
40 301 et al., 2008) (localities g and j respectively on Fig. 1; Table 1). Although volcanic successions
41
42 302 from both localities are intercalated with or overlain by marine sedimentary rocks with
43
44 303 brachiopod, conodont and ostracod assemblages assigned to the late Llandovery (Noble, 1976;
45
46 304 Nowlan, 1983; David and Gariépy, 1990; Wilson et al., 2008), a U-Pb date of 429.2 ± 0.5 Ma
47
48 305 was obtained from a dacitic tuff of the Weir Formation (Wilson et al., 2008), which is late
49
50
51
52
53
54
55
56
57
58
59
60
61
62
63
64
65

1
2
3
4
5
6
7
8
9
10
11
12
13
14
15
16
17
18
19
20
21
22
23
24
25
26
27
28
29
30
31
32
33
34
35
36
37
38
39
40
41
42
43
44
45
46
47
48
49
50
51
52
53
54
55
56
57
58
59
60
61
62
63
64
65

306 Wenlock according to the current Silurian subdivisions of the International Commission on
307 Stratigraphy (Melchin et al., 2020). As biostratigraphic constraints imply that volcanic rocks of
308 the Lac Raymond and Pointe aux Trembles formations are time-equivalent to those of the Weir
309 Formation, they were possibly deposited near 429 Ma and are herein included within the
310 Llandoverly to Wenlock (~444–428 Ma) bracket. These rocks are in part equivalent to the
311 Ristigouche volcanic rocks in the Gaspé Peninsula of southeastern Quebec (locality k on Fig. 1;
312 Table 1) based on biostratigraphic constraints (Bourque and Lachambre, 1980; Bourque et al.,
313 2000), but the latter succession is basaltic and does not include intermediate to intermediate-
314 felsic rocks (Doyon and Dalpé, 1993).

315 Following a volcanic hiatus of a few million years and a period of uplift and erosion
316 (Salinic B unconformity of Wilson et al., 2017), voluminous volcanism was recorded in the
317 Pridoli Dickie Cove Group of northwest New Brunswick (Dostal et al., 2016, 2021, 2022)
318 (locality h on Fig. 1; Table 1). This group yielded U-Pb zircon ages of 422.3 ± 0.3 Ma in the
319 basal Bryant Point Formation, and of 420.8 ± 0.4 and 419.7 ± 0.3 Ma in respectively the lower
320 and upper parts of the Benjamin Formation at the top of the succession (Wilson and Kamo, 2008,
321 2012). The two volcanic formations are separated by coarse volcanoclastic conglomerate of the
322 New Mills Formation. This group is in part equivalent to the Siluro-Devonian Tobique Group of
323 central-west New Brunswick (locality e on Fig. 1; Table 1), in which stratigraphic relationships
324 are less well constrained (Wilson, 2017).

325
326 *4.2.1.1. Geochemistry.* North of the Dog Bay Line along the composite Laurentian margin of
327 northeastern North America, available data on intermediate to intermediate-felsic rocks of the
328 Llandoverly to Wenlock interval (~444–428 Ma) dominantly plot within the slab failure range in

1
2
3
4
5
6
7
8
9
10
11
12
13
14
15
16
17
18
19
20
21
22
23
24
25
26
27
28
29
30
31
32
33
34
35
36
37
38
39
40
41
42
43
44
45
46
47
48
49
50
51
52
53
54
55
56
57
58
59
60
61
62
63
64
65

329 the Nb+Y vs Nb/Y and Ta+Yb vs La/Yb diagrams of Whalen and Hildebrand (2019; Fig. 7c,d),
330 including those from the Lac Raymond, Pointe aux Trembles and Weir formations, which were
331 previously attributed to arc volcanism (David and Gariépy, 1990; Wilson et al., 2008). In
332 contrast, volcanic rocks from the late Pridoli (the ~421–420 Ma Benjamin Formation of the
333 Dickie Cove Group in northwest New Brunswick) plot entirely within the A2-type range. These
334 two clearly differentiated populations are somewhat linked by rocks that are dated as Ludlow
335 (the ~427–424 Ma Topsails intrusive suite of northwest Newfoundland) to early Pridoli (the
336 ~423–422 Ma Bryant Point Formation of the Dickie Cove Group). Based on limited age
337 constraints, the Llandovery to Ludlow interval records a gradual increase in HFSE contents
338 accompanied by a gradual decrease in Nb/Y and La/Yb ratios, whereas the Pridoli interval
339 mostly shows a pronounced increase in HFSE contents (Fig. 7c,d).

340
341 *4.2.2. Lochkovian to earliest Emsian interval (~419–405 Ma)*

342
343 Early Devonian igneous rocks in northeastern North America include a series of felsic
344 intrusions in the Miramichi Highlands (Brunswick subduction complex of the North Ganderian
345 assemblage) in northern New Brunswick (locality f on Fig. 1; Table 1), which range between
346 ~418 and ~402 Ma (Whalen et al., 1996), as well as coeval volcanic rocks of the Dalhousie
347 Group, which straddle the New Brunswick / Quebec border (locality i on Fig. 1; Table 1), and
348 which range between 417.5 ± 0.4 Ma (Wilson et al., 2017) and 407.4 ± 0.8 Ma (Wilson et al.,
349 2004). The latter group disconformably overlies the Silurian Ristigouche volcanics and Dickie
350 Cove Group (Doyon and Dalpé, 1993; Bourque et al., 2000; Wilson, 2017). Based on
351 stratigraphic constraints, the Baldwin and Lyall volcanic rocks in the Gaspé Peninsula of eastern

1
2
3
4
5
6
7
8
9
10
11
12
13
14
15
16
17
18
19
20
21
22
23
24
25
26
27
28
29
30
31
32
33
34
35
36
37
38
39
40
41
42
43
44
45
46
47
48
49
50
51
52
53
54
55
56
57
58
59
60
61
62
63
64
65

352 Quebec (locality k on Fig. 1; Table 1) are possibly time-equivalent to volcanic rocks of the
353 Dalhousie Group (Doyon and Dalpé, 1993).

354 Early Devonian plutons also occur in the Fogo Island Batholith of northern
355 Newfoundland, with a monzogranite yielding a 408 ± 0.8 Ma U-Pb zircon age, and a quartz
356 diorite yielding a 410 ± 2 Ma U-Pb titanite age and a 420 ± 2 Ma U-Pb zircon age (Aydin, 1995).
357 We consider the significantly older zircon population as probably inherited.

358
359 *4.2.2.1. Geochemistry.* Although the Lower Devonian volcanic rocks of northern New
360 Brunswick and southeastern Quebec are traditionally linked to the same post-Taconic overstep
361 succession as the Pridoli Dickie Cove Group (the Matapedia cover sequence of Fyffe and
362 Fricker, 1987), they differ from the latter unit by the lack of a gap in the intermediate range
363 (*sensu* Daly, 1925) when the succession is taken as a whole (Wilson, 2017). They also show
364 distinct trace element contents that straddle all three ranges in the Nb+Y vs Nb/Y and Ta+Nb vs
365 La/Yb diagrams of Whalen and Hildebrand (2019) (Fig. 8c,d), but that are skewed towards the
366 arc and slab failure ranges, whereas data from the Dickie Cove Group are skewed towards the
367 A2-type range (Fig. 7c,d). Moreover, contrary to the Silurian successions, an overall decrease in
368 HFSE contents is observed with time (Fig. 8c,d). Hence, a change in tectono-magmatic setting
369 must have occurred in association with the disconformity at the Siluro-Devonian boundary in the
370 region.

371 In northern Newfoundland, available data on Lower Devonian igneous rocks are
372 constrained to the Pragian, and although they are compatible with age-equivalent rocks in
373 northern New Brunswick (Figs. 8 and 9), they show a tendency for lower Nb/Y and therefore a
374 stronger affinity with typical arc environments (Fig. 9c).

1
2
3
4
5
6
7
8
9
10
11
12
13
14
15
16
17
18
19
20
21
22
23
24
25
26
27
28
29
30
31
32
33
34
35
36
37
38
39
40
41
42
43
44
45
46
47
48
49
50
51
52
53
54
55
56
57
58
59
60
61
62
63
64
65

375

376 *4.3. Laurentian margin in the British Isles*

377

378 Following the Middle Ordovician Grampian Orogeny, evidence from structures and syn-
379 tectonic sedimentary rocks reviewed by Strachan (2012b), Stone et al. (2012) and McConnell et
380 al. (2021) indicates that a northwest-dipping subduction zone developed beneath Laurentia,
381 although the Late Ordovician magmatic record for this subduction is scarce because of
382 subsequent burial beneath younger rocks covering the Midland Valley terrane of Scotland and its
383 extension in Ireland. Badenszki et al. (2019) obtained a 453.6 ± 8 Ma U-Pb zircon age
384 (Sandbian/Katian boundary) from a metadioritic xenolith within upper Palaeozoic intrusive rocks
385 of the Midland Valley terrane (locality s on Fig. 1; Table 1).

386 In northwest Ireland, the polymodal Donegal composite batholith (locality r on Fig. 1;
387 Table 1) yielded U-Pb zircon ages ranging from 428 ± 4 to ~ 424 Ma (latest Wenlock to Ludlow)
388 in the Ardara Pluton and in an enclave within the Thorr Pluton, but the composite batholith is
389 volumetrically dominated by Early Devonian plutons with U-Pb zircon ages ranging between
390 420 ± 3 and ~ 400 Ma, and clustering between ~ 418 and 411 Ma (Lochkovian) (Archibald et al.,
391 2021).

392 An appinite and lamprophyre suite near the Donegal composite batholith yielded a U-Pb
393 zircon age of 437 ± 5 Ma (Kirkland et al., 2013), $^{40}\text{Ar}/^{39}\text{Ar}$ hornblende ages ranging from 434.2
394 ± 2.1 to 433.7 ± 5.5 Ma (Murphy et al., 2019), and U-Pb titanite ages ranging from 431 ± 6 to
395 419 ± 5 Ma (Archibald et al., 2021) (late Llandovery to early Lochkovian). However, these rocks
396 have an aluminium saturation index greater than 1.1 and therefore cannot be used in the
397 discrimination diagrams of Whalen and Hildebrand (2019). Samples from this suite plotted in

1
2
3
4
5
6
7
8
9
10
11
12
13
14
15
16
17
18
19
20
21
22
23
24
25
26
27
28
29
30
31
32
33
34
35
36
37
38
39
40
41
42
43
44
45
46
47
48
49
50
51
52
53
54
55
56
57
58
59
60
61
62
63
64
65

Fig. 10a,b are from rocks ranging from 434.2 ± 2.1 to 431 ± 6 Ma (Murphy et al., 2019) (late Llandovery to Wenlock).

In terms of Early Devonian occurrences, an Rb/Sr age of 408 ± 1.5 Ma (Pragian) was obtained by Piper (2007) for the Loch Doon pluton in the Southern Uplands of Scotland (locality t on Fig. 1; Table 1), and U-Pb zircon dates of 410 ± 1 and 406 ± 2 Ma were reported by Stone et al. (2012) for the same pluton. Badenszki et al. (2019) obtained a weighted average of 415 ± 3 Ma (Lochkovian) for U-Pb zircon ages obtained from metadioritic xenoliths within Permo–Carboniferous igneous rocks of Scotland’s Midland Valley (locality s on Fig. 1; Table 1).

4.4.2. Geochemistry

The only retrieved sample from Katian to Hirnantian (~553-444 Ma) igneous rocks along the Laurentian margin in the British Isles plots into the arc range defined by Whalen and Hildebrand (2019), whereas mid–Silurian to Early Devonian igneous rocks plot almost exclusively within the slab failure range (Fig. 10c,d). However, the Pragian Loch Doon pluton (data from Tindle and Pearce, 1981) plots notably closer to the A-type range than the Lochkovian xenoliths as well as the mid–Silurian to Lochkovian Donegal plutons, and the associated increase in HFSE contents is paired with a decrease in Nb/Y and La/Yb ratios.

4.5. Terranes associated with the former micro-continents of West and composite East Avalonia

Late Ordovician to earliest Silurian plutonic and volcanic rocks intercepted by wells in northeast England to the southeast of the Solway Line (locality y on Fig. 1; Table 1) have been interpreted as related to subduction of the Tornquist slab beneath Avalonia (Pharaoh et al., 1993). These rocks yielded U-Pb zircon dates of $452 \pm 8-5$ Ma (Pidgeon and Aftalion, 1978), as

1
2
3
4
5
6
7
8
9
10
11
12
13
14
15
16
17
18
19
20
21
22
23
24
25
26
27
28
29
30
31
32
33
34
35
36
37
38
39
40
41
42
43
44
45
46
47
48
49
50
51
52
53
54
55
56
57
58
59
60
61
62
63
64
65

422 well as 449 ± 13 Ma, 457 ± 20 Ma, and 442 ± 3 Ma (Noble et al., 1993). They are thought to be
423 related to calc-alkaline rocks of approximately the same age in the Brabant Massif of Belgium
424 (locality z on Fig. 1; Table 1) (André et al., 1986).

425 At the southernmost end of the British Isles, Silurian volcanic rocks are distributed along
426 an east-west trend (Woodcock et al, 2007; Woodcock, 2012b). They include the Llandovery
427 Skomer Volcanic Group of south Wales (Thorpe et al., 1989) (locality w on Fig. 1; Table 1), the
428 Llandovery to Wenlock Tortworth volcanics of southern England (van de Kamp, 1969; Pharaoh
429 et al., 1991) (locality x on Fig. 1; Table 1), and the late Wenlock Dunquin Group of southern
430 Ireland (Sloan and Bennett, 1990) (locality u on Fig. 1; Table 1), with ages that are based on
431 biostratigraphic constraints.

432 Also within the composite East Avalonian assemblage, southeast of the Solway Line,
433 intrusive units in the northern part of the Leinster Batholith of southeast Ireland yielded U-Pb
434 zircon ages ranging from 417.4 ± 1.7 to 404.9 ± 2.6 Ma (Fritschle et al., 2018a) (locality v on
435 Fig. 1; Table 1). However, trace element geochemical data that would be relevant to this study
436 are only available for southern units of the batholith (Sweetman, 1987) that were long considered
437 to be Early Devonian, but from which U-Pb zircon dates of 462.0 ± 2.7 Ma and 460.5 ± 3.2 Ma
438 (Middle Ordovician) were subsequently obtained (Fritschle et al., 2018b). Furthermore, mafic to
439 intermediate sills at Cape St. Mary's in the Avalon Peninsula of Newfoundland (West Avalonia)
440 (locality q on Fig. 1; Table 1) yielded a U-Pb baddeleyite date of 441 ± 2 Ma (Greenough et al.,
441 1993).

442
443
444

1
2
3
4
5
6
7
8
9
10
11
12
13
14
15
16
17
18
19
20
21
22
23
24
25
26
27
28
29
30
31
32
33
34
35
36
37
38
39
40
41
42
43
44
45
46
47
48
49
50
51
52
53
54
55
56
57
58
59
60
61
62
63
64
65

445 4.5.2. *Geochemistry*

446 Late Ordovician to earliest Silurian intermediate to intermediate-felsic rocks along the
447 inferred Thor Suture to the northeast of the Midland Microcraton (locality y on Fig. 1; Table 1)
448 straddle the arc and slab failure ranges (Fig. 11c,d). Along the inferred Rheic Suture (*sensu*
449 Woodcock et al., 2007, and Woodcock, 2012b) at the southern edge of composite East Avalonia,
450 Silurian andesites and dacites mostly plot into the arc range (Fig. 11c,d), which is consistent with
451 the conclusions of previous workers (van de Kamp, 1969; Thorpe et al., 1989; Sloan and
452 Bennett, 1990; Pharaoh et al., 1991). In contrast, the Cape St. Mary's sills of West Avalonia
453 (Greenough, 1984) are constrained within the A2-type range (Fig. 11c,d).

454 455 **5. Discussion**

456 457 *5.1. General chronological trends in the geochemical signature of slab-failure-related* 458 *magmatism*

459
460 Along the composite Laurentian margin in northeastern North America and the British
461 Isles, a trend towards increasing HFSE contents as well as decreasing Nb/Y and La/Yb ratios is
462 observed with time in igneous rocks associated with slab failure (Figs. 6c,d and 11c,d).
463 Hildebrand and Whalen (2017) and Whalen and Hildebrand (2019) interpreted the rise in Nb/Y
464 and LREE/HREE ratios from arc to slab failure magmatism as being related to partial melting of
465 the Nb-enriched metabasaltic/gabbroic upper portion of the failing slab, leaving HREE-rich
466 residual garnet in the eclogitic residue. This would be especially true in the early stages of slab
467 failure, when the failing slab is still close to the base of the lithosphere. Hence, although slab-
468 failure-related magmatic systems will tend to develop high Nb/Y and La/Yb ratios, the observed

1
2
3
4
5
6
7
8
9
10
11
12
13
14
15
16
17
18
19
20
21
22
23
24
25
26
27
28
29
30
31
32
33
34
35
36
37
38
39
40
41
42
43
44
45
46
47
48
49
50
51
52
53
54
55
56
57
58
59
60
61
62
63
64
65

469 decrease of these ratios with time could reflect a gradually fading contribution of the sinking slab
470 at the source, whereas the observed increase in HFSE contents (Nb+Y and Ta+Yb) suggests that
471 a gradual dehydration of the mantle source occurs in such setting due to a lack of new water
472 input from subduction.

473
474 *5.2. Katian to Hirnantian interval (~453–444 Ma)*

475
476
477 The Katian to Hirnantian igneous rock record is very scarce in the Appalachian–
478 Caledonian Belt, and the subduction zones depicted in Fig. 5 are mainly inferred from structures
479 and metamorphic features (eg. Woodcock, 2012a; van Staal et al., 1998, 2008, 2012, 2016;
480 Wilson et al., 2017; and references therein) as well as evidence for convergence from
481 palaeomagnetic (Johnson and Van der Voo, 1985, 1990; Mac Niocaill, C., 2000; Cocks and
482 Torsvik, 2002; Smethurst and McEnroe, 2003; Torsvik and Rehnström, 2003; Thompson et al.,
483 2010, 2022) and palaeontologic data (McKerrow et al., 1977; Ziegler et al., 1977; Landing and
484 Murphy, 1991; Landing, 1996, 2007; Landing et al., 2008, 2022). However, where recorded
485 along the composite Laurentian margin and the inferred Thor Suture of composite East Avalonia,
486 those igneous rocks are geochemically consistent with an arc environment (Figs. 10 and 11).
487 According to Pharaoh et al. (1995) and Torsvik and Rehnström (2003), Baltica and composite
488 East Avalonia had already collided by early Silurian times in association with the poorly
489 recorded Shelveian tectonic event in northeast England (Woodcock, 2012b) (Figs. 2 and 12,
490 Table 2).

491
492

1
2
3
4 493 5.3. *The Llandovery to Ludlow interval (~444–424 Ma)*
5

6 494
7

8
9 495 5.3.1. *Composite Laurentian margin north of the Dog Bay Line in northeastern North America*
10

11 496 A clear slab-failure signature in Llandovery to Wenlock (~444–428 Ma) igneous rocks
12
13
14 497 within North Ganderian and southeasternmost Laurentian terranes in northeastern North America
15
16 498 (Fig. 8c,d) suggests that, although final closure of the Tetagouche–Exploits back-arc basin was
17
18
19 499 previously associated with the Wenlock to Ludlow Salinic B unconformity (Wilson et al., 2017),
20
21 500 it most likely occurred in association with the latest Ordovician to early Llandovery Salinic A
22
23 501 deformation event (Figs. 2 and Fig. 12), which is characterized by an unconformity separating
24
25
26 502 the Ordovician Brunswick subduction complex from overlying Silurian sedimentary and
27
28
29 503 volcanic rocks (Wilson and Kamo, 2012). A similar timing for the closure is suggested by
30
31 504 reports of Laurentian detrital zircons in the Llandovery Hayes Brook Formation (Dokken, 2017)
32
33 505 to the south of the Dog Bay Line. Hence, closure of the Tetagouche–Exploits basin must have
34
35
36 506 been constrained within the ~453–440 Ma interval, for which a record of arc volcanic rocks is
37
38 507 currently lacking. It should be noted that the Tetagouche–Exploits slab was composed of young
39
40
41 508 oceanic crust that was unlikely to subduct steeply and produce abundant arc volcanism.
42

43 509
44

45 510 5.3.2. *Laurentian margin in the British Isles*
46

47
48 511 Based on available data from the Donegal composite batholith of northwest Ireland, the
49
50 512 Iapetan slab had failed beneath Laurentian rocks of the British Isles by ~428 Ma (Archibald and
51
52
53 513 Murphy, 2021; Archibald et al., 2021, 2022) (Fig. 10c,d). This event was most likely linked to
54
55 514 the *circa* 430 Ma culmination of the Scandian Orogeny, which was the result of the collision
56
57
58 515 between Laurentia and Baltica, and which affected rocks of Scotland, east Greenland and
59
60
61
62
63
64
65

1
2
3
4 516 Scandinavia (Strachan, 2012b; Hollocher et al., 2016; Chew and Strachan, 2014; Bender et al.,
5
6
7 517 2019; Jakob et al., 2022) (Fig. 13).

8
9 518

10 11 519 *5.3.3. South Ganderia*

12
13
14 520 Based on data from the Kingston terrane of southern New Brunswick (Fig. 6c,d),
15
16 521 northwest-dipping subduction beneath South Ganderian terranes was already ongoing by ~442
17
18
19 522 Ma (earliest Llandovery) (Barr et al., 2002), and two closely spaced northwest dipping
20
21 523 subduction zones may therefore have coexisted for a while along the two parts of Ganderia
22
23
24 524 (*sensu* van Staal et al., 2009, Tremblay and Pinet, 2016, and Wilson et al., 2017). Based on
25
26 525 radiometric and stratigraphic constraints (Wilson et al., 2017), it is also possible that the onset of
27
28
29 526 Acadian Seaway slab subduction accompanied the Salinic A deformation and final closure of the
30
31 527 Tetagouche–Exploits back-arc basin (Figs. 2 and 12). The tendency for relatively high Nb/Y and
32
33
34 528 Nb+Y in these inferred Silurian arc igneous rocks in South Ganderian terranes suggests shallow
35
36 529 subduction, which can result in poorly hydrated arc magmatism as much of the well-hydrated
37
38
39 530 uppermost part of the subducting slab is left behind in the accretionary prism in such settings.

40
41 531

42 43 532 *5.3.4. West and composite East Avalonia*

44
45
46 533 Inferred subduction of the Rheic Ocean slab beneath composite East Avalonia during the
47
48 534 Silurian (Woodcock et al., 2007; Woodcock, 2012b) is supported by the geochemistry of Silurian
49
50
51 535 igneous rocks distributed along an east-west trend at the south end of the British Isles (Fig.
52
53 536 11c,d). Based on the available record, onset of this subduction occurred near the beginning of the
54
55
56 537 Silurian (Figs. 2 and 12). In this context, the 441 ± 2 Ma Cape Saint Mary's sills of
57
58 538 Newfoundland (Greenough et al., 1993), which show geochemical evidence for anhydrous

59
60
61
62
63
64
65

1
2
3
4
5
6
7
8
9
10
11
12
13
14
15
16
17
18
19
20
21
22
23
24
25
26
27
28
29
30
31
32
33
34
35
36
37
38
39
40
41
42
43
44
45
46
47
48
49
50
51
52
53
54
55
56
57
58
59
60
61
62
63
64
65

539 volcanism (Fig. 11c), are pictured as probable products of back-arc extension or transtension.

540 Associated arc volcanic rocks in West Avalonia are possibly buried beneath continental shelf

541 strata along the northwest Atlantic margin.

542

543 *5.4. The Pridoli interval (~423–420 Ma)*

544

545 *5.4.1. Ganderian and West Avalonian terranes*

546 As no coeval deformation is recorded in West Avalonia, which had not yet accreted with
547 composite Laurentia, no continental collision is inferred to have caused the minor pre–Pridoli
548 orogenic phase responsible for the Salinic B unconformity (*sensu* Wilson et al., 2017) in
549 Ganderian terranes, which was most likely caused by a shallowing of Acadian Seaway slab
550 subduction in Wenlock to Ludlow times (Figs. 2 and 13). To explain the rapid switch from arc
551 volcanism in the ~424 Ma Cranberry Island volcanic series to anhydrous, extensional volcanism
552 in the ~423 Ma Passamaquoddy Bay volcanic sequence on South Ganderian terranes (Fig. 6c,d),
553 we propose that the warm and slowly sinking Tetagouche–Exploits slab may have interfered
554 with the neighbouring shallow subduction of the Acadian Seaway slab, causing chain failure at
555 depth (Fig. 14, cross-section A-B, ~423 Ma). Because the second tear would have occurred deep
556 below the asthenosphere-lithosphere boundary, the associated volcanism would not have
557 developed a clear slab failure signature, but it would have generated sufficient stress release to
558 cause significant extensional magmatism at the level of the composite Laurentian margin (Figs. 2
559 and 14).

560 Failure of the Acadian Seaway slab at the onset of the Pridoli is consistent with the
561 contemporaneous record of a very rapid and short-lived sea regression in the Silurian Arisaig
562 Group on West Avalonia (Boucot et al., 1974) (Fig. 2, and Fig. 14, cross-section C-D), which

1
2
3
4 563 had drifted very close to the composite Laurentian margin by then based on palaeomagnetic
5
6 564 studies (Cocks and Torsvik, 2002) and detrital zircon data (Murphy et al., 2004). The Arisaig
7
8
9 565 Group displays an undisturbed marine succession that spans the entire Silurian with the
10
11 566 exception of a thin interval of continental red beds in the upper member of the Moydart
12
13 567 Formation (Fig. 15A), which were deposited near the Ludlow–Pridoli boundary (Boucot et al.,
14
15 568 1974). Within a ~2 m interval, the succession conformably passes upward from green mudrock
16
17 569 with coquina lenses and hummocky cross-stratified siltstone intervals deposited below the mean
18
19 570 fairweather wave base (late Ludlow Lower Member of the Moydart Formation) to mottled red
20
21 571 mudrock with pedogenic calcretes deposited in the supratidal zone (undated Upper Member of
22
23 572 the Moydart Formation), the two facies being separated by rhythmic alternations of red mudrock
24
25 573 and green biosparudite presumably deposited in the intertidal zone (Fig. 15b,c). Considering the
26
27 574 high sedimentation rate of tidal rhythmites, this section seems to have experienced several metres
28
29 575 of base-level lowering in a matter of months. Such rapid regression would be difficult to explain
30
31 576 without invoking a sudden event of tectonic relaxation, which could be related to retrogressive
32
33 577 movement of the remnant Acadian Seaway oceanic lithosphere following failure, as the latter
34
35 578 was still attached to West Avalonia (Fig. 14). Shallow marine sedimentation resumed a few
36
37 579 metres higher in the succession from a recrudescence of basin subsidence recorded in the Pridoli
38
39 580 Stonehouse Formation (Waldron et al., 1996) (Figs. 2 and 15c), which is also consistent with the
40
41 581 short-lived nature of slab-failure-related uplift.

42
43 582 On the Ganderian side, post–Salinic relaxation associated with the inferred failure of the
44
45 583 Acadian Seaway slab seemingly migrated landward during the Pridoli, generating profuse
46
47 584 volcanism recorded in the ~422 Ma Bryant Point Formation at the base of the Dickie Cove
48
49 585 Group, which still marginally plots within the arc failure range, but which shows a significant
50
51
52
53
54
55
56
57
58
59
60
61
62
63
64
65

1
2
3
4 586 offset towards the A-type ranges (Fig. 7c,d). Because the significant increase in Nb+Y does not
5
6 587 show a corresponding decrease in Nb/Y, we attribute the former to the onset of A-type
7
8 588 extensional tectonics rather than to a fading contribution of the sinking Tetagouche–Exploits
9
10 589 slab; the latter having been most likely too deep by then to be part of the magmatic source, as
11
12 590 both numerical models and the geological record suggest that slab-failure-related magmatism is a
13
14 591 short-lived event of a few million years (eg. Zhu et al., 2015; Freeburn et al., 2017; Kant et al.,
15
16 592 2018; Dostal and Jutras, 2021). We therefore attribute the relatively low HFSE contents of the
17
18 593 Bryant Point Formation to inheritance from a previous history of hydrated arc volcanism at the
19
20 594 base of the sub-continental lithospheric mantle (SCLM), and we associate this unit to the onset of
21
22 595 an increasingly anhydrous extensional tectonic regime during the Pridoli in North Ganderian
23
24 596 terranes in relation to failure of the Acadian Seaway slab at depth (Fig. 14, cross-section A-B,
25
26 597 ~422 Ma).

32
33 598 The possibility of two distinct Silurian tectono-magmatic events in the area is supported
34
35 599 by the identification of a large time gap separating the original Llandovery to early Ludlow pulse
36
37 600 of slab-failure-related volcanic rocks (Lac Raymond, Pointe aux Trembles, and Weir formations)
38
39 601 from bimodal magmatism associated with the Pridoli Bryant Point Formation; the latter
40
41 602 corresponding to a significant magmatic pulse that left a ~2000 m thick succession dominated by
42
43 603 volcanic rocks (Wilson, 2017). An increase in extensional rates may have generated the coarse,
44
45 604 fault-controlled deposits of the overlying New Mills Formation (Bourque et al., 2000; Tremblay
46
47 605 and Pinet, 2016), which are overlain by thick, bimodal volcanic rocks with a clear A2-type
48
49 606 composition that form the bulk of the ~421–420 Ma Benjamin Formation (Figs. 7c,d, and 14,
50
51 607 cross-section A-B, ~421 Ma). A similar setting is inferred for Pridoli felsic volcanic rocks in
52
53
54
55
56
57
58
59
60
61
62
63
64
65

1
2
3
4
5
6
7
8
9
10
11
12
13
14
15
16
17
18
19
20
21
22
23
24
25
26
27
28
29
30
31
32
33
34
35
36
37
38
39
40
41
42
43
44
45
46
47
48
49
50
51
52
53
54
55
56
57
58
59
60
61
62
63
64
65

608 Newfoundland based on scarce geochemical data that suggest an A-type affinity (Sandeman and
609 Malpas, 1995; Currie, 2003).

610
611 *5.4. Lochkovian to earliest Emsian interval (~419–405 Ma)*

612
613 *5.4.1. The Brabantian event in composite East Avalonia*

614 The Siluro-Devonian boundary approximately marked the onset of Brabantian
615 deformation in easternmost portions of the Avalonian domain (Dewaele et al., 2002; Debacker et
616 al., 2005; Sintubin et al., 2009; Linnemann et al., 2012; Pharaoh, 2018). There is still much
617 debate regarding what caused this Early Devonian event and the subsequent and partly
618 overprinting Middle Devonian Acadian Orogeny in Europe. The Midlands Microcraton
619 seemingly acted as a rigid internal indenter that rotated counter-clockwise with respect to the rest
620 of composite East Avalonia during the Brabantian and Acadian events (Sintubin et al., 2009;
621 partly based on palaeomagnetic data from Piper, 2007). This rotation implies that the region
622 experienced shortening concentrated over a discrete area due to the docking of an external
623 indenter. According to Soper et al. (1987, 1992) and Martinez Catalan et al. (2007), this external
624 indenter was a peri-Gondwanan terrane associated with Armorica (or Cadomia, *sensu* Nance et
625 al., 2012), which, according to Kroner and Romer (2013), was in the form of a promontory (the
626 Armorican Spur) attached to Gondwana (Fig. 16). Resistance of the Scandinavian Shield to this
627 rotation generated the Brabantian belt in the area of the inferred Thor Suture to the northeast of
628 the Midland Microcraton, whereas rocks to the northwest of the microcraton experienced
629 sinistral transpression evolving towards sinistral transtension to the southeast (Sintubin et al.,
630 2009; Pharaoh, 2018).

631

1
2
3
4 632 *5.4.2. Early Devonian foreland basin development in West Avalonia*

5
6 633 In West Avalonian terranes of northern Nova Scotia, the Siluro-Devonian boundary is
7
8
9 634 marked by a transition from passive-margin marine sedimentation in the Pridoli Stonehouse
10
11 635 Formation to coarsening-upward foreland basin deposits of the Lochkovian to Pragian Knoydart
12
13
14 636 Formation, which bear palaeocurrent vectors that indicate a source to the southwest (Boucot et
15
16 637 al., 1974; Murphy, 1987; Waldron et al., 1996). This suggests that collision between Gondwana
17
18
19 638 and West Avalonia was already occurring in earliest Devonian times (Fig. 16, cross-section C-
20
21 639 D). In contrast, the now juxtaposed Meguma Belt of southern Nova Scotia was then
22
23
24 640 accommodating quiet marine sediments (Jensen, 1975) that were hosting brachiopods with
25
26 641 Rhenish affinities (Boucot, 1960). This suggests that rocks of the Meguma Terrane were
27
28
29 642 proximal to Armorica/Cadomia, which is consistent with provenance data from the Silurian
30
31 643 (White et al., 2018), but uninvolved in the early Devonian collisions that affected both West and
32
33 644 composite East Avalonia (Fig. 16).

34
35 645
36
37
38 646 *5.4.3. Final closure of the Acadian Seaway*

39
40
41 647 One of the most challenging tectono-magmatic events to explain in the Appalachian–
42
43 648 Caledonian is the onset of andesite-rich Early Devonian volcanism in the Matapedia cover
44
45
46 649 sequence of northeastern North America, unconformably above Pridoli bimodal volcanic rocks
47
48 650 that are clearly associated with extension or transtension (Wilson et al., 2017). The progressive
49
50
51 651 depletion in HFSEs within these rocks (Fig. 8c,d) suggests a gradual reintroduction of hydrous
52
53 652 conditions at the source. We propose that this volcanic succession may be the record of a
54
55 653 reactivation of Acadian Seaway slab subduction beneath composite Laurentia (including the
56
57
58 654 accreted Ganderian terranes) due to the Early Devonian docking of a Gondwanan promontory
59
60
61
62
63
64
65

1
2
3
4
5
6
7
8
9
10
11
12
13
14
15
16
17
18
19
20
21
22
23
24
25
26
27
28
29
30
31
32
33
34
35
36
37
38
39
40
41
42
43
44
45
46
47
48
49
50
51
52
53
54
55
56
57
58
59
60
61
62
63
64
65

655 against West Avalonia to the southwest, which forced convergence to resume between the latter
656 and composite Laurentia (Figs. 2 and 16, Cross-section A-B). Hence, the previously aborted
657 subduction zone beneath the South Ganderian margin of composite Laurentia would have
658 provided a weak zone that could have partly accommodated the shortening generated by the
659 convergence of Gondwana against West Avalonia (Fig. 16), which was still separated from
660 composite Laurentia by a small remnant of the Acadian Seaway at the Siluro-Devonian boundary
661 (Fig. 14).

662 Final closure of the Acadian Seaway and accretion of West Avalonia to composite
663 Laurentia occurred in late Emsian to Middle Devonian times and caused the Acadian Orogeny in
664 northeastern North America (Figs. 2 and 17). A synchronous episode of shortening to the
665 northwest of the Midland Microcraton in the British Isles has also been attributed to the Acadian
666 Orogeny (eg. Soper et al., 1987; Woodcock et al., 2007) (Fig. 17). At the time, the Cornubian
667 Basin of southern England (Fig. 1) was located outside of the collision zone, to the east
668 (Woodcock, 2012c). Its post-Acadian westward migration may have been associated with the
669 same east-west fault system that caused the Meguma Terrane of Atlantic Canada to migrate
670 westward by ~900-1000 km in relation to Avalonian domains along a large Middle Devonian to
671 Carboniferous dextral strike-slip fault corridor (Keppie, 1982; Murphy et al., 2011).

672
673 **6. Conclusions**

674
675 Katian to earliest Emsian igneous rocks in the Appalachian-Caledonian Belt all share
676 characteristics of plate-margin magmatism (Figs. 6a,b-11a,b). However, differentiation between
677 arc, slab-failure and plate-margin A2-type magmatism (Figs. 6c,d-11c,d) allowed us to draw a

1
2
3
4
5
6
7
8
9
10
11
12
13
14
15
16
17
18
19
20
21
22
23
24
25
26
27
28
29
30
31
32
33
34
35
36
37
38
39
40
41
42
43
44
45
46
47
48
49
50
51
52
53
54
55
56
57
58
59
60
61
62
63
64
65

678 clearer picture on the series of tectono-magmatic events that took place in terranes of that belt
679 during the interval separating the Taconic–Grampian and Acadian orogenies. Furthermore,
680 relatively well constrained ages for these rocks allowed the identification of evolutionary trends
681 in the geochemical data. Based on the latter as well as palaeomagnetic, palaeontologic,
682 structural, stratigraphic and sedimentologic constraints, the following nuances can be added to
683 the closure history of the Iapetus and Rheic oceans as well as their associated segments
684 (Tornquist Sea, Tetagouche–Exploits back-arc basin, and Acadian Seaway):

- 685 Based on the slab-failure signature of early to mid-Silurian igneous rocks to the north
686 of the Dog Bay Line in the North Ganderian and Laurentian margin terranes of
687 northeastern North America (Fig. 7c,d), closure of the Tetagouche–Exploits back-arc
688 basin took place earlier than previously thought (eg. Wilson et al., 2017), and in
689 association with the early Silurian Salinic A unconformity rather than the late Silurian
690 Salinic B unconformity.
- 691 In Ireland, slab failure occurred in mid-Silurian times (*circa* 428 Ma) prior to final
692 closure of Iapetus, with no associated local deformation. However, Iapetus closure
693 was already completed by then farther to the northeast, as recorded by Scandian
694 deformation in terranes of northern Scotland and Greenland, which may have
695 generated post-collisional slab failure (Fig. 13).
- 696 Based on geochronological constraints, igneous rocks produced in association with
697 failure of the Iapetus and Tetagouche–Exploits slabs show a gradual increase in
698 HFSE contents with time (Figs. 7c,d and 10c,d), which we associate with a gradual
699 dehydration of the mantle source due to the abortion of subduction. This trend is
700 paired with a corresponding decrease in Nb/Y and La/Yb ratios with time, which we

1
2
3
4
5
6
7
8
9
10
11
12
13
14
15
16
17
18
19
20
21
22
23
24
25
26
27
28
29
30
31
32
33
34
35
36
37
38
39
40
41
42
43
44
45
46
47
48
49
50
51
52
53
54
55
56
57
58
59
60
61
62
63
64
65

701 attribute to a fading contribution of the failed slab at the source as it sinks to greater
702 depths.

703 - A switch from shallow subduction and arc magmatism to extensional, A2-type
704 bimodal magmatism occurred at the Ludlow–Pridoli boundary in South Ganderian
705 terranes of coastal Maine and southwest New Brunswick (Fig. 7c,d)). This may have
706 been caused by chain failure of the Acadian Seaway slab deep within the
707 asthenosphere due to its interaction with the slowly sinking Tetagouche–Exploits slab
708 (Fig. 14, transect A-B), which had previously failed at a short distance inboard near
709 the beginning of the Silurian (Fig. 12, transect A-B). Such conclusion is supported by
710 the synchronous record of a rapid and short-lived regression along the north margin
711 of West Avalonia (Fig. 15), which was nearby at the time and attached to the Acadian
712 Seaway slab (Fig. 14, transect C-D).

713 - Extensional tectonics associated with failure of the Acadian Seaway slab at depth
714 seemingly migrated towards north Ganderian terranes during the Pridoli and produced
715 extensional, A2-type bimodal volcanic rocks and coarse clastic deposits of the Dickie
716 Cove Group (Fig. 14, sections A-B and A’-B’). Evidence for more hydrated
717 volcanism at the base of the group than at the top (Fig. 7c,d) suggests an inheritance
718 from the preceding subduction and slab failure settings and an associated delay in the
719 development of a complete A2-type signature.

720 - The Early Devonian Dalhousie Group, which overlaps the North Ganderian–
721 Laurentian suture in northern New Brunswick and eastern Quebec (locality i in Fig.
722 1), records a gradual return to hydrated, andesite-rich arc magmatism (Fig. 8c,d),
723 which is synchronous with foreland basin development in West Avalonia (Table 2). It

1
2
3
4 724 is here proposed that these igneous rocks were produced by a reactivation of Acadian
5
6 725 Seaway slab subduction beneath composite Laurentia forced by the prograding
7
8
9 726 collision of Gondwana into West Avalonia, which was still attached to that remnant
10
11 727 of oceanic lithosphere (Fig. 16). Final closure of the Acadian Seaway generated the
12
13
14 728 laterally extensive Acadian Orogeny (Fig. 17 and Table 2).
15

16 729

17 730 **Acknowledgements**

18
19 731

20
21 732 We wish to thank J.D. Greenough and J.B. Whalen for their positive and constructive
22
23
24 733 reviews, as well as R.S. Hildebrand and J.W. Waldron for their helpful advice on an earlier
25
26 734 version of this manuscript. This project was supported by an operational grant (249658-07) from
27
28
29 735 the Natural Sciences and Engineering Council of Canada (NSERC) to P. Jutras.
30
31
32

33 736

34 737 **References**

35
36 738

37
38
39
40 739 André, L., Hertogen, J. and Deutsch, S., 1986. Ordovician–Silurian magmatic provinces in
41
42
43 740 Belgium and the Caledonian orogeny in middle Europe. *Geology* 14 (10), 879–882.

44
45 741 Archibald, D.B., Murphy, J.B., 2021. A slab failure origin for the Donegal composite
46
47
48 742 batholith, Ireland as indicated by trace-element geochemistry. *Geological Society,*
49
50
51 743 London, Special Publications, vol. 503, pp. 347–370.

52
53 744 Archibald, D.B., Macquarrie, L.M., Murphy, J.B., Strachan, R.A., McFarlane, C.R.,
54
55 745 Button, M., Larson, K.P., Dunlop, J., 2021. The construction of the Donegal
56
57
58
59
60
61
62
63
64
65

1
2
3
4
5
6
7
8
9
10
11
12
13
14
15
16
17
18
19
20
21
22
23
24
25
26
27
28
29
30
31
32
33
34
35
36
37
38
39
40
41
42
43
44
45
46
47
48
49
50
51
52
53
54
55
56
57
58
59
60
61
62
63
64
65

746 composite batholith, Irish Caledonides: Temporal constraints from U-Pb dating of
747 zircon and titanite. *Geol. Soc. Am. Bull.* 133 (11–12), 2335–2354.

748 Archibald, D.B., Murphy, J.B., Fowler, M., Strachan, R.A., Hildebrand, R.S., 2022.
749 Testing petrogenetic models for contemporaneous mafic and felsic to intermediate
750 magmatism within the ‘Newer Granite’ suite of the Scottish and Irish Caledonides,
751 *in* Kuiper, Y., Murphy, J.B., Nance, R.D., Strachan, R.S., Thompson, M.D., eds.,
752 *New Developments in the Appalachian–Caledonian–Variscan Orogen*. Geological
753 Society of America - Special Paper, vol. 554, pp. 375–400.

754 Aydin, N.S., 1995. Petrology of the composite mafic-felsic rocks of the Fogo Island
755 batholith: A window to mafic magma chamber processes and the role of mantle in
756 the petrogenesis of granitoid rocks. Unpublished PhD thesis, Memorial University
757 of Newfoundland, St. John’s, NL, 191 p.

758 Badenszki, E., Daly, J.S., Whitehouse, M.J., Kronz, A., Upton, B.G., Horstwood, M.S.,
759 2019. Age and origin of deep crustal meta-igneous xenoliths from the Scottish
760 Midland Valley: vestiges of an early Palaeozoic arc and ‘Newer Granite’
761 magmatism. *J. of Petrol.* 60 (8), 1543–1574.

762 Barr, S.M., White, C.E., Miller, B.V., 2002. The Kingston terrane, southern New
763 Brunswick, Canada: evidence for an Early Silurian volcanic arc. *Geol. Soc. Am.*
764 *Bull.* (8), 964–982.

765 Becker, R.T., Marshall, J.E.A., Da Silva, A.-C., 2020. Chapter 22—The Devonian Period,
766 *in* Gradstein, F.M., Ogg, J.G., Schmitz, M.D., Ogg, G.M., eds., *The Geologic Time*
767 *Scale 2020, Volume 2*. Elsevier: Boston, MA, USA, pp. 733–810. ISBN: 978-0-
768 128-24361-9.

1
2
3
4 769 Bender, H., Glodny, J., Ring, U., 2019. Absolute timing of Caledonian orogenic wedge
5
6 770 assembly, Central Sweden, constrained by Rb–Sr multi-mineral isochron data.
7
8
9 771 Lithos, 344, 339–359.

10
11 772 Bergström, S.M., Chen, X., Gutiérrez- Marco, J.C., Dronov, A., 2009. The new
12
13
14 773 chronostratigraphic classification of the Ordovician System and its relations to
15
16 774 major regional series and stages and to $\delta^{13}\text{C}$ chemostratigraphy. *Lethaia* 42 (1), 97-
17
18 775 107, DOI 10.1111/j.1502-3931.2008.00136.x.

19
20
21 776 Boucot, A.J., 1960. A New Lower Devonian Stropheodontid Brachiopod: *J. Paleontol.* 34
22
23 777 (3), 483–485.

24
25
26 778 Boucot, A.J., Dewey, J.F., Dineley, D.L., Fletcher, R., Fyson, W.K., Griffin, J.G., Hickox,
27
28 779 C.F., Mckerrow, W.S., Ziegler, A.M., 1974. Geology of the Arisaig area, Antigonish
29
30 780 County, Nova Scotia. Geological Society of America - Special Paper, vol. 139, 191
31
32 781 p.

33
34
35
36 782 Bourque, P.A., Lachambre, G., 1980. Stratigraphie du Silurien et du Dévonien basal du sud
37
38 783 de la Gaspésie. Québec Ministry of Energy and Ressources, Special Paper ES–30,
39
40 784 123 p.

41
42
43 785 Bourque, P.A., Malo, M., Kirkwood, D., 2000. Paleogeography and tectono-sedimentary
44
45 786 history at the margin of Laurentia during Silurian to earliest Devonian time: The
46
47 787 Gaspé Belt, Québec. *Geol. Soc. Am. Bull.* 112 (1), 4–20.

48
49
50 788 Brem, A.G., Lin, S., Van Staal, C.R., Davis, D.W., McNicoll, V.J., 2007. The Middle
51
52 789 Ordovician to Early Silurian voyage of the Dashwoods microcontinent, West
53
54 790 Newfoundland; based on new U/Pb and $^{40}\text{Ar}/^{39}\text{Ar}$ geochronological, and
55
56 791 kinematic constraints. *Am. J. Sci.* 307, 311–338.

57
58
59
60
61
62
63
64
65

1
2
3
4
5
6
7
8
9
10
11
12
13
14
15
16
17
18
19
20
21
22
23
24
25
26
27
28
29
30
31
32
33
34
35
36
37
38
39
40
41
42
43
44
45
46
47
48
49
50
51
52
53
54
55
56
57
58
59
60
61
62
63
64
65

792 Cawood, P.A., Dunning, G.R., 1993. Silurian age for movement on the Baie Verte Line:
793 implications for accretionary tectonics in the northern Appalachians. In Geological
794 Society of America, Abstracts with Programs 25, p. A422.

795 Cawood, P.A., van Gool, J.A.M., Dunning, G.R., 1996. Geological development of eastern
796 Humber and western Dunnage zones: Corner Brook-Glover Island region,
797 Newfoundland. *Can. J. Earth Sci.* 33, 182–198.

798 Chew, D.M., Strachan, R.A., 2014. The Laurentian Caledonides of Scotland and Ireland.
799 Geological Society, London, Special Publications, vol. 390, pp. 45–91.

800 Chew, D.M., Daly, J.S., Magna, T., Page, L.M., Kirkland, C.L., Whitehouse, M.J., Lam, R.,
801 2010. Timing of ophiolite obduction in the Grampian orogen. *Geol. Soc. Am. Bull.*
802 122, 1787–1799.

803 Churchill-Dickson, L., 2004. A Late Silurian (Pridolian) age for the Eastport Formation,
804 Maine: A review of the fossil, stratigraphic, and radiometric-age data. *Atl. Geol.* 40,
805 189–195.

806 Cocks, L.R.M., Torsvik, T.H., 2002. Earth geography from 500 to 400 million years ago; a
807 faunal and palaeomagnetic review. *J. Geol. Soc.* 159, 631–644.

808 Currie, K.L., 2003, Emplacement of the Fogo Island Batholith, Newfoundland. *Atl. Geol.*
809 39, 79–96.

810 Daly, R.A., 1925. The geology of Ascension Island. *Proceedings to American Academy of*
811 *Arts and Sciences* 60, 3–80.

812 David, J., Gariépy, C., 1990. Early Silurian orogenic andesites from the central Quebec
813 Appalachians. *Can. J. Earth Sci.* 27 (5), 632–643.

1
2
3
4
5
6
7
8
9
10
11
12
13
14
15
16
17
18
19
20
21
22
23
24
25
26
27
28
29
30
31
32
33
34
35
36
37
38
39
40
41
42
43
44
45
46
47
48
49
50
51
52
53
54
55
56
57
58
59
60
61
62
63
64
65

814 Debacker, T.N., Dewaele, S., Sintubin, M., Verniers, J., Muechez, P., Boven, A., 2005.
815 Timing and duration of the progressive deformation of the Brabant Massif,
816 Belgium. *Geol. Belg.* 8 (4), 20–34.

817 Dewaele, S., Boven, A., Muechez, P.H., 2002. $^{40}\text{Ar}/^{39}\text{Ar}$ dating of mesothermal, orogenic
818 mineralization in a low-angle reverse shear zone in the Lower Palaeozoic of the
819 Anglo–Brabant fold belt, Belgium. *Applied Earth Sci.* 111 (3), 215–220.

820 Dewey, J.F., Dalziel, I.W., Reavy, R.J., Strachan, R.A., 2015. The Neoproterozoic to Mid-
821 Devonian evolution of Scotland: a review and unresolved issues. *Scott. J. Geol.* 51,
822 5–30.

823 Doig, R., Nance, R.D., Murphy, J.B., Casseday, R.P., 1990. Evidence for Silurian sinistral
824 accretion of Avalon composite terrane in Canada. *J. Geol. Soc.* 147 (6), 927–930.

825 Dokken, R., 2017. Detrital zircon studies in Silurian basins of southern New Brunswick.
826 MSc thesis, University of Alberta.

827 Dostal, J., Jutras, P., 2021. Tectonic and petrogenetic settings of the Eocene Challis–
828 Kamloops volcanic belt of western Canada and the northwestern United States. *Int.*
829 *Geol. Rev.* 64 (18), 2565–2583. <https://doi.org/10.1080/00206814.2021.1992800>.

830 Dostal, J., Wilson, R.A., Keppie, J.D., 1989. Geochemistry of Siluro-Devonian Tobique
831 volcanic belt in northern and central New Brunswick (Canada): tectonic
832 implications. *Can. J. Earth Sci.* 26, 1282–1296.

833 Dostal, J., Laurent, R., Keppie, J.D., 1993. Late Silurian–Early Devonian rifting during
834 dextral transpression in the southern Gaspé Peninsula (Quebec): petrogenesis of
835 volcanic rocks. *Can. J. Earth Sci.* 30, 2283–2294.

1
2
3
4
5
6
7
8
9
10
11
12
13
14
15
16
17
18
19
20
21
22
23
24
25
26
27
28
29
30
31
32
33
34
35
36
37
38
39
40
41
42
43
44
45
46
47
48
49
50
51
52
53
54
55
56
57
58
59
60
61
62
63
64
65

836 Dostal, J., Keppie, J.D., Wilson, R.A., 2016. Nd isotopic and trace element constraints on
837 the source of Silurian–Devonian mafic lavas in the Chaleur Bay Synclinorium of
838 New Brunswick (Canada): Tectonic implications. *Tectonophysics* 681, 364–375.

839 Dostal, J., Wilson, R., Jutras, P., 2021. Petrogenesis of Siluro-Devonian rhyolites of the
840 Tobique Group in the northwestern Appalachians (northern New Brunswick,
841 Canada): Tectonic implications for the accretion history of peri–Gondwanan
842 terranes along the Laurentian margin, *in* Quesada, C., Strachan, R., Murphy, B.,
843 eds., *Pannotia to Pangea: Neoproterozoic and Paleozoic orogenic cycles in the*
844 *circum–North Atlantic region*. Geological Society, London, Special Publications,
845 vol. 503, pp. 391–407.

846 Dostal, J., Jutras, P., Wilson, R., 2022. Geochemical and Nd isotopic constraints on the
847 origin of Upper Silurian rhyolitic rocks in the northern Appalachians (northern New
848 Brunswick): tectonic implications, *in* Kuiper, Y., Murphy, J.B., Nance, R.D.,
849 Strachan, R.S., Thompson, M.D., eds., *New Developments in the Appalachian–*
850 *Caledonian–Variscan Orogen*. Geological Society of America - Special Paper, vol.
851 554, pp. 121–134.

852 Doyon, M., Dalpé, C., 1993. *Roches magmatiques siluro-dévonniennes de la Gaspésie*.
853 Québec Ministry of Energy and Resources, MB 93–16, 128 p.

854 Dunning, G.R., 1992, U–Pb geochronological research agreement final report for the
855 Newfoundland Department of Mines and Energy. Unpublished report (results
856 published in van Staal et al., 2014).

1
2
3
4
5
6
7
8
9
10
11
12
13
14
15
16
17
18
19
20
21
22
23
24
25
26
27
28
29
30
31
32
33
34
35
36
37
38
39
40
41
42
43
44
45
46
47
48
49
50
51
52
53
54
55
56
57
58
59
60
61
62
63
64
65

857 Dunning, G.R., O'brien, S.J., Colman-Sadd, S.P., Blackwood, R.F., Dickson, W.L., O'neill,
858 P.P., Krogh, T.E., 1990. Silurian orogeny in the Newfoundland Appalachians. The
859 J. Geol. 98 (6), 895–913.

860 Eby, N., 1992. Chemical subdivision of the A-type granitoids: petrogenetic and tectonic
861 implications. Geology 20, 641–644.

862 Elliott, C.G., Dunning, G.R., Williams, P.F., 1991. New U/Pb zircon age constraints on the
863 timing of deformation in north-central Newfoundland and implications for early
864 Paleozoic Appalachian orogenesis. Geol. Soc. Am. Bull. 103, 125–135.

865 Freeburn, R., Bouilhol, P., Maunder, B., Magni, V., van Hunen, J., 2017. Numerical
866 models of the magmatic processes induced by slab breakoff. Earth Planet. Sci. Lett.
867 478, 203–213.

868 Fritschle, T., Daly, J.S., Whitehouse, M.J., McConnell, B., Buhre, S., 2018a. Multiple
869 intrusive phases in the Leinster Batholith, Ireland: geochronology, isotope
870 geochemistry and constraints on the deformation history. J. Geol. Soc. 175 (2), 229-
871 246.

872 Fritschle, T., Daly, J.S., McConnell, B., Whitehouse, M.J., Menuge, J.F., Buhre, S., Mertz-
873 Kraus, R., Döpke, D., 2018b. Peri-Gondwanan Ordovician arc magmatism in
874 southeastern Ireland and the Isle of Man: Constraints on the timing of Caledonian
875 deformation in Ganderia. Geol. Soc. Am. Bull. 130 (11-12), 1918-1939.

876 Fyffe, L., Fricker, A., 1987. Tectonostratigraphic terrane analysis of New Brunswick. Atl.
877 Geol. 23 (3), 113–122.

878 Giggie, K.V., 1999. Ground follow-up to the multi-sensor airborne geophysical survey in
879 central Restigouche County, New Brunswick: results and interpretation. New

1
2
3
4
5
6
7
8
9
10
11
12
13
14
15
16
17
18
19
20
21
22
23
24
25
26
27
28
29
30
31
32
33
34
35
36
37
38
39
40
41
42
43
44
45
46
47
48
49
50
51
52
53
54
55
56
57
58
59
60
61
62
63
64
65

880 Brunswick Department of Natural Resources and Energy, Minerals and Energy
881 Division, Open File Report, vol. 99–9, 41 p.

882 Greenough, J.D. 1984. Petrology and geochemistry of Cambrian volcanic rocks from the
883 Avalon Zone in Newfoundland and New Brunswick. Ph.D. thesis, Memorial
884 University of Newfoundland, St. John's.

885 Greenough, J.D., Kamo, S.L., Krogh, T.E., 1993. A Silurian U–Pb age for the Cape St
886 Mary’s sills, Avalon Peninsula, Newfoundland, Canada: implications for Silurian
887 orogenesis in the Avalon Zone. *Can. J. Earth Sci.* 30, 1607–1612.

888 Greiner, H.R., 1970. Geology of the Charlo area, 21O/16, Restigouche County, New
889 Brunswick. New Brunswick Department of Natural Resources, Mineral Resources
890 Branch, Map Series 70–2, 18 p.

891 Heaman, L.M., Erdmer, P., Owen, J.V., 2002. U–Pb geochronologic constraints on the
892 crustal evolution of the Long Range Inlier, Newfoundland. *Can. J. Earth Sci.* 39,
893 845–865.

894 Hamilton, M.A., Kerr, A., 2016. New U–Pb dates from Silurian rocks on Fogo Island:
895 Preliminary stratigraphic and tectonic implications. Newfoundland and Labrador
896 Department of Natural Resources Geological Survey, Current Research, vol. 16, pp.
897 123-132.

898 Hildebrand, R.S., Whalen, J.B., 2017. The Tectonic Setting and Origin of Cretaceous
899 Batholiths Within the North American Cordillera: The Case for Slab Failure
900 Magmatism and Its Significance for Crustal Growth. Geological Society of
901 America - Special Paper, vol. 532, 113 p.

1
2
3
4
5
6
7
8
9
10
11
12
13
14
15
16
17
18
19
20
21
22
23
24
25
26
27
28
29
30
31
32
33
34
35
36
37
38
39
40
41
42
43
44
45
46
47
48
49
50
51
52
53
54
55
56
57
58
59
60
61
62
63
64
65

902 Holland, C.H., 1988. The fossiliferous Silurian rocks of the Dunquin inlier, Dingle
903 peninsula, County Kerry, Ireland. *Trans. R. Soc. Edinb. Earth Sci.* 19, 347–360.

904 Hollocher, K., Robinson, P., Seaman, K., Walsh, E., 2016. Ordovician–early Silurian
905 intrusive rocks in the northwest part of the Upper Allochthon, mid-Norway: Plutons
906 of an Iapetan volcanic arc complex. *Am. J. Sci.* 316 (10), 925–980.

907 Irrinki, R.R., 1990. Geology of the Charlo area, Restigouche County, New Brunswick.
908 New Brunswick Department of Natural Resources and Energy, Minerals and
909 Energy Division, Report of Investigation 24, 118 p.

910 Jakob, J., Andersen, T.B., Mohn, G., Kjøll, H.J., Beyssac, O., 2022. A Revised Tectono-
911 Stratigraphic Scheme for the Scandinavian Caledonides and Its Implications for
912 Our Understanding of the Scandian Orogeny, *in* Kuiper, Y., Murphy, J.B., Nance,
913 R.D., Strachan, R.S., Thompson, M.D., eds., *New Developments in the*
914 *Appalachian–Caledonian–Variscan Orogen*. Geological Society of America -
915 Special Paper, vol. pp. 554, 335–374.

916 Jensen, L.R., 1975. The Torbrook Formation. *Atl. Geol.* 11 (3), 107–118.

917 Johnson, R.J.E., Van der Voo, R., 1985. Middle Cambrian paleomagnetism of the Avalon
918 Terrane in Cape Breton Island, Nova Scotia. *Tectonics* 4, 629–651.
919 <https://doi.org/10.1029/TC004i007p00629>.

920 Johnson, R.J.E., Van der Voo, R., 1990. Pre-folding magnetization reconfirmed for the Late
921 Ordovician–Early Silurian Dunn Point volcanics, Nova Scotia. *Tectonophysics* 178,
922 193–205. [https://doi.org/10.1016/0040-1951\(90\)90146-Y](https://doi.org/10.1016/0040-1951(90)90146-Y).

1
2
3
4
5
6
7
8
9
10
11
12
13
14
15
16
17
18
19
20
21
22
23
24
25
26
27
28
29
30
31
32
33
34
35
36
37
38
39
40
41
42
43
44
45
46
47
48
49
50
51
52
53
54
55
56
57
58
59
60
61
62
63
64
65

923 Jutras, P., Murphy, J.B., Quick, D., Dostal, J., 2020. Evolution of subduction dynamics
924 beneath West Avalonia in Middle to Late Ordovician times. *Lithosphere*, Article
925 8837633, 22 p., <https://doi.org/10.2113/2020/8837633>.

926 Kant, L.B., Tepper, J.H., Eddy, M.P., Nelson, B.K., 2018. Eocene basalt of Summit Creek:
927 slab breakoff magmatism in the central Washington Cascades, USA. *Lithosphere*
928 10 (6), 792–805.

929 Karabinos, P., Macdonald, F.A., Crowley, J., 2017. Bridging the gap between the foreland
930 and hinterland 1: geochronology and plate tectonic geometry of Ordovician
931 magmatism and terrane accretion on the Laurentian margin of New England. *Am. J.*
932 *Sci.* 317, 515–554.

933 Keppie, J.D., 1982. The Minas Geofracture. In St-Julien, Pierre (editor); Beland, J (editor).
934 Geological Association of Canada - Special Paper, vol. 24, pp. 263–280.

935 Kirkland, C.L., Alsop, G.I., Daly, J.S., Whitehouse, M.J., Lam, R., Clark, C., 2013.
936 Constraints on the timing of Scandian deformation and the nature of a buried
937 Grampian terrane under the Caledonides of northwestern Ireland. *J. Geol. Soc.* 170
938 (4), 615–625.

939 Kroner, U., Romer, R.L., 2013. Two plates—many subduction zones: the Variscan
940 orogeny reconsidered. *Gondwana Res.* 24 (1), 298–329.

941 Landing, E., 1996. Avalon; insular continent by the latest Precambrian, *in* Nance, R.D.,
942 Thompson, M.D., eds., *Avalonian and Related Peri-Gondwanan Terranes of the*
943 *Circum-North Atlantic*. Geological Society of America - Special Paper, vol. 304,
944 pp. 29–63.

1
2
3
4
5
6
7
8
9
10
11
12
13
14
15
16
17
18
19
20
21
22
23
24
25
26
27
28
29
30
31
32
33
34
35
36
37
38
39
40
41
42
43
44
45
46
47
48
49
50
51
52
53
54
55
56
57
58
59
60
61
62
63
64
65

945 Landing, E., 2007. Ediacaran–Ordovician of East Laurentia. S. W. Ford Memorial Volume,
946 Bulletin 510 - New York State Museum, University of The State of New York,
947 Albany, NY, United States.

948 Landing, E., Murphy, J.B., 1991. Uppermost Precambrian(?)–Lower Cambrian of
949 mainland Nova Scotia; faunas, depositional environments, and stratigraphic
950 revision. *J. Paleontol.* 65, 382–396.

951 Landing, E., Johnson, S.C., Geyer, G., 2008. Faunas and Cambrian volcanism on the
952 Avalonian marginal platform, southern New Brunswick. *J. Paleontol.* 82, 884–905.
953 <https://doi.org/10.1666/07-007.1>.

954 Landing, E., Keppie, J.D., Keppie, D.F., Geyer, G., Westrop, S.R., 2022. Greater
955 Avalonia—latest Ediacaran–Ordovician “peribaltic” terrane bounded by continental
956 margin prisms (“Gander,” Harlech Dome, Meguma): review, tectonic implications,
957 and paleogeography. *Earth-Sci. Rev.* 224, 103863.
958 <https://doi.org/10.1016/j.earscirev.2021.103863>.

959 Leggett, J.K., McKerrow, W.S., Eales, M.H., 1979. The Southern Uplands of Scotland: a
960 Lower Palaeozoic accretionary prism. *J. Geol. Soc.* 136, 755–770.

961 Linnemann, U., Herbolch, A., Liégeois, J.P., Pin, C., Gärtner, A., Hofmann, M., 2012. The
962 Cambrian to Devonian odyssey of the Brabant Massif within Avalonia: a review
963 with new zircon ages, geochemistry, Sm–Nd isotopes, stratigraphy and
964 palaeogeography. *Earth-Sci. Rev.* 112 (3–4), 126–154.

965 Lissenberg, C.J., van Staal, C.R., 2002. The relationships between the Annieopsquotch
966 ophiolite belt, the Dashwoods block and the Notre Dame arc in southwestern

1
2
3
4 967 Newfoundland. Newfoundland Department of Energy and Mines, Current
5
6 968 Research, vol. 02-1, pp. 45–153.
7
8
9 969 Lissenberg, C.J., Zagorevski, A., McNicoll, V.J., van Staal, C.R., Whalen, J.B., 2005.
10
11 970 Assembly of the Annieopsquotch Accretionary Tract, Newfoundland Appalachians:
12
13
14 971 age and geodynamic constraints from syn-kinematic Intrusions. *J. Geol.* 113, 553–
15
16 972 570.
17
18
19 973 Lusty, P.A.J., Lacinska, A.M, Millar, I.L., Barrie, C.D., Boyce, A.J., 2017. Wales, UK; a
20
21 974 failed volcanogenic massive sulfide system in the Avalon Zone of the British
22
23
24 975 Caledonides. *Ore Geol. Rev.* 89, 557–586.
25
26 976 Macdonald, F.A., Ryan-Davis, J., Coish, R.A., Crowley, J.L., Karabinos, P., 2014. A
27
28
29 977 newly identified Gondwanan terrane in the northern Appalachian Mountains:
30
31 978 Implications for the Taconic orogeny and closure of the Iapetus Ocean. *Geology* 42
32
33 979 (6), 539–542.
34
35
36 980 Mac Niocaill, C., 2000. A new Silurian paleolatitude for eastern Avalonia and evidence for
37
38 981 crustal rotations in the Avalonian margin of southwestern Ireland. *Geophys. J. Int.*
39
40 982 141 (3), 661–671. doi:10.1046/j.1365-246x.2000.00101.x.
41
42
43 983 Martinez Catalan, J.R., Arenas, R., García, F.D., Cuadra, P.G., Gómez-Barreiro, J., Abati,
44
45 984 J., Castiñeiras, P., Fernández-Suárez, J., Martínez, S.S., Andonaegui, P., Clavijo,
46
47
48 985 E.G., 2007. Space and time in the tectonic evolution of the northwestern Iberian
49
50 986 Massif: Implications for the Variscan belt, *in* Hatcher, R.D. Jr, Carlson, M.P.,
51
52
53 987 McBride, J.H., Martinez Catalan, J.R., eds., 4-D framework of continental crust.
54
55 988 Geological Society of America Memoir, vol. 200, pp. 403–423.
56
57
58 989 doi:10.1130/2007.1200(21).
59
60
61
62
63
64
65

- 1
2
3
4 990 McConnell, B., Riggs, N., Fritschle, T., 2021. Tectonic history across the Iapetus suture
5
6 991 zone in Ireland. Geological Society, London, Special Publications, vol. 503 (1), pp.
7
8
9 992 333-345.
10
11 993 McGregor, D.C., 1992. Palynology of Upper Silurian/Lower Devonian rock samples from
12
13
14 994 the western margin of the Elmtree inlier of northern New Brunswick (NTS 21
15
16 995 P/13). Geological Survey of Canada, unpublished paleontological report F1-1-
17
18
19 996 1992-DCM, 2 p.
20
21 997 McKerrow, W.S., Leggett, J.K., Eales, M.H., 1977. Imbricate thrust model of the Southern
22
23
24 998 Uplands of Scotland. *Nature* 267, 237-239.
25
26 999 McNicoll, V., Squires, G.C., Kerr, A., Moore, P.J., 2008. Geological and metallogenic
27
28
29 1000 implications of U-Pb zircon geochronological data from the Tally Pond area,
30
31 1001 central Newfoundland. Newfoundland and Labrador Department of Natural
32
33
34 1002 Resources, Geological Survey, Report 8, pp. 173-193.
35
36 1003 Melchin, M.J., Sadler, P.M., Cramer, B.D., 2020. The Silurian Period, *in* *Geologic Time*
37
38 1004 *Scale* 2020, Elsevier, p. 695-732.
39
40
41 1005 Miller, B.V., Fyffe, L.R., 2002. Geochronology of the Letete and Waweig Formations,
42
43 1006 Mascarene Group, southwestern New Brunswick. *Atl. Geol.* 38, 29-36.
44
45
46 1007 Murphy, J., 1987. The stratigraphy and depositional environment of upper Ordovician to
47
48 1008 lower Devonian rocks in the Antigonish Highlands, Nova Scotia. *Atl. Geol.* 23 (2),
49
50
51 1009 63-75.
52
53 1010 Murphy, R.B., 1989. Geochemistry of Siluro-Devonian mafic volcanic rocks and
54
55 1011 associated gabbroic intrusions, Upsalquitch Forks area, New Brunswick.
56
57
58 1012 Unpublished M.Sc. thesis, Acadia University, Wolfville, Nova Scotia, 274 p.
59
60
61
62
63
64
65

- 1
2
3
4 1013 Murphy, J.B., Fernández-Suárez, J., Jeffries, T.E., 2004. Lithogeochemical, Sm-Nd and U-
5
6
7 1014 Pb isotopic data from the Silurian–Early Devonian Arisaig Group clastic rocks,
8
9 1015 Avalon terrane, Nova Scotia: a record of terrane accretion in the Appalachian–
10
11
12 1016 Caledonide orogeny. *Geol. Soc. Am. Bull.* 116, 1183–1201.
13
14 1017 Murphy, J.B., Dostal, J., Keppie, J.D., 2008. Neoproterozoic–Early Devonian magmatism
15
16 1018 in the Antigonish Highlands, Avalon terrane, Nova Scotia: Tracking the evolution
17
18
19 1019 of the mantle and crustal sources during the evolution of the Rheic Ocean.
20
21 1020 *Tectonophysics* 461, 181–201.
22
23
24 1021 Murphy, J.B., Waldron, J.W., Kontak, D.J., Pe-Piper, G., Piper, D.J., 2011. Minas Fault
25
26 1022 Zone: Late Paleozoic history of an intra-continental orogenic transform fault in the
27
28
29 1023 Canadian Appalachians. *J. Struct. Geol.* 33 (3), 312–328.
30
31 1024 Murphy, J.B., Hamilton, M.A., Leblanc, B., 2012. Tectonic significance of Late
32
33 1025 Ordovician silicic magmatism, Avalon terrane, northern Antigonish Highlands,
34
35
36 1026 Nova Scotia. *Can. J. Earth Sci.* 49, 346–358.
37
38 1027 Murphy, J.B., Nance, R.D., Gabler, L.B., Martell, A., Archibald, D.A., 2019. Age,
39
40
41 1028 geochemistry and origin of the Ardara appinite plutons, northwest Donegal, Ireland.
42
43 1029 *Geoscience Canada. Geosci. Can.* 46 (1), 31–48.
44
45
46 1030 Nance, R.D., Gutiérrez-Alonso, G., Keppie, J.D., Linnemann, U., Murphy, J.B., Quesada,
47
48 1031 C., Strachan, R.A., Woodcock, N.H., 2010. Evolution of the Rheic ocean.
49
50
51 1032 *Gondwana Res.* 17, 194–222.
52
53 1033 Nance, R.D., Gutiérrez-Alonso, G., Keppie, J.D., Linnemann, U., Murphy, J.B., Quesada,
54
55 1034 C., Strachan, R.A., Woodcock, N.H., 2012. A brief history of the Rheic Ocean.
56
57
58 1035 *Geosci. Frontiers* 3, 125–135.
59
60
61
62
63
64
65

- 1
2
3
4 1036 Noble, J.P.A., 1976. Silurian stratigraphy and paleogeography, Pointe Verte area, New
5
6
7 1037 Brunswick, Canada. *Can. J. Earth Sci.* 13 (4), 537-546.
8
9 1038 Noble, S.R., Tucker, R.D., Pharaoh, T.C., 1993. Lower Palaeozoic and Precambrian
10
11 1039 igneous rocks from eastern England, and their bearing on late Ordovician closure of
12
13
14 1040 the Tornquist Sea: constraints from U-Pb and Nd isotopes. *Geol. Mag.* 130 (6),
15
16 1041 835–846.
17
18
19 1042 Nowlan, G.S., 1983. Early Silurian conodonts of eastern Canada. *Fossils and Strata* 15, 95–
20
21 1043 110.
22
23
24 1044 Pharaoh, T., 2018. The Anglo–Brabant Massif: persistent but enigmatic palaeo-relief at the
25
26 1045 heart of western Europe. *Proc. Geol. Assoc.* 129 (3), 278–328.
27
28
29 1046 Pharaoh, T.C., Merriman, R.J., Evans, J.A., Brewer, T.S., Webb, P.C., Smith, N.J.P., 1991.
30
31 1047 Early Palaeozoic arc-related volcanism in the concealed Caledonides of southern
32
33 1048 Britain. *Annales de la Société Géologique de Belgique* 114, 63–91.
34
35
36 1049 Pharaoh, T.C., Brewer, T.S., Webb, P.C., 1993. Subduction-related magmatism of late
37
38 1050 Ordovician age in eastern England. *Geol. Mag.* 130, 647–656.
39
40
41 1051 Pharaoh, T., England, R., Lee, M., 1995. The concealed Caledonide basement of eastern
42
43 1052 England and the southern North Sea—a review. *Studia geophysica et geodaetica*
44
45 1053 39, 330–346.
46
47
48 1054 Phillips, B.A., Kerr, A.C., Bevins, R., 2016. A re-appraisal of the petrogenesis and tectonic
49
50
51 1055 setting of the Ordovician Fishguard volcanic group, SW Wales. *Geol. Mag.* 153,
52
53 1056 410–425.
54
55 1057 Pidgeon R.T., Aftalion M., 1978. Cogenetic and Inherited Zircon U-Pb Systems in
56
57 1058 Palaeozoic granites of Scotland and England, *in* Bowes, R.D. and Leake, B.E., eds.,
59
60
61
62
63
64
65

- 1
2
3
4 1059 Crustal evolution in Northwest Britain and adjacent regions. *Geology Journal*
5
6
7 1060 Special Issue 10, 183–220.
8
9 1061 Piñán-Llamas, A., Hepburn, J.C., 2013. Geochemistry of Silurian–Devonian volcanic rocks
10
11 1062 in the Coastal Volcanic belt, Machias–Eastport area, Maine: Evidence for a pre–
12
13
14 1063 Acadian arc. *Geol. Soc. Am. Bull.* 125, 1930–1942.
15
16 1064 Piper, J.D.A., 2007. Palaeomagnetism of the Loch Doon Granite Complex, Southern
17
18
19 1065 Uplands of Scotland: the Late Caledonian palaeomagnetic record and an early
20
21 1066 Devonian Episode of true polar wander. *Tectonophysics* 432 (1–4), 133–157.
22
23
24 1067 Pothier, H.D., Waldron, J.W.F., Schofield, D.I., DuFrane, A., 2015. Peri–Gondwanan
25
26 1068 terrane interactions recorded in the Cambrian–Ordovician detrital zircon
27
28
29 1069 geochronology of North Wales. *Gondwana Res.* 28 (3), 987–1001.
30
31 1070 Rogers, N., Van Staal, C.R., 2003. Volcanology and tectonic setting of the northern
32
33 1071 Bathurst Mining Camp: Part II. Mafic volcanic constraints on back-arc opening, *in*
34
35
36 1072 Goodfellow, W.D., McCutcheon, S.R., Peter, J.M., eds., *Massive Sulfide Deposits*
37
38 1073 of the Bathurst Mining Camp, New Brunswick, and Northern Maine. *Economic*
39
40
41 1074 *Geology Monograph* 11, 181–201.
42
43 1075 Ross, P.S., Bédard, J.H., 2009. Magmatic affinity of modern and ancient subalkaline
44
45
46 1076 volcanic rocks determined from trace-element discriminant diagrams. *Can. J. Earth*
47
48 1077 *Sci.* 46 (11), 823–839.
49
50
51 1078 Ryan, P.D., Dewey, J.F., 1991. A geological and tectonic cross-section of the Caledonides
52
53 1079 of western Ireland. *J. Geol. Soc.* 148, 173–180.
54
55 1080 Sandeman, H.A., Malpas, J., 1995. Epizonal I-and A-type granites and associated ash-flow
56
57
58 1081 tuffs, Fogo Island, northeast Newfoundland. *Can. J. Earth Sci.* 32, 1835–1844.
59
60
61
62
63
64
65

- 1
2
3
4 1082 Schofield, D.I., Potter, J., Barr, S.M., Horák, J.M., Millar, I.L., Longstaffe, F.J., 2016.
5
6 1083 Reappraising the Neoproterozoic ‘East Avalonian’ terranes of southern Great
7
8 Britain. *Gondwana Res.* 35, 257–271.
9 1084
10
11 1085 Seaman, S.J., Wobus, R.A., Wiebe, R.A., Lubick, N., Bowring, S.A., 1995. Volcanic
12
13 expression of bimodal magmatism: the Cranberry Island–Cadillac Mountain
14 1086
15 complex, coastal Maine. *J. Geol.* 103 (3), 301–311.
16 1087
17
18 1088 Seaman, S.J., Scherer, E.E., Wobus, R.A., Zimmer, J.H., Sales, J.G., 1999. Late Silurian
19
20 volcanism in coastal Maine: the Cranberry Island series. *Geol. Soc. Am. Bull.* 111
21 1089
22 (5), 686–708.
23 1090
24
25 1091 Sintubin, M., Debacker, T.N., Van Baelen, H., 2009. Early Palaeozoic orogenic events
26
27 north of the Rheic suture (Brabant, Ardenne): A review. *Comptes Rendus*
28 1092
29 Geoscience 341, 156–173.
30
31 1093
32
33 1094 Sloan, R.J., Bennett, M.C., 1990. Geochemical character of Silurian volcanism in SW
34
35 Ireland. *J. Geol. Soc.* 147 (6), 1051–1060.
36 1095
37
38 1096 Smethurst, M.A., McEnroe, S.A., 2003. The palaeolatitude controversy in the Silurian of
39
40 Newfoundland resolved: New palaeomagnetic results from the central mobile belt.
41 1097
42 *Tectonophysics* 362, 83–104, doi:10.1016/S0040-1951(02)00632-7.
43 1098
44
45 1099 Soper, N.J., Webb, B.C., Woodcock, N.H., 1987. Late Caledonian (Acadian) transpression
46
47 in north-west England: timing, geometry and geotectonic significance. *Proc. Yorks.*
48 1100
49 *Geol. Soc.* 46 (3), 175–192.
50 1101
51
52 1102 Soper, N.J., Strachan, R.A., Holdsworth, R.E., Gayer, R.A., Greiling, R.O., 1992. Sinistral
53
54 transpression and the Silurian closure of Iapetus. *J. Geol. Soc.* 149 (6), 871–880.
55 1103
56
57
58
59
60
61
62
63
64
65

- 1
2
3
4 1104 Stone, P., McMillan, A.A., Floyd, J.D., Barnes, R.P., Phillips, E.R., 2012. British Regional
5
6
7 1105 Geology: South of Scotland, 4th Edition. British Geological Survey, Nottingham.
8
9 1106 247 p. ISBN 978-085272-694-5.
10
11 1107 Strachan, R.A., 2012a. The Grampian Orogeny: Mid-Ordovician Arc–Continent Collision
12
13
14 1108 along the Laurentian Margin of Iapetus, *in* Woodcock, N.H., Strachan, R., eds.,
15
16 1109 Geological history of Britain and Ireland. Second Edition: Geological history of
17
18
19 1110 Britain and Ireland, Chapter 6, Wiley–Blackwell.
20
21 1111 Strachan, R.A., 2012b. Mid- Ordovician to Silurian Subduction and Collision: Closure of
22
23
24 1112 the Iapetus Ocean, *in* Woodcock, N.H., Strachan, R., eds., Geological history of
25
26 1113 Britain and Ireland. Second Edition: Geological history of Britain and Ireland,
27
28
29 1114 Chapter 7, Wiley–Blackwell.
30
31 1115 Strong, D.F., Dupuy, C., 1982. Rare earth elements in the bimodal Mount Peyton batholith:
32
33
34 1116 Evidence of crustal anatexis by mantle-derived magma. *Can. J. Earth Sci.* 19 (2),
35
36 1117 308-315.
37
38 1118 Sweetman, T.M., 1987. The geochemistry of the Blackstairs unit of the Leinster granite,
39
40
41 1119 Ireland. *J. Geol. Soc.* 144 (6), 971–984.
42
43 1120 Thompson, M.D., Grunow, A.M., Ramezani, J., 2010. Cambro–Ordovician
44
45
46 1121 paleogeography of the Southeastern New England Avalon Zone: implications for
47
48 1122 Gondwana breakup. *Geol. Soc. Am. Bull.* 122, 76–88.
49
50
51 1123 <https://doi.org/10.1130/b26581.1>.
52
53 1124 Thompson, M.D., Barr, S.M., Pollock, J.C., 2022. Evolving views of West Avalonia:
54
55 1125 Perspectives from southeastern New England, USA, *in* Kuiper, Y.D., Murphy, J.B.,
56
57
58 1126 Nance, R.D., Strachan, R.A., Thompson, M.D., eds., *New Developments in the*
59
60
61
62
63
64
65

1
2
3
4 1127 Appalachian–Caledonian– Variscan Orogen. Geological Society of America -
5
6
7 1128 Special Paper, vol. 554, pp. 47-72. [https://doi.org/10.1130/2022.2554\(03\)](https://doi.org/10.1130/2022.2554(03)).
8
9 1129 Thorpe, R.S., Leat, P.T., Bevins, R.E., Hughes, D.J., 1989. Late-orogenic
10
11 alkaline/subalkaline Silurian volcanism of the Skomer Volcanic Group in the
12 1130
13 Caledonides of south Wales. *J. Geol. Soc.* 146 (1), 125–132.
14 1131
15
16 1132 Tindle, A.G., Pearce, J.A., 1981. Petrogenetic modelling of in situ fractional crystallization
17
18 in the zoned Loch Doon Pluton, Scotland. *Cont. Min. Pet.* 78 (2), 196–207.
19 1133
20
21 1134 Torsvik, T.H., Rehnström, E.F., 2003 The Tornquist Sea and Baltica–Avalonia docking.
22
23 *Tectonophysics* 362, 67–82.
24 1135
25
26 1136 Tremblay, A., Pinet, N., 2016. Late Neoproterozoic to Permian tectonic evolution of the
27
28 Quebec Appalachians, Canada. *Earth-Sci. Rev.* 160, 131–170.
29 1137
30
31 1138 van de Kamp, P.C., 1969. The silurian volcanic rocks of the Mendip hills, Somerset; and
32
33 the Tortworth area, Gloucestershire, England. *Geol. Mag.* 106 (6), 542–553.
34 1139
35
36 1140 van Staal, C.R., 1994, Brunswick subduction complex in the Canadian Appalachians:
37
38 record of the Late Ordovician to Late Silurian collision between Laurentia and the
39 1141
40 Gander margin of Avalon. *Tectonics* 13, 946–962.
41 1142
42
43 1143 van Staal, C.R., Ravenhurst, C.E., Roddick, J.C., Winchester, J.A., Langton, J.P., 1990.
44
45 Post-Taconic blueschist suture in the northern Appalachians of northern New
46 1144
47 Brunswick, Canada. *Geology* 18, 1073–1077.
48 1145
49
50 1146 van Staal, C.R., Dewey, J.F., MacNiocaill, C., McKerrow, W.S., 1998. The Cambrian–
51
52 Silurian tectonic evolution of the northern Appalachians and British Caledonides:
53 1147
54 history of a complex, west and southwest Pacific-type segment of Iapetus, *in*
55 1148
56
57
58
59
60
61
62
63
64
65

1
2
3
4 1149 Blundell, D.J., Scott, A.C., eds., Lyell: The Past Is the Key to the Present.
5
6
7 1150 Geological Society, London, Special Publications, vol. 143, pp. 199–242.
8
9 1151 van Staal, C.R., Whalen, J.B., McNicoll, V.J., Pehrsson, S., Lissenberg, C.J., Zagorevski,
10
11
12 1152 A., Van Breemen, O., Jenner, G.A., 2007. The Notre Dame arc and the Taconic
13
14 1153 orogeny in Newfoundland. Geological Society of America Memoir, vol. 200, pp.
15
16 1154 511–552.
17
18
19 1155 van Staal, C.R., Whalen, J.B., Valverde-Vaquero, P., Zagorevski, and A., Rogers, N.,
20
21 1156 2009. Pre Carboniferous, episodic accretion-related, orogenesis along the
22
23
24 1157 Laurentian margin of the northern Appalachians, *in* Murphy, J. B., Keppie, J.D.,
25
26 1158 Hynes, A.J., eds., Ancient Orogens and Modern Analogues. Geological Society,
27
28
29 1159 London, Special Publications, vol. 327, pp. 271–316.
30
31 1160 van Staal, C.R., Barr, S.M., Murphy, J.B., 2012. Provenance and tectonic evolution of
32
33
34 1161 Ganderia: Constraints on the evolution of the Iapetus and Rheic Oceans. *Geology*
35
36 1162 40, 987–990.
37
38
39 1163 van Staal, C.R., McNicoll, V.J., Rogers, N., 2014. Time-transgressive Salinic and Acadian
40
41 1164 orogenesis, magmatism and Old Red Sandstone sedimentation in Newfoundland.
42
43 1165 *Geosci. Can.* 41, 138-164.
44
45
46 1166 van Staal, C.R., Wilson, R.A., Kamo, S.L., McClelland, W.C., McNicoll, V., 2016.
47
48 1167 Evolution of the Early to Middle Ordovician Popelogan arc in New Brunswick,
49
50
51 1168 Canada, and adjacent Maine, USA: Record of arc-trench migration and multiple
52
53 1169 phases of rifting. *Geol. Soc. Am. Bull.* 128, 122–146, doi: 10.1130/B31253.1.
54
55
56 1170 van Staal, C.R., Barr, S.M., Waldron, J.W., Schofield, D.I., Zagorevski, A., White, C.E.,
57
58 1171 2021. Provenance and Paleozoic tectonic evolution of Ganderia and its
59
60
61
62
63
64
65

1
2
3
4 1172 relationships with Avalonia and Megumia in the Appalachian-Caledonide orogen.
5
6
7 1173 Gondwana Res. 98, 212-243.
8
9 1174 van Wagoner, N.A., Leybourne, M.I., Dadd, K.A., Huskins, M.L., 2001. The Silurian (?)
10
11 1175 Passamaquoddy Bay mafic dyke swarm, New Brunswick: petrogenesis and tectonic
12
13
14 1176 implications. *Can. J. Earth Sci.* 38, 1565–1578.
15
16 1177 van Wagoner, N.A., Leybourne, M.I., Dadd, K.A., Baldwin, D.K., McNeil, W., 2002. Late
17
18
19 1178 Silurian bimodal volcanism of southwestern New Brunswick, Canada: Products of
20
21 1179 continental extension. *Geol. Soc. Am. Bull.* 114 (4), 400–418.
22
23
24 1180 Waldron, J.W., Murphy, J.B., Melchin, M.J. and Davis, G., 1996. Silurian tectonics of
25
26 1181 western Avalonia: strain-corrected subsidence history of the Arisaig Group, Nova
27
28
29 1182 Scotia. *J. Geol.* 104 (6), 677–694.
30
31 1183 Waldron, J.W.F., Schofield, D.I., White, C.E., Barr, S.M., 2011. Cambrian successions of
32
33 1184 the Meguma Terrane, Nova Scotia, Canada, and Harlech Dome, North Wales, UK:
34
35
36 1185 dispersed fragments of a peri-Gondwanan basin? *J. Geol. Soc.* 168, 83–98.
37
38 1186 Waldron, J.W.F., Schofield, D.I., DuFrane, S.A., Floyd, J.D., Crowley, Q.G., Simonetti,
39
40
41 1187 A., Dokken, R.J., Pothier, H.D., 2014. Ganderia–Laurentia collision in the
42
43 1188 Caledonides of Great Britain and Ireland. *J. Geol. Soc.* 171, 555–569.
44
45
46 1189 Waldron, J.W., Schofield, D.I., Murphy, J.B., 2019. Diachronous Paleozoic accretion of
47
48 1190 peri-Gondwanan terranes at the Laurentian margin. Geological Society, London,
49
50
51 1191 Special Publications, vol. 470, pp. 289–310.
52
53 1192 Waldron, J.W., Phil J.A. McCausland, P.J.A., Barr S.M., Schofield, D.I., Reusch, D., Wu,
54
55 1193 L., 2022. Terrane history of the Iapetus Ocean as preserved in the northern
56
57
58 1194 Appalachians and western Caledonides. *Earth-Sci. Rev.* 233, 104163.
59
60
61
62
63
64
65

1
2
3
4 1195 Walker, J.A., 2010. Stratigraphy and lithogeochemistry of Early Devonian volcano-
5
6
7 1196 sedimentary rocks hosting the Nash Creek Zn-Pb-Ag deposit, northern New
8
9 1197 Brunswick, *in* Martin, G.L., ed., Geological Investigations in New Brunswick for
10
11 1198 2009. New Brunswick Department of Natural Resources; Lands, Minerals and
12
13
14 1199 Petroleum Division, Mineral Resource Report 2010–1, pp. 52–97.
15
16 1200 Whalen, J.B., 1989. The Topsails igneous suite, western Newfoundland: an Early Silurian
17
18
19 1201 subduction-related magmatic suite? *Can. J. Earth Sci.* 26 (12), 2421–2434.
20
21 1202 Whalen, J.B., Hildebrand, R.S., 2019. Trace element discrimination of arc, slab failure, and
22
23
24 1203 A-type granitic rocks. *Lithos* 348–349, 105179.
25
26 1204 Whalen, J.B., Currie, K.L., Van Breemen, O., 1987. Episodic Ordovician–Silurian
27
28
29 1205 plutonism in the Topsails igneous terrane, western Newfoundland. *Earth Env. Sci.*
30
31 1206 *Trans. R. Soc. Edinb.* 78 (1), 17–28.
32
33 1207 Whalen, J.B., Jenner, G.A., Longstaffe, F.J., Hegner, E., 1996. Nature and evolution of the
34
35
36 1208 eastern margin of Iapetus: geochemical and isotopic constraints from Siluro-
37
38 1209 Devonian granitoid plutons in the New Brunswick Appalachians. *Can. J. Earth Sci.*
39
40
41 1210 33, 140–155.
42
43 1211 Whalen, J.B., McNicoll, V.J., van Staal, C.R., Lissenberg, C.J., Longstaffe, F.J., Jenner,
44
45
46 1212 G.A., van Breeman, O., 2006. Spatial, temporal and geochemical characteristics of
47
48 1213 Silurian collision-zone magmatism, Newfoundland Appalachians: An example of a
49
50
51 1214 rapidly evolving magmatic system related to slab break-off. *Lithos* 89 (3–4), 377–
52
53 1215 404.
54
55 1216 White, C.E., Barr, S.M., Linnemann, U., 2018. U–Pb (zircon) ages and provenance of the
56
57
58 1217 White Rock Formation of the Rockville Notch Group, Meguma terrane, Nova
59
60
61
62
63
64
65

1
2
3
4 1218 Scotia, Canada. evidence for the “Sardian gap” and West African origin. Can. J.
5
6
7 1219 Earth Sci. 55 (6), 589–603.
8
9 1220 Whitehead, J., Reynolds, P.H., Spray, J.G., 1996. $^{40}\text{Ar}/^{39}\text{Ar}$ age constraints on Taconian
10
11 and Acadian events in the Quebec Appalachians. Geology 24, 359–362.
12
13
14 1222 Williams, H., 1979. Appalachian orogen in Canada. Can. J. Earth Sci. 16 (3), 792–807.
15
16 1223 Wilson, R.A., 2017. The Middle Paleozoic rocks of northern and western New Brunswick,
17
18
19 1224 Canada. New Brunswick Department of Energy and Resource Development,
20
21 1225 Geological Surveys Branch Memoir, vol. 4, 319 p.
22
23
24 1226 Wilson, R.A., Kamo, S., 2008. New U-Pb ages from the Chaleurs and Dalhousie groups:
25
26 1227 Implications for regional correlations and tectonic evolution of northern New
27
28
29 1228 Brunswick, *in* Martin, G.L., ed., Geological Investigations in New Brunswick for
30
31 1229 2007. New Brunswick Department of Natural Resources; Minerals, Policy and
32
33
34 1230 Planning Division, Mineral Resource Report 2008–1, pp. 55–77.
35
36 1231 Wilson, R.A., Kamo, S.L., 2012. The Salinic Orogeny in northern New Brunswick:
37
38 1232 Geochronological constraints and implications for Silurian stratigraphic
39
40
41 1233 nomenclature. Can. J. Earth Sci. 49, 222–238.
42
43 1234 Wilson, R.A., Burden, E.T., Bertrand, R., Asselin, E., McCracken, A.D., 2004,
44
45
46 1235 Stratigraphy and tectono-sedimentary evolution of the Late Ordovician to Middle
47
48 1236 Devonian Gaspé Belt in northern New Brunswick: Evidence from the Restigouche
49
50
51 1237 area. Can. J. Earth Sci. 41, 527–551.
52
53 1238 Wilson, R.A., Kamo, S., Burden, E.T., 2005. Geology of the Val d’Amour Formation:
54
55 1239 Revisiting the type area of the Dalhousie Group, northern New Brunswick, *in*
56
57
58 1240 Martin, G.L., ed., Geological Investigations in New Brunswick for 2004. New
59
60
61
62
63
64
65

1
2
3
4 1241 Brunswick Department of Natural Resources; Minerals, Policy and Planning
5
6
7 1242 Division, Mineral Resource Report 2005–1, pp. 167–212.
8
9 1243 Wilson, R.A., van Staal, C.R., Kamo, S., 2008. Lower Silurian subduction-related volcanic
10
11 1244 rocks in the Chaleurs Group, northern New Brunswick, Canada. *Can. J. Earth Sci.*
12
13
14 1245 45, 981–998.
15
16 1246 Wilson, R.A., Van Staal, C.R., McClelland, W.C., 2015. Synaccretionary sedimentary and
17
18
19 1247 volcanic rocks in the Ordovician Tetagouche backarc basin, New Brunswick,
20
21 1248 Canada: Evidence for a transition from foredeep to forearc basin sedimentation.
22
23
24 1249 *Am. J. Sci.* 315, 958-1001.
25
26 1250 Wilson, R.A., van Staal, C.R., Kamo, S. L., 2017. Rapid transition from the Salinic to
27
28
29 1251 Acadian orogenic cycles in the Northern Appalachian orogen: evidence from
30
31 1252 Northern New Brunswick, Canada. *Am. J. Sci.* 317, 448–481.
32
33 1253 Wood, D.A., 1980. The application of a Th-Hf-Ta diagram to problems of
34
35
36 1254 tectonomagmatic classification and to establishing the nature of crustal
37
38 1255 contamination of basaltic lavas of the British Tertiary volcanic province. *Earth*
39
40
41 1256 *Planet. Sci. Lett.* 50, 11–30.
42
43 1257 Woodcock, N.H., 2012a. Ordovician Volcanism and Sedimentation on Eastern Avalonia,
44
45
46 1258 *in* Woodcock, N.H., Strachan, R., eds., *Geological history of Britain and Ireland:*
47
48 1259 *Second Edition.* Wiley–Blackwell, Chapter 10.
49
50
51 1260 Woodcock, N.H., 2012b. Late Ordovician to Silurian Evolution of Eastern Avalonia during
52
53 1261 Iapetus Closure, *in* Woodcock, N.H., Strachan, R., eds., *Geological history of*
54
55 1262 *Britain and Ireland: Second Edition.* Wiley–Blackwell, Chapter 11.
56
57
58
59
60
61
62
63
64
65

1
2
3
4 1263 Woodcock, N.H., 2012c. The Acadian Orogeny and its Mid-Late Devonian Depositional
5
6
7 1264 Aftermath, *in* Woodcock, N.H., Strachan, R., eds., Geological history of Britain and
8
9 1265 Ireland: Second Edition. Wiley–Blackwell, Chapter 13.
10
11
12 1266 Woodcock, N.H., Soper, N.J., Strachan, R.A., 2007. A Rheic cause for the Acadian
13
14 1267 deformation in Europe. *J. Geol. Soc.* 164 (5), 1023–1036.
15
16 1268 Zagorevski, A., van Staal, C.R., McNicoll, V., Rogers, N., Valverde-Vaquero, P., Draut,
17
18
19 1269 A., Clift, P.D., Scholl, D.W., 2008. Tectonic architecture of an arc-arc collision
20
21 1270 zone, Newfoundland Appalachians, *in* Draut, A. et al., eds., Formation and
22
23
24 1271 applications of the sedimentary record in arc-collision zones. Geological Society of
25
26 1272 America - Special Paper, vol. 436, pp. 309–333, doi:10.1130/2008.2436(14).
27
28
29 1273 Zagorevski, A., van Staal, C.R., Rogers, N., McNicoll, V., Dunning, G.R., Pollock, J.C.,
30
31 1274 2010. Middle Cambrian to Ordovician arc-backarc development on the leading
32
33 1275 edge of Ganderia, Newfoundland Appalachians, *in* Tollo, R.P., et al., eds., From
34
35
36 1276 Rodinia to Pangea: the lithotectonic record of the Appalachian region. Geological
37
38 1277 Society of America Memoir, vol. 206, pp. 367–396.
39
40
41 1278 Zagorevski, A., van Staal, C.R., McNicoll, V.J., Hartree, L., Rogers, N., 2012. Tectonic
42
43 1279 evolution of the Dunnage mélange tract and its significance to the closure of
44
45
46 1280 Iapetus. *Tectonophysics* 568–569, 371–387.
47
48 1281 Ziegler, A.M., Mckerrow, W.S., Burne, R.V., Baker, P.E., 1969. Correlation and
49
50
51 1282 environmental setting of the Skomer Volcanic Group, Pembrokeshire. *Proc. Geol.*
52
53 1283 *Assoc.* 80, 409–39.
54
55 1284 Ziegler, A.M., Scotese, C.R., McKerrow, W.S., Johnson, M.E., Bambach, R.K., 1977.
56
57
58 1285 Paleozoic biogeography of continents bordering the Iapetus (pre–Caledonian) and
59
60
61
62
63
64
65

1
2
3
4
5
6
7
8
9
10
11
12
13
14
15
16
17
18
19
20
21
22
23
24
25
26
27
28
29
30
31
32
33
34
35
36
37
38
39
40
41
42
43
44
45
46
47
48
49
50
51
52
53
54
55
56
57
58
59
60
61
62
63
64
65

1286 Rheic (pre–Hercynian) oceans, *in* Paleontology and Plate Tectonics, Milwaukee
1287 Public Museum Special Publication in Biology and Geology, vol. 2, pp. 1–21.
1288 Zhu, D.C., Wang, Q., Zhao, Z.D., Chung, S.L., Cawood, P.A., Niu, Y., Liu, S.A., Wu,
1289 F.Y., Mo, X.X., 2015. Magmatic record of India–Asia collision. Scientific Reports
1290 5 (1), 1–9.

Figure and Table captions

Table 1. Katian to early Emsian igneous rock units at the localities featuring in Figure 1.

Abbreviations: badd.: baddeleyite; biostrat.: biostratigraphic; constr.: constraints; Ems.: Emsian;

Fm: Formation; Gp: Group; Lland.: Llandovery; Loch.: Lochkovian; Mon.: monazite; Ord.:

Ordovician; Settl.: Settlement; strat.: stratigraphic; tit.: titanium; zirc.: zircon.

~~**Table 1. Igneous rock units at the localities featuring in Figure 1. Abbreviations: voles:**~~

~~volcanics; ig.: igneous; Fm : Formation; Gp : Group; C.: Cove; Dal.: Dalhousie; Settl.:~~

~~Settlement; lampr.: lamprophyre; inter.: intermediate; Lland.: Llandovery; Lochk: Lochkovian;~~

~~Ems.: Emsian; Ord.: Ordovician; strat.: stratigraphic; biostrat.: biostratigraphic.~~

Fig. 1. Map of northeastern North America and Europe showing the main continental terrane assemblages that were involved in the formation of the Appalachian–Caledonian Belt. Details on the lettered localities are included in the text and compiled in Table 1.

Fig. 2. Main tectono-magmatic events recorded in the study area. Ordovician, Silurian and Devonian subdivisions are respectively from Bergström et al. (2008), Melchin et al. (2020), and Becker et a. (2020). Letters in triangles and circles correspond respectively to intrusive and

1
2
3
4 1309 extrusive rocks at localities indicated in Fig. 1, with references for estimated ages indicated in
5
6
7 1310 Table 1. Previous work and references therein include, 1: van Staal et al. (2016); 2: van Staal et
8
9 1311 al. (2012); 3: van Staal et al. (2009); 4: Jutras et al. (2020); 5: Woodcock (2012a); 6: Chew and
10
11 1312 Strachan (2014); 7: Rogers and van Staal, 2003; 8: Wilson et al. (2017); 9: Pharaoh et al. (1993);
12
13 1313 10: Piñán-Llamas and Hepburn (2013); 11: Woodcock (2012b); 12: Boucot et al. (1974); 13:
14
15 1314 Jakob et al. (2022); 14: Woodcock et al. (2007); 15: Murphy et al. (2004); 16: Kroner and Romer
16
17
18
19 1315 (2013); 17: Tremblay and Pinet (2016), and Woodcock (2012c).
20

21 1316 **Fig. 3.** Palaeocontinental reconstruction at ~462 Ma based on Woodcock (2012a), Zagorevski et
22
23 1317 al. (2010), Murphy et al. (2008, 2012), Waldron et al. (2014), Phillips et al. (2016), van Staal et
24
25 1318 al. (2016), Wilson et al. (2017), and Jutras et al. (2020).
26
27

28 1319 **Fig. 4.** Accretion of North Ganderia to composite Laurentia near 455 Ma (Taconic phase C of
29
30 1320 van Staal et al., 2007) followed by slab-window volcanism *circa* 454 Ma in the McGillivray
31
32 1321 Brook Formation of Nova Scotia (Jutras et al., 2020) and the Snowdon Group of Wales
33
34 1322 (Woodcock, 2012a; Lusty et al., 2017) due to the incomplete subduction of the Iapetan ridge
35
36 1323 beneath Avalonia.
37
38
39

40 1324 **Fig. 5.** Development of new, post-Taconic-Grampian subduction zones *circa* 453 Ma based on
41
42 1325 Pharaoh et al., (1991, 1993), Noble et al. (1993) and Torsvik and Rehnström (2003), Woodcock
43
44 1326 (2012a), and Wilson et al. (2017). Intrusive rocks from localities s and y are described in Table
45
46 1327 1.
47
48
49

50 1328 **Fig. 6.** Late Ordovician to Early Devonian igneous rocks in South Ganderian terranes of coastal
51
52 1329 Maine and southern New Brunswick (data from Seaman et al., 1999; Barr et al., 2002; van
53
54 1330 Wagoner et al., 2002; Llamas and Hepburn, 2013) plotted in (a) the Hf/3-Ta-Th diagram of
55
56
57
58
59
60
61
62
63
64
65

1
2
3
4 1331 Wood (1980), (b) the Zr/Y vs Th/Yb diagram of Ross and Bédard (2009), and (c) the Nb+Y vs
5
6
7 1332 Nb/Y and (d) Ta+Yb vs La/Yb diagrams of Whalen and Hildebrand (2019).

8
9 1333 **Fig. 7.** Late Ordovician to Silurian igneous rocks in North Ganderian and Laurentian margin
10
11
12 1334 terranes of northeastern North America (data from Whalen, 1989; David and Gariépy, 1990;
13
14 1335 Giggie, 1999; Whalen et al., 2006; Wilson and Kamo, 2008; Wilson et al., 1995; Wilson, 2017)
15
16 1336 plotted in (a) the Hf/3–Ta–Th diagram of Wood (1980), (b) the Zr/Y vs Th/Yb diagram of Ross
17
18
19 1337 and Bédard (2009), and (c) the Nb+Y vs Nb/Y and (d) Ta+Yb vs La/Yb diagrams of Whalen and
20
21 1338 Hildebrand (2019).

22
23
24 1339 **Fig. 8.** Lower Devonian igneous rocks in North Ganderian and Laurentian margin terranes of
25
26 1340 northern New Brunswick and eastern Quebec (data from Murphy, 1989; Whalen et al., 1996;
27
28
29 1341 Wilson et al., 2005; Walker, 2010; Wilson, 2017) plotted in (a) the Hf/3–Ta–Th diagram of
30
31 1342 Wood (1980), (b) the Zr/Y vs Th/Yb diagram of Ross and Bédard (2009), and (c) the Nb+Y vs
32
33 1343 Nb/Y and (d) Ta+Yb vs La/Yb diagrams of Whalen and Hildebrand (2019).

34
35
36 1344 **Fig. 9.** Lower Devonian igneous rocks in North Ganderian terranes of northern Newfoundland
37
38 1345 (data from Aydin, 1995; Currie, 2003) plotted in (a) the Hf/3–Ta–Th diagram of Wood (1980),
39
40
41 1346 (b) the Zr/Y vs Th/Yb diagram of Ross and Bédard (2009), and (c) the Nb+Y vs Nb/Y and (d)
42
43 1347 Ta+Yb vs La/Yb diagrams of Whalen and Hildebrand (2019).

44
45
46 1348 **Fig. 10.** Late Ordovician to Early Devonian igneous rocks along the Laurentian margin in the
47
48 1349 British Isles (data from Tindle and Pearce, 1981; Badenszki et al., 2019; Murphy et al., 2019;
49
50
51 1350 Archibald and Murphy, 2021) plotted in (a) the Hf/3–Ta–Th diagram of Wood (1980), (b) the
52
53 1351 Zr/Y vs Th/Yb diagram of Ross and Bédard (2009), and (c) the Nb+Y vs Nb/Y and (d) Ta+Yb vs
54
55 1352 La/Yb diagrams of Whalen and Hildebrand (2019).

56
57
58
59
60
61
62
63
64
65

1
2
3
4 1353 **Fig. 11.** Late Ordovician to Early Devonian igneous rocks (data from van de Kamp, 1969;
5
6 1354 Greenough, 1984; Sloan and Bennett, 1990; Pharaoh et al., 1991, 1993) in the former micro-
7
8
9 1355 continents of West and composite East Avalonia plotted in (a) the Hf/3–Ta–Th diagram of Wood
10
11
12 1356 (1980), (b) the Zr/Y vs Th/Yb diagram of Ross and Bédard (2009), and (c) the Nb+Y vs Nb/Y
13
14 1357 and (d) Ta+Yb vs La/Yb diagrams of Whalen and Hildebrand (2019).

15
16 1358 **Fig. 12.** Proposed model for tectono-magmatic events that occurred during the ~441-429 Ma
17
18
19 1359 interval (Llandovery to Wenlock) in rocks of the Appalachian–Caledonian Belt. Isolated letters
20
21 1360 correspond to localities on Fig. 1 described in Table 1, with red letters indicating the record of
22
23
24 1361 intrusive rocks, black letters indicating the record of extrusive rocks, and red-and-black letters
25
26 1362 indicating the record of both. Igneous rock units from that interval include the Dennys Formation
27
28
29 1363 at locality b (Piñán-Llamas and Hepburn, 2013), intrusive and extrusive rocks from the Kingston
30
31 1364 terrane at locality d (Barr et al., 2002), the Lac Raymond and Pointe aux Trembles formations at
32
33
34 1365 locality g (David and Gariépy, 1990), the Weir Formation at locality j (Wilson et al., 2008),
35
36 1366 various plutons at localities m and l (Whalen et al. (2006), the Topsails volcanic group at locality
37
38 1367 o (Whalen, 1989), the Cape St. Mary’s sills at locality q (Greenough et al., 1993), the Skomer
39
40
41 1368 Volcanic Group at locality w (Thorpe et al., 1989), and the Tortworth volcanics at locality x (van
42
43 1369 de Kamp, 1969; Pharaoh et al., 1991).

44
45
46 1370 **Fig. 13.** Proposed model for tectono-magmatic events that occurred during the ~428-424 Ma
47
48 1371 interval (latest Wenlock to Ludlow) in rocks of the Appalachian–Caledonian Belt. Isolated letters
49
50
51 1372 correspond to localities on Fig. 1 described in Table 1, with red letters indicating the record of
52
53 1373 intrusive rocks, and black letters indicating the record of extrusive rocks. Igneous rock units from
54
55 1374 that interval include the Cranberry Islands volcanic series at locality a (Seaman et al., 1999), the
56
57
58 1375 Edmunds Formation, and possibly the Leighton and Eastport formations at locality b (Piñán-

59
60
61
62
63
64
65

1
2
3
4 1376 Llamas and Hepburn, 2013), the Topsails intrusive suite at locality n (Whalen, 1989), early
5
6
7 1377 intrusions in the Donegal composite pluton at locality r (Archibald and Murphy, 2021), the
8
9 1378 Dunquin Group at locality u (Sloan and Bennett, 1990), and possibly the Tortworth volcanics at
10
11
12 1379 locality x (van de Kamp, 1969; Pharaoh et al., 1991).

13
14 1380 **Fig. 14.** Proposed model for tectono-magmatic events that occurred during the 423–421 Ma
15
16 1381 interval (Pridoli) in rocks of the Appalachian–Caledonian Belt. Isolated letters correspond to
17
18
19 1382 localities on Fig. 1 described in Table 1, with red letters indicating the record of intrusive rocks,
20
21 1383 and black or white letters indicating the record of extrusive rocks. Igneous rock units from that
22
23
24 1384 interval include the Passamaquoddy Bay volcanic sequence at locality c (van Wagoner et al.,
25
26 1385 2002), the Dickie Cove and lower Tobique groups at localities h and e, respectively (Dostal et
27
28
29 1386 al., 2020, 2021), and intrusive rocks in the Donegal composite pluton at locality r (Archibald and
30
31 1387 Murphy, 2021).

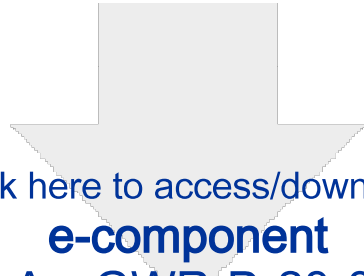
32
33 1388 **Fig. 15.** (a) Thin interval of early Pridoli continental red beds (Upper Member of the Moydart
34
35
36 1389 Formation) between thick intervals of green marine mudrock in the Arisaig Group of northern
37
38
39 1390 Nova Scotia (West Avalonia); (b) intertidal rhythmites in the gradational, but rapid transition
40
41 1391 from subtidal to supratidal deposits near the Ludlow–Pridoli boundary; (c) calcretes within the
42
43 1392 barren Upper Member of the Moydart Formation, which is latest Ludlow to earliest Pridoli based
44
45
46 1393 on biostratigraphic constraints.

47
48 1394 **Fig. 16.** Proposed model for tectono-magmatic events that occurred during the ~417–407 Ma
49
50
51 1395 interval (Lochkovian to earliest Emsian) in rocks of the Appalachian–Caledonian Belt. Isolated
52
53 1396 letters correspond to localities on Fig. 1 described in Table 1, with red letters indicating the
54
55 1397 record of intrusive rocks, and black letters indicating the record of extrusive rocks. Igneous rock
56
57
58 1398 units from that interval include the Dalhousie and upper Tobique groups at localities i and e,
59
60
61
62
63
64
65

1
2
3
4
5
6
7
8
9
10
11
12
13
14
15
16
17
18
19
20
21
22
23
24
25
26
27
28
29
30
31
32
33
34
35
36
37
38
39
40
41
42
43
44
45
46
47
48
49
50
51
52
53
54
55
56
57
58
59
60
61
62
63
64
65

1399 respectively (Wilson, 2017), the Lyall and Baldwin volcanics at locality k (Doyon and Dalpé,
1400 1993), various plutons in the Miramichi Highlands of northern New Brunswick (locality f;
1401 Whalen et al., 1996), the Fogo Island Batholith at locality p (Aydin, 1995; Currie, 2003),
1402 intrusive rocks in the Donegal composite pluton at locality r (Archibald and Murphy, 2021), the
1403 Loch Doon Pluton at locality s (Tindle and, 1981), and a xenolith within upper Palaeozoic
1404 intrusive rocks at locality t (Badenszki et al., 2019).

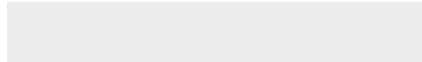
Fig. 17. Proposed model for the Middle Devonian Acadian Orogeny.

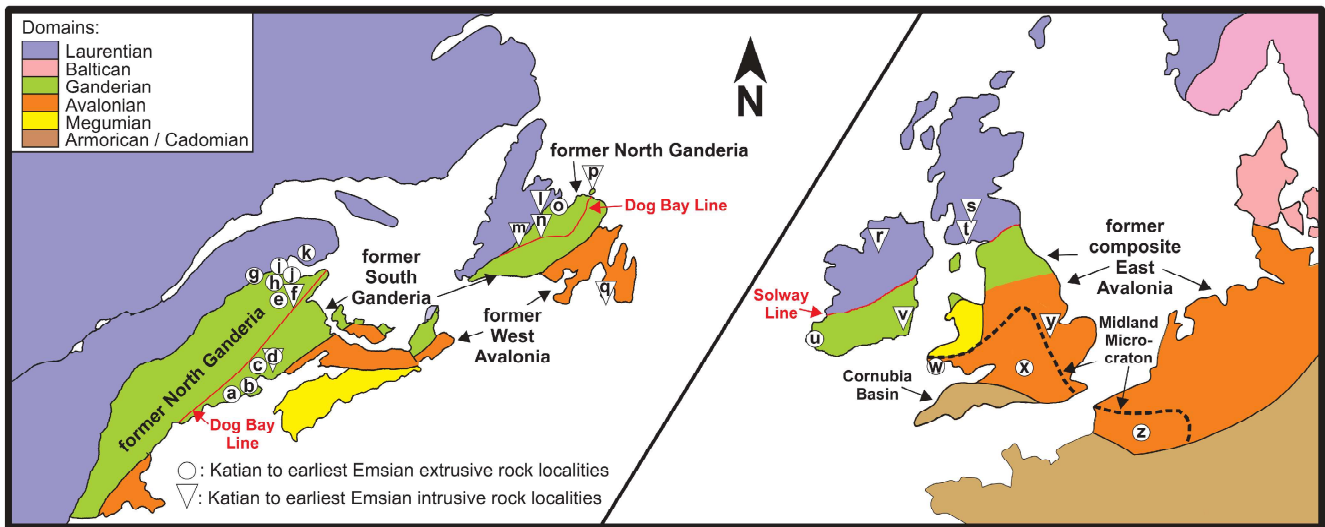


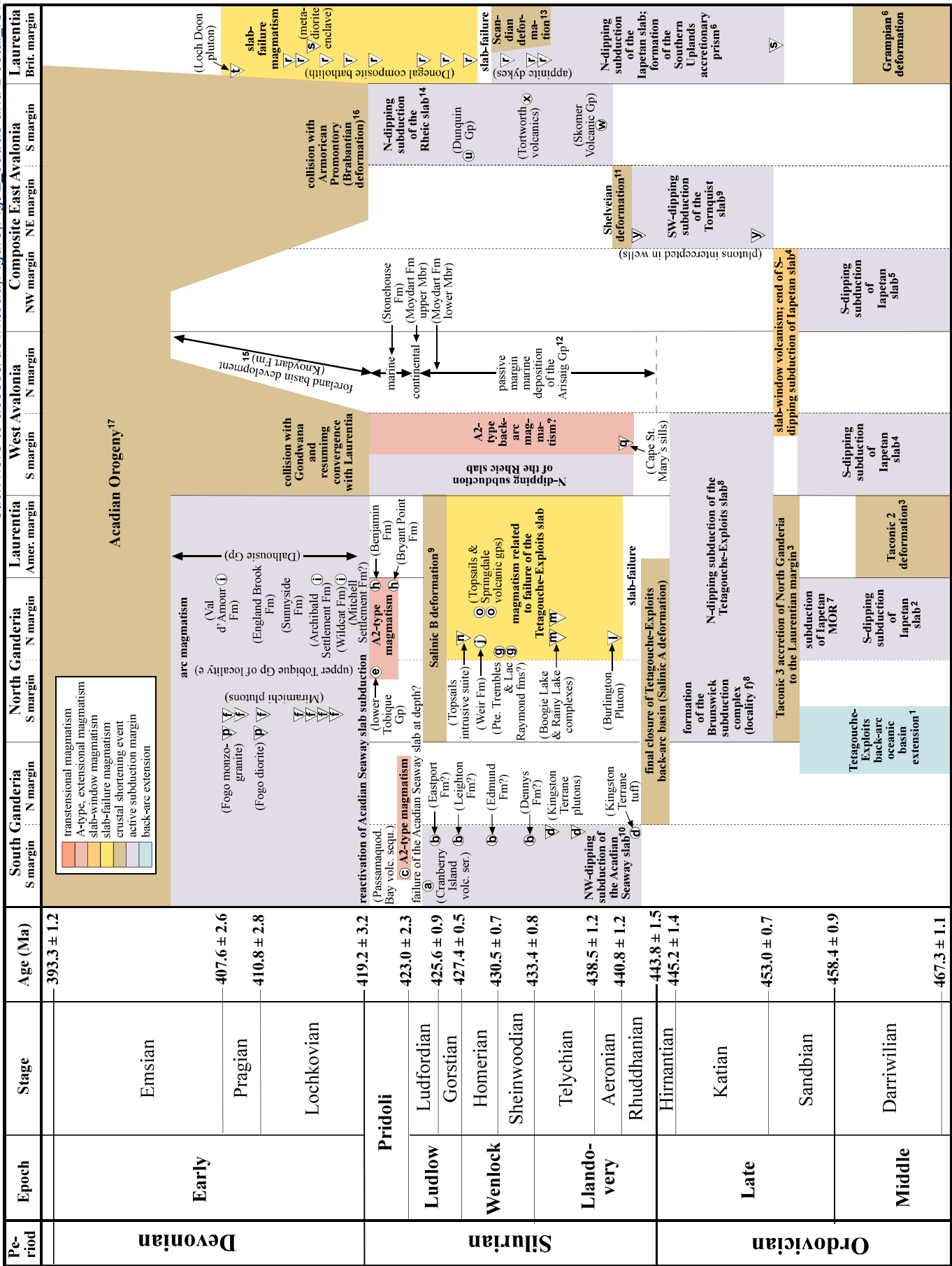
Click here to access/download

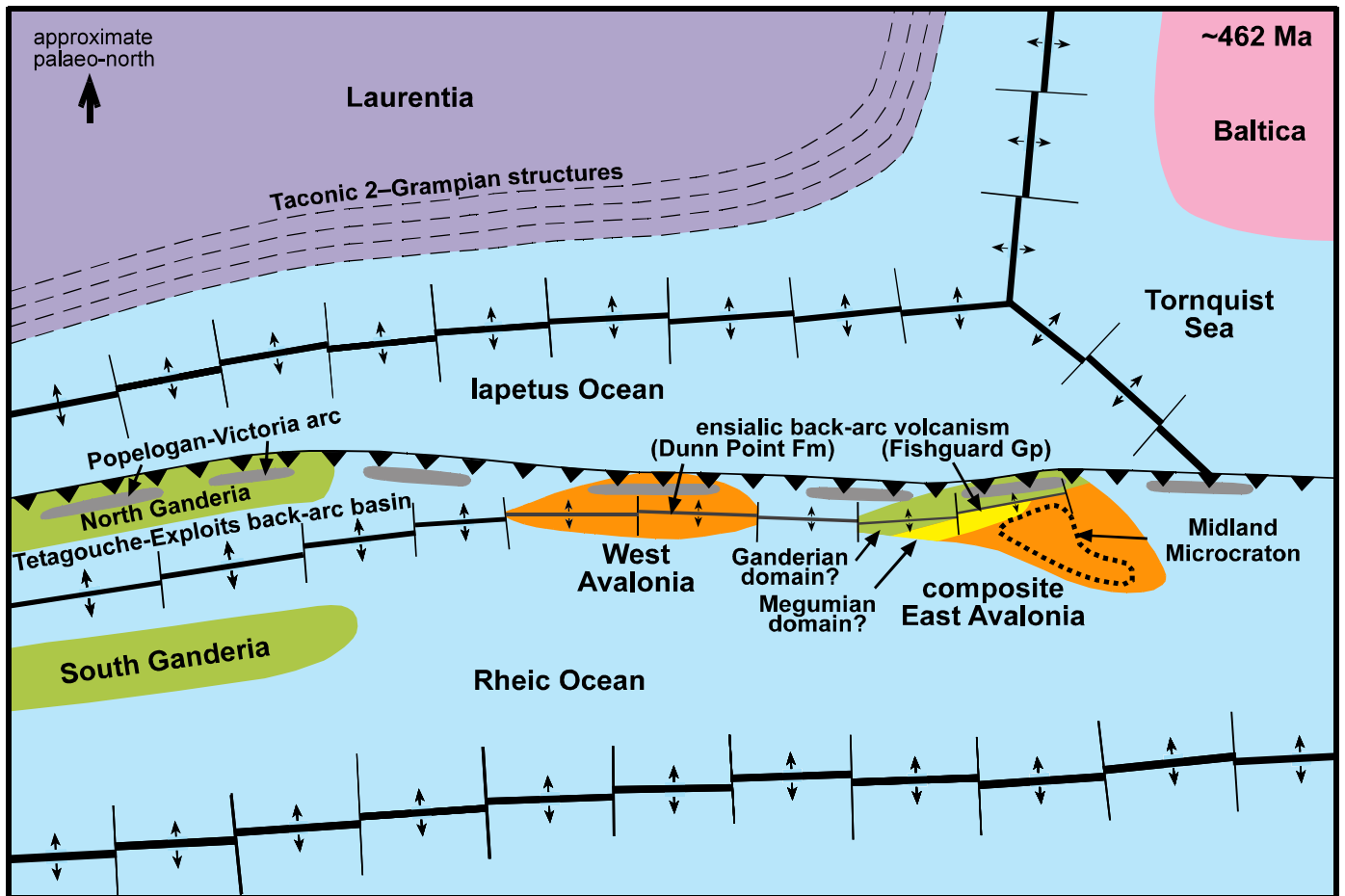
e-component

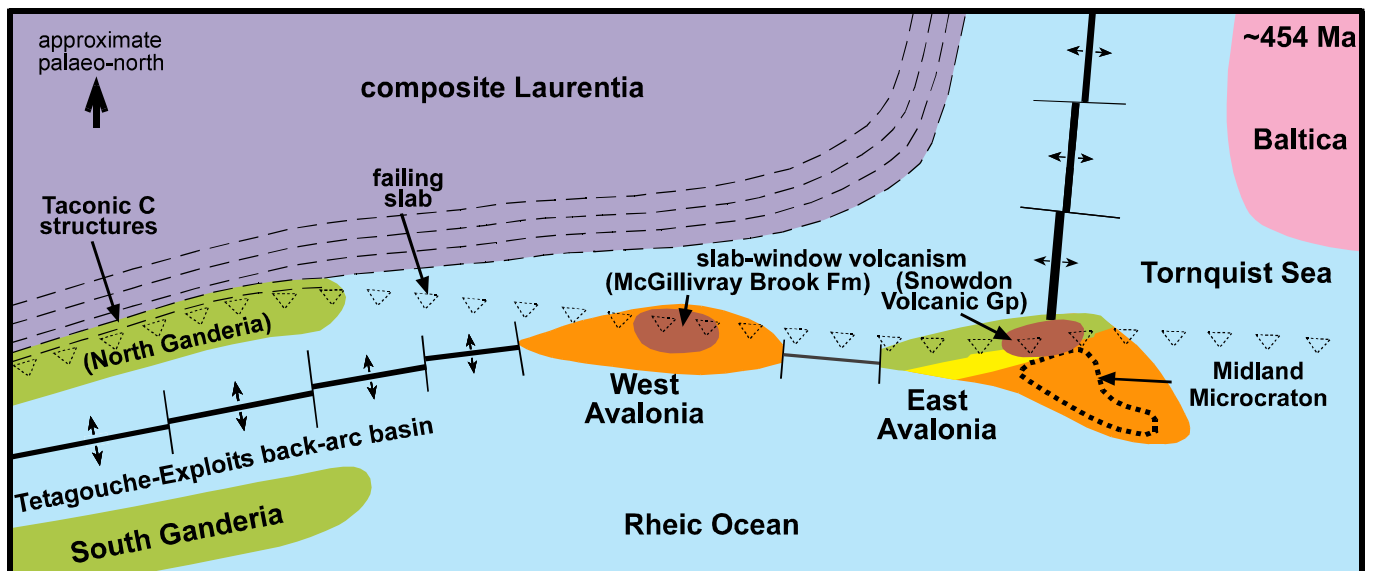
Appendix A__GWR-D-23-00172.xlsx

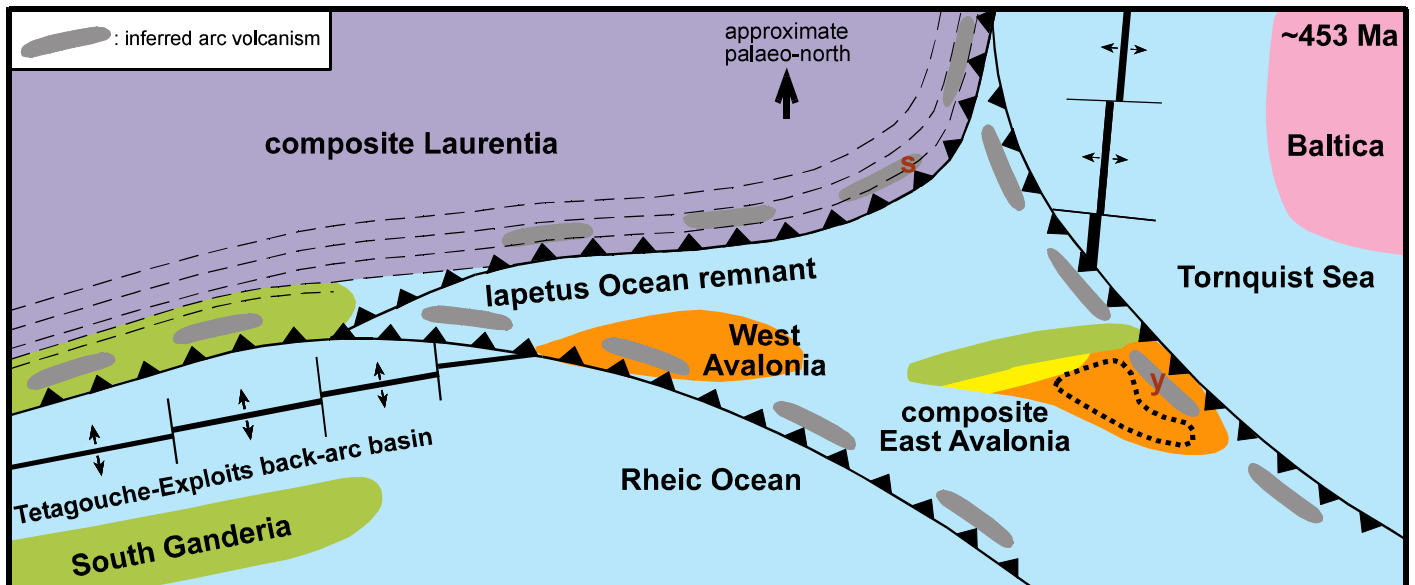


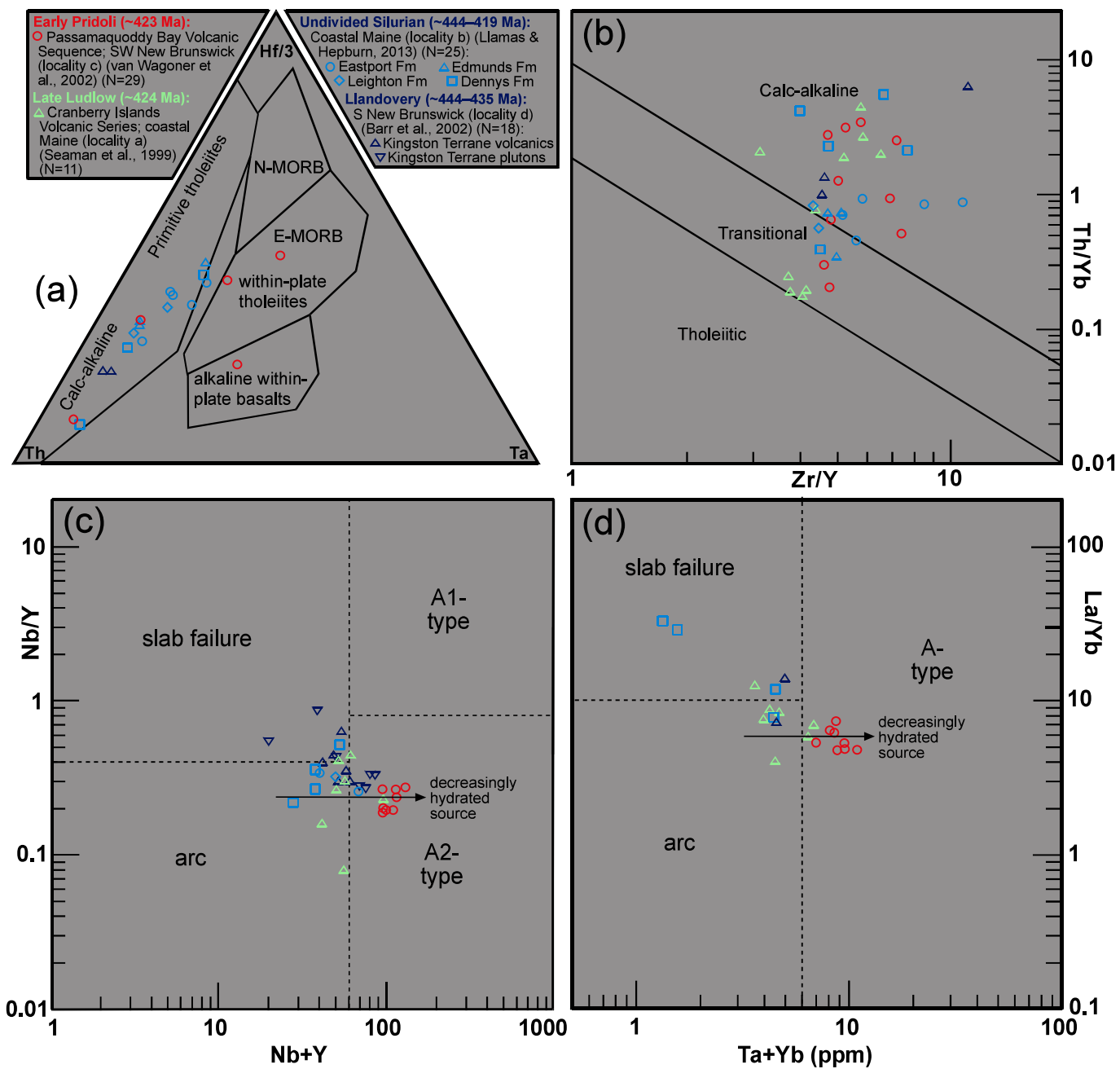


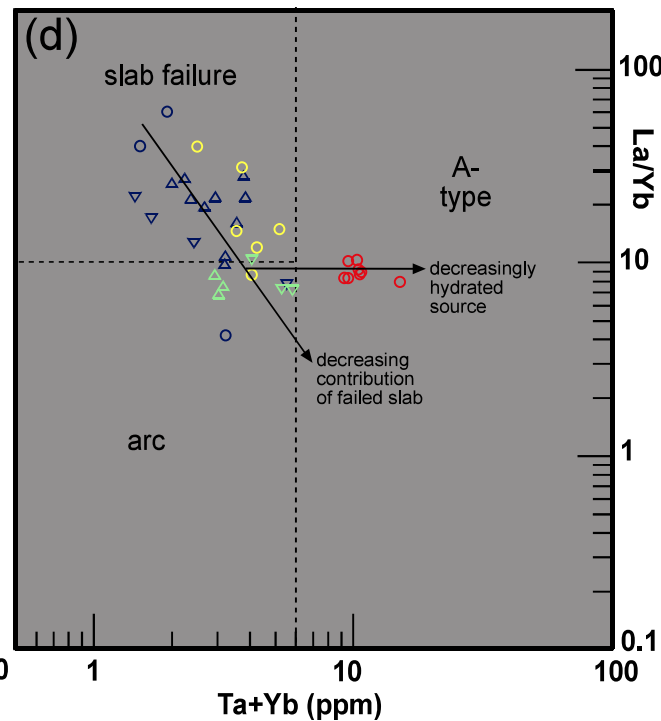
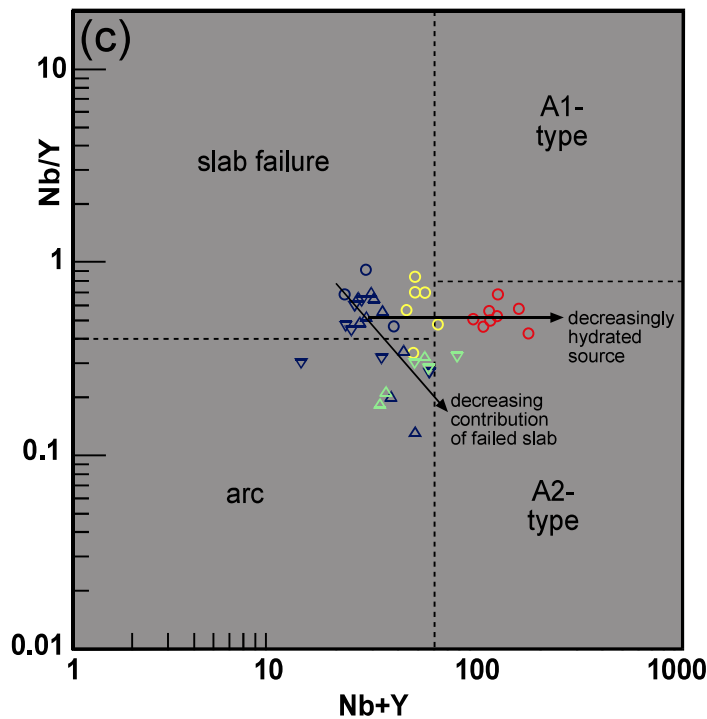
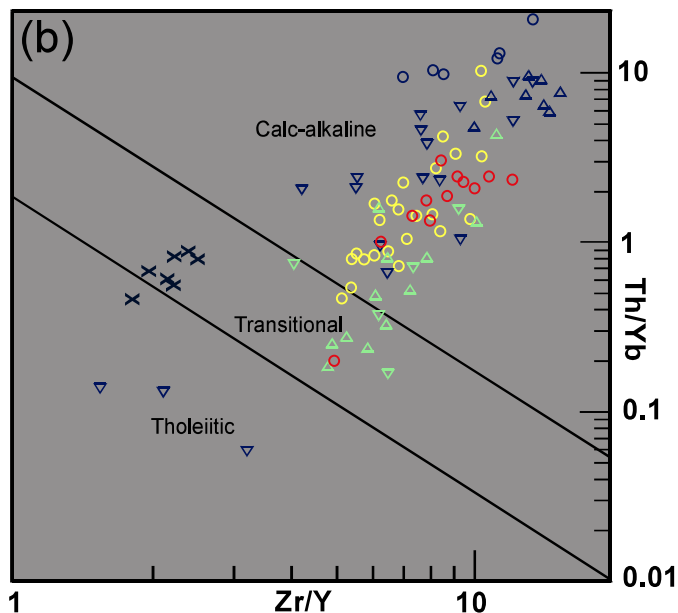
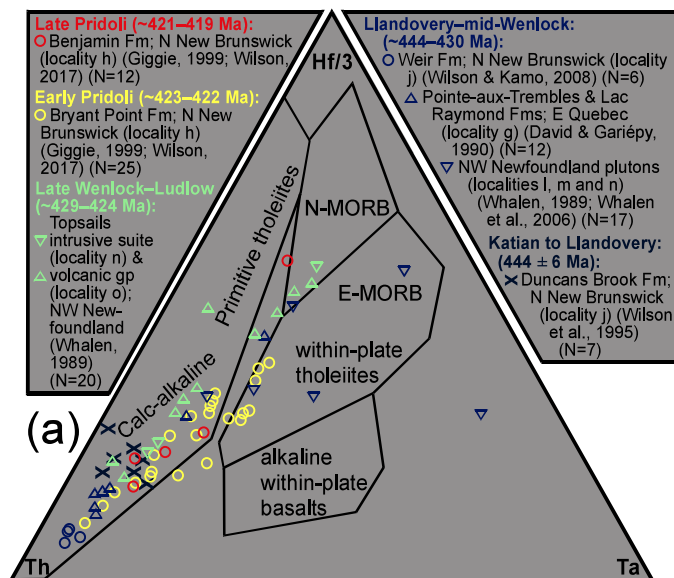


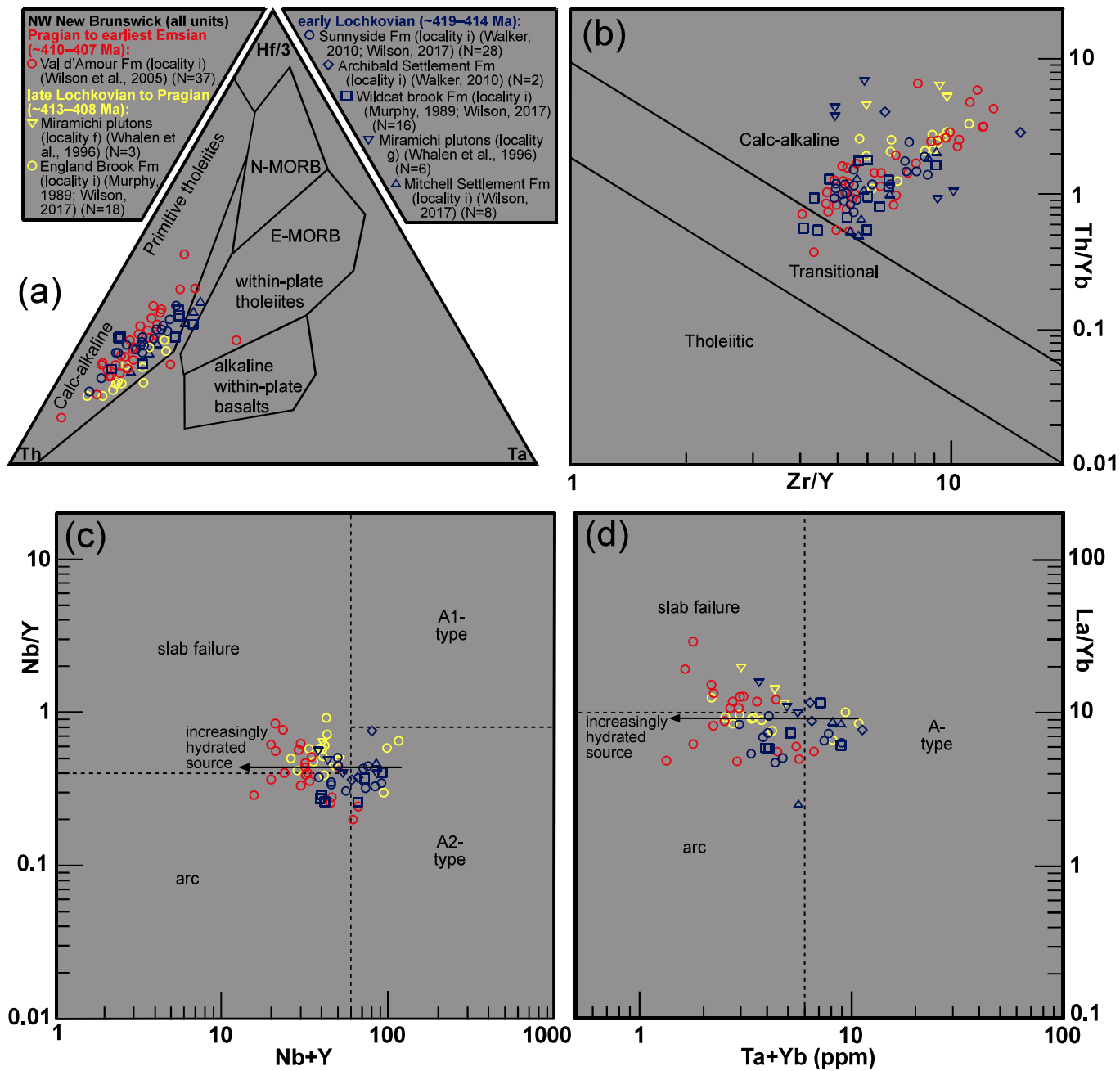


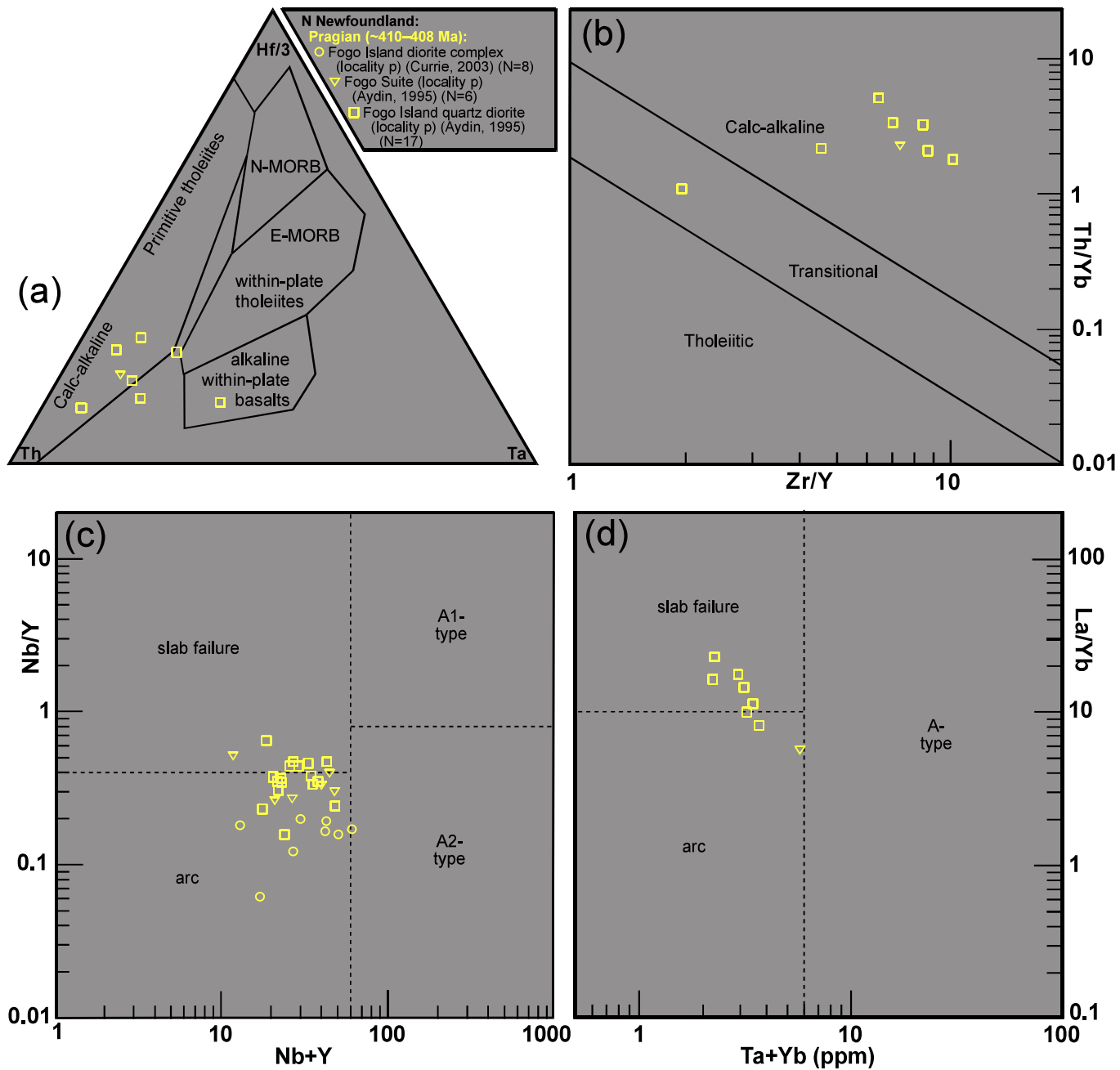


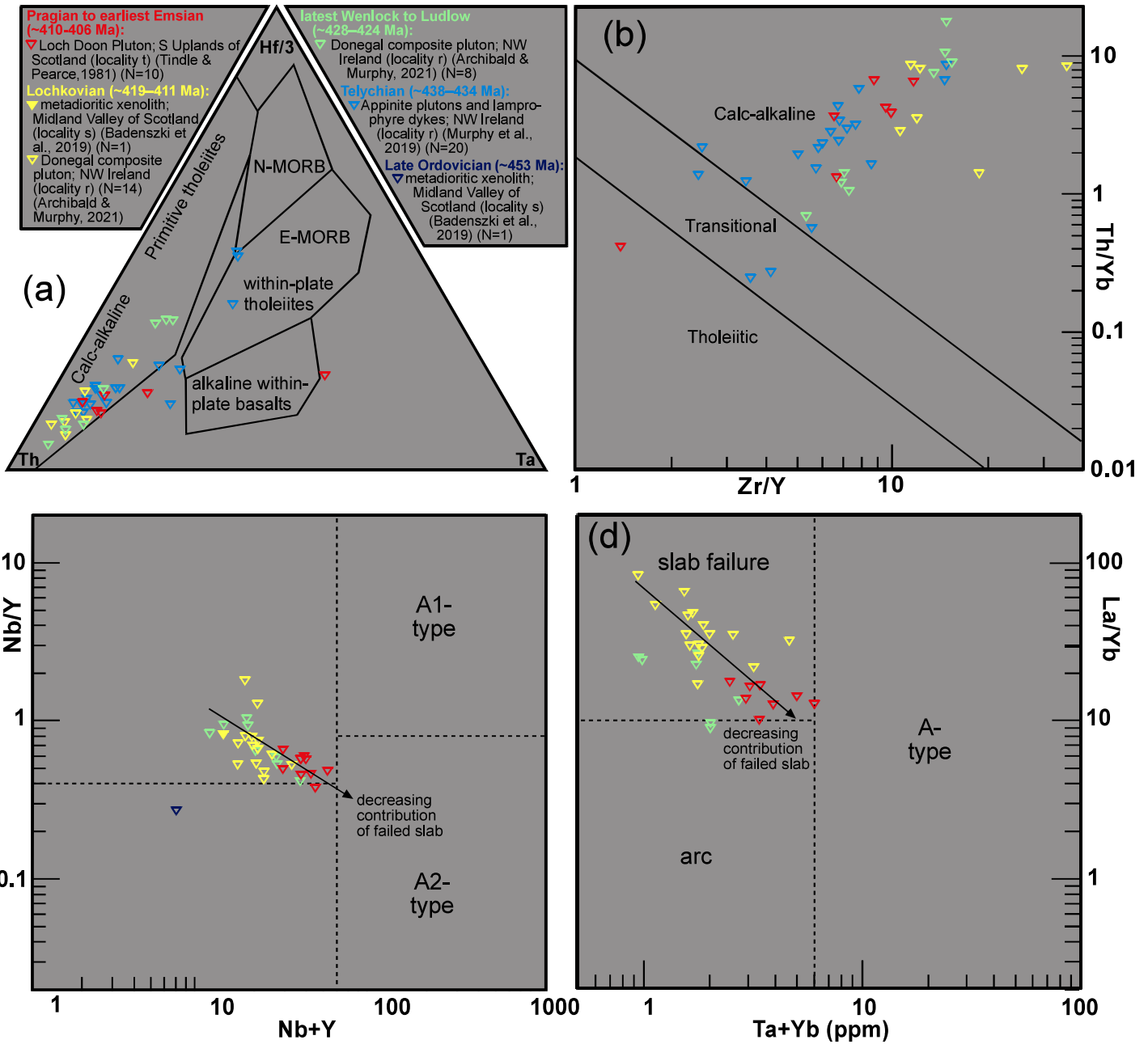


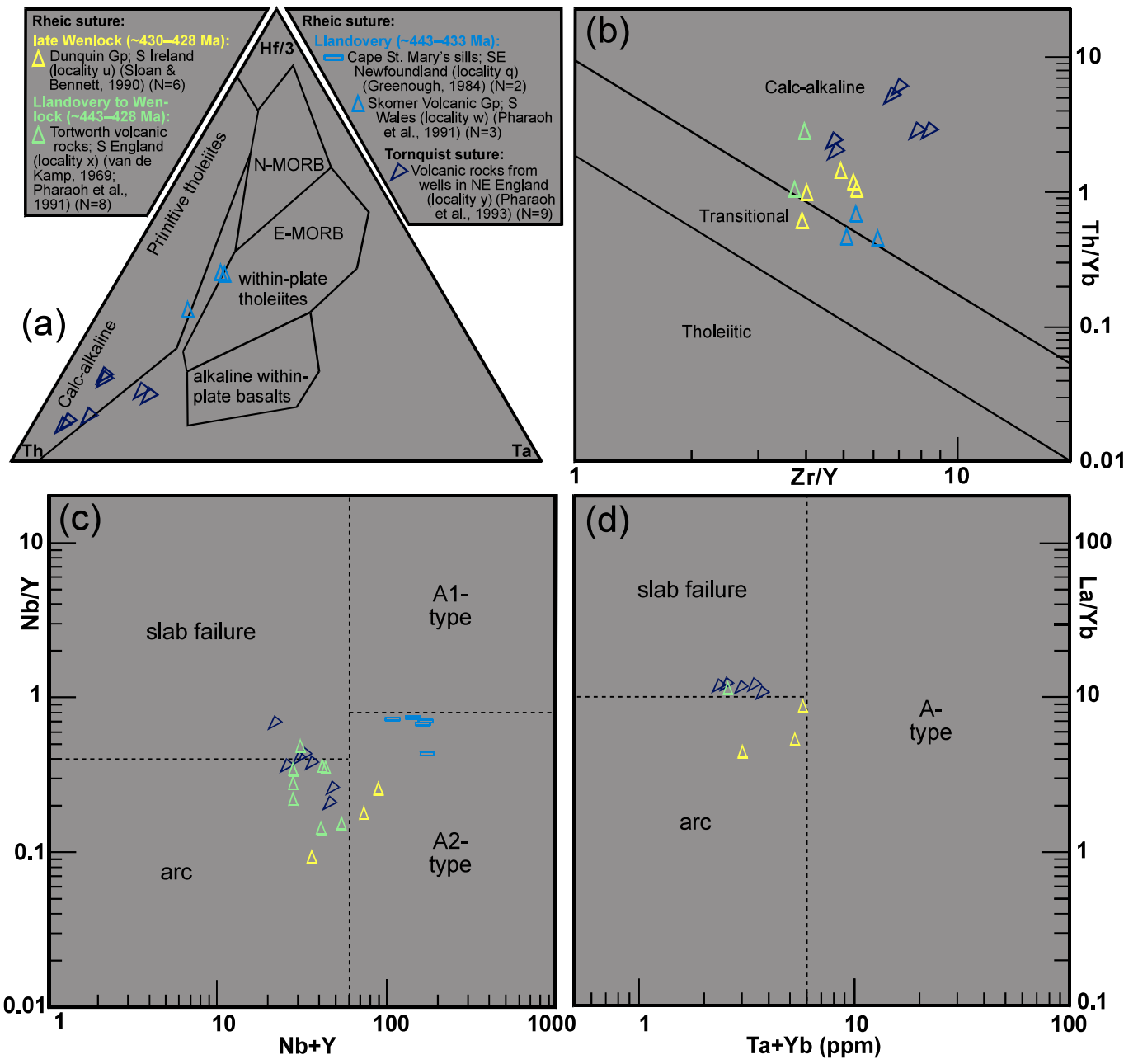


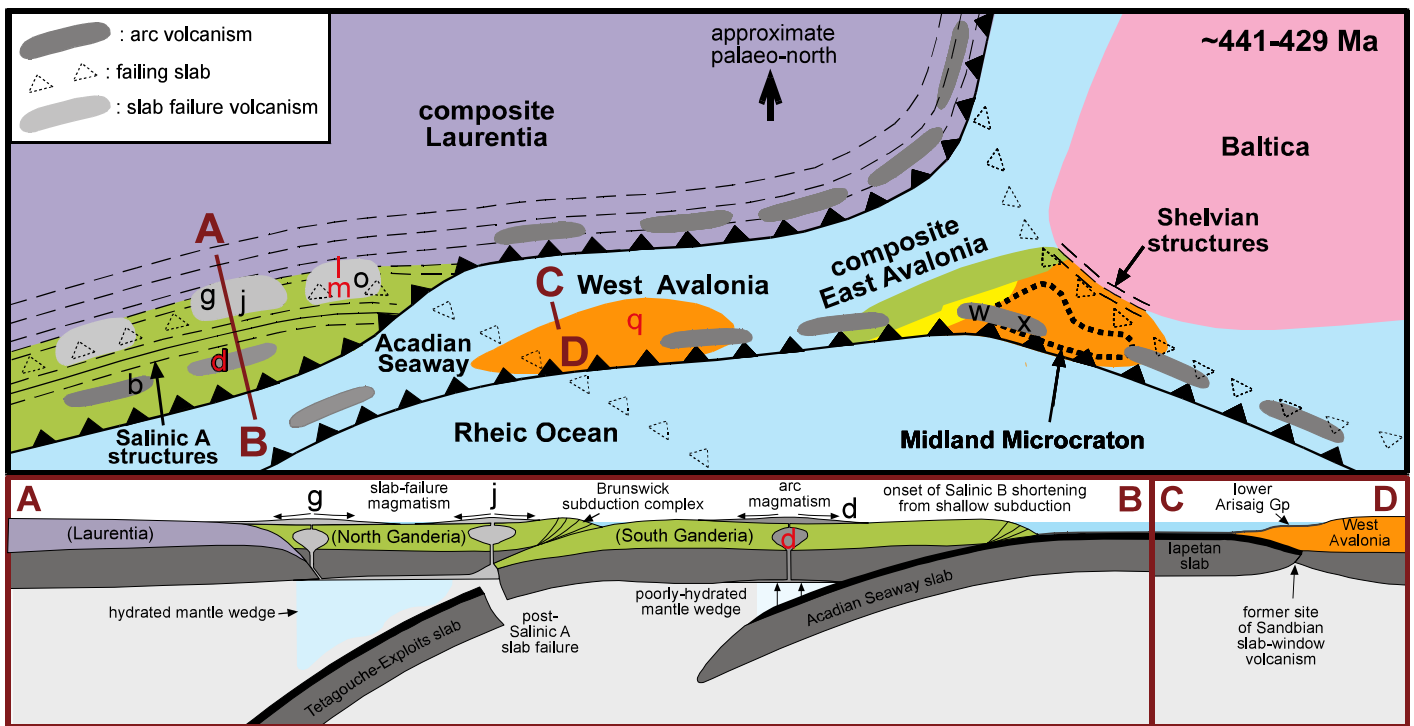


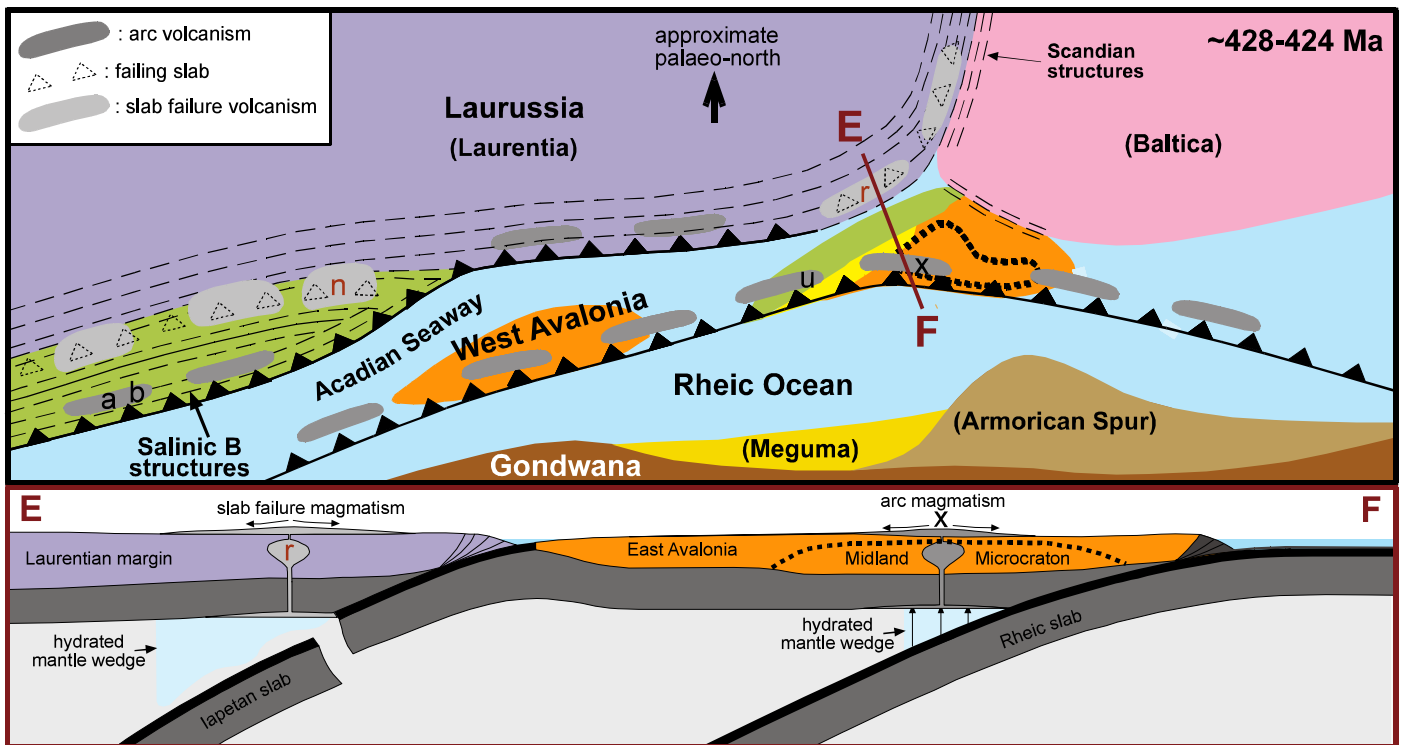


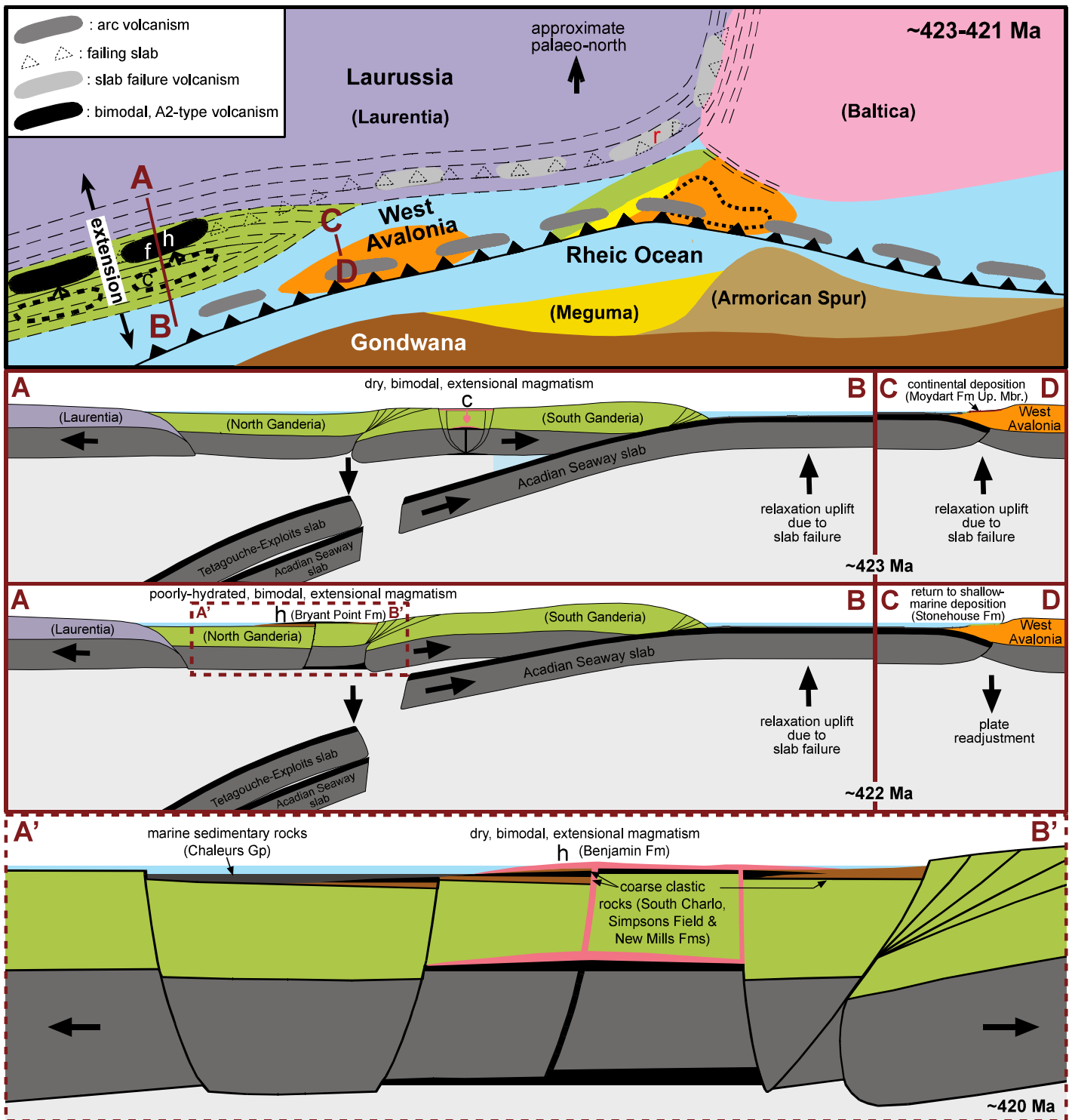


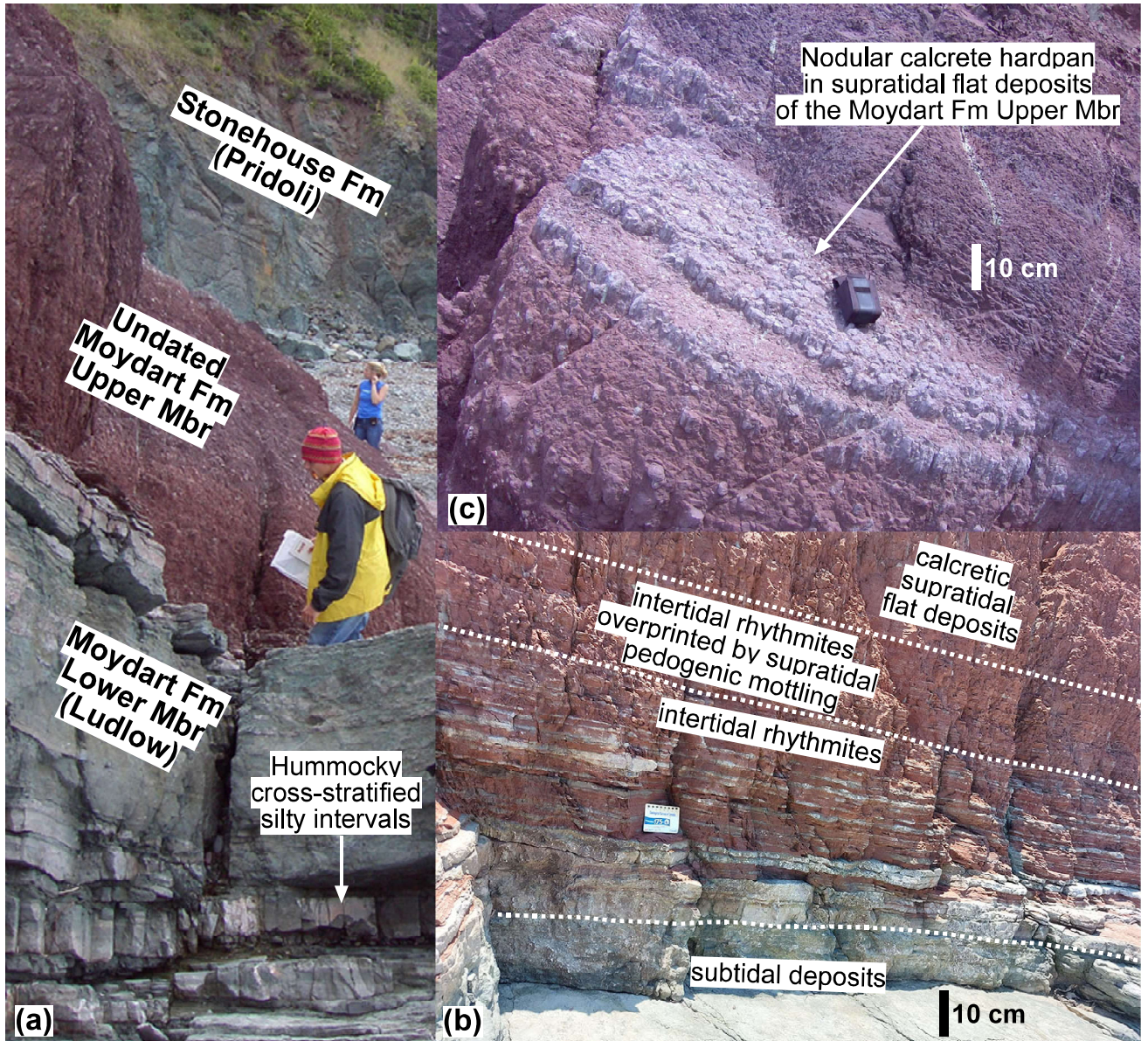


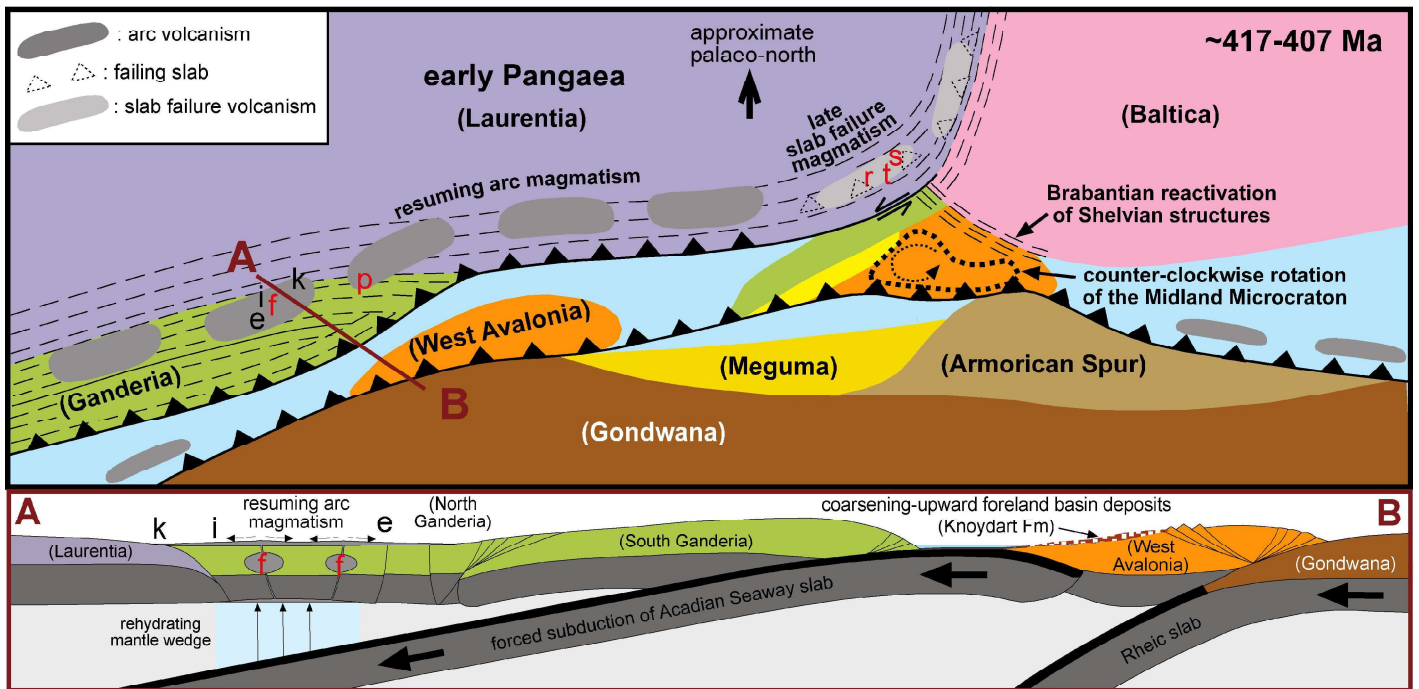












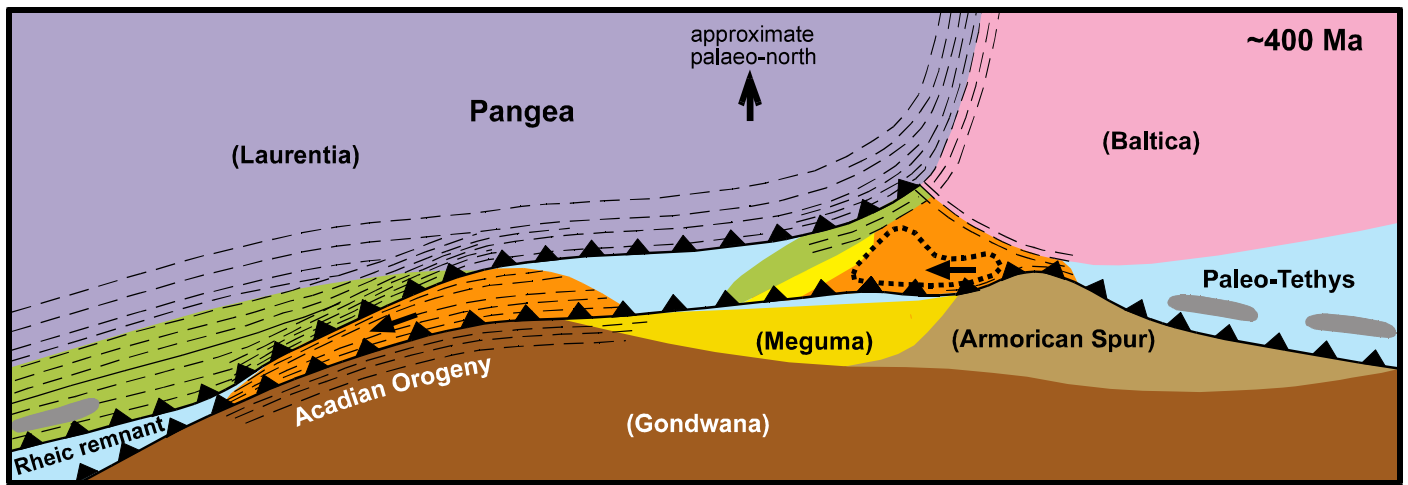


Table 1.

Katian to early Emsian igneous rock units at the localities featuring in Figure 1.

Locality	Region	Unit	Age	Dating method	Age data	Geochemical data		
a	Coastal Maine	Cranberry Island volcanics	424±1 Ma	U-Pb zircon	Seaman et al., 1995	Seaman et al., 1999		
b	Coastal Maine	Eastport Fm	Pridoli?	biostrat. constraints	Gates & Moench, 1981	Llamas & Hepburn, 2013		
		Leighton Fm	Pridoli?	biostrat. constraints	Gates & Moench, 1981	Llamas & Hepburn, 2013		
		Edmunds Fm	Ludlow?	biostrat. constraints	Gates & Moench, 1981	Llamas & Hepburn, 2013		
		Dennys Fm	late Lland. to Wenlock?	biostrat. constraints	Gates & Moench, 1981	Llamas & Hepburn, 2013		
		Passamaquoddy Bay volcanics	423±1 Ma	U-Pb zircon	van Wagoner et al., 2001	van Wagoner et al., 2002		
c	S New Brunswick	Kingston terrane igneous suite	442±6 & 437±10 Ma	U-Pb zircon	Barr et al., 2002	Barr et al., 2002		
			435±1.5 Ma	U-Pb zircon	Doig et al., 1990			
e	W New Brunswick	Tobique Gp	Pridoli to Lochkovian	biostrat. constraints	Dostal et al., 2021	Dostal et al., 2021		
f	N New Brunswick	Miramichi plutons	~418 to ~402 Ma	U-Pb zirc., tit. & mon.	Whalen et al., 1996	Whalen et al., 1996		
g	E Quebec	Lac Raymond Fm	late Llandovery	ostracods	David & Gariépy, 1990	David & Gariépy, 1990		
		Pointe aux Trembles Fm	late Llandovery	ostracods	David & Gariépy, 1990	David & Gariépy, 1990		
h	NW New Brunswick	Benjamin Fm (Dickie Cove Gp)	419.7±0.3 &	U-Pb zircon	Wilson & Kamo, 2012	Giggie, 1989; Wilson, 2017		
			420.8±0.4 Ma	U-Pb zircon	Wilson & Kamo, 2008			
			422.3±0.3 Ma	U-Pb zircon	Wilson & Kamo, 2012	Giggie, 1989; Wilson, 2017		
i	NW New Brunswick	Bryant Point Fm (Dickie Cove Gp)	late Loch. to early Ems.	biostrat. constraints &	Wilson, 2017	Wilson et al., 2005		
		Val d'Amour Fm (Dalhousie Gp)	407.4±0.8 Ma	U-Pb zircon	Wilson et al., 2004			
		England Brook Fm (Dalhousie Gp)	mid-Lochkovian	biostrat. constraints	Wilson, 2017	Murphy, 1989; Wilson, 2017		
		Sunnyside Fm (Dalhousie Gp)	early mid-Lochkovian	biostrat. constraints	Greiner, 1970; Irrinki, 1990	Walker, 2010; Wilson, 2017		
		Archibald Settl. Fm (Dalhousie Gp)	415.6±0.4 Ma	U-Pb zircon	Wilson & Kamo, 2008	Walker, 2010; Wilson, 2017		
j	NW New Brunswick	Wildcat Brook Fm (Dalhousie Gp)	417.5±0.4 Ma	U-Pb zircon	Wilson et al., 2017	Wilson, 2017		
		Mitchell Settl. Fm (Dalhousie Gp)	early Lochkovian	spores & strat. constr.	McGregor, 1992;	Wilson, 2017		
		Weir Fm (Chaleurs Gp)	429.2±0.5 Ma	U-Pb zircon	Wilson et al., 2008	Wilson et al., 2008		
		k	E Quebec	Baldwin & Lyall volcanics	Loch. to early Emsian	biostrat. constraints	Doyon & Dalpé, 1993	Doyon & Dalpé, 1993
				Ristigouche Volcanics	Wenlock to Pridoli	biostrat. constraints	Bourque et al., 2000	Doyon & Dalpé, 1993
l	NW Newfoundland	Burlington pluton	440±2 Ma	U-Pb monazite	Cawood & Dunning, 1993	Whalen et al., 2006		
m	NW Newfoundland	Boogie Lake complex	435±6 Ma	U-Pb zircon	Dunning et al., 1990	Whalen et al., 2006		
		Main Gut complex	431±2 Ma	U-Pb zircon	Dunning et al., 1990	Whalen et al., 2006		
		Rainy Lake complex	435±1 Ma	U-Pb zircon	Whalen et al., 2006	Whalen et al., 2006		
		Silver Pond complex	431.6±4 Ma	U-Pb zircon	Whalen et al., 2006	Whalen et al., 2006		
		Puddle Pond complex	432.4±1 Ma	U-Pb zircon	Lissenberg et al., 2005	Whalen et al., 2006		
		Taylor Brook complex	430.5±2 Ma	U-Pb zircon	Heaman et al., 2002	Whalen et al., 2006		
		Topsails intrusive suite	427±1 Ma	U-Pb zircon	Whalen et al., 2006	Whalen, 1989		
n	NW Newfoundland	Topsails volcanic gp	425 ± 4 Ma	U-Pb zircon	Whalen et al., 2014	van Staal et al., 2014		
			429±4 Ma	U-Pb zircon	Whalen et al., 1987	Whalen, 1989		
o	NW Newfoundland	Springdale volcanic gp	430±5 Ma	U-Pb zircon	Chandler et al., 1987	Whalen et al., 2006		
		Mount Peyton Batholith	424±2 Ma	U-Pb zircon	Dunning, 1992	Strong & Dupuy, 1982		
p	N Newfoundland	Patch Valley rhyolite	423±3.5 Ma	U-Pb zircon	McNicoll et al., 2008			
		Stony Lake Volcanics	423+3-2 Ma	U-Pb zircon	Dunning et al., 1990			
		Port Albert dykes	422 ± 2 Ma	U-Pb zircon	Elliott et al., 1991			
		Lawrenceton Fm	421±4 Ma	U-Pb zircon	van Staal et al., 2014			
		Port Albert Fm	418.5±4 Ma	U-Pb zircon	van Staal et al., 2014			
		Fogo Island quartz diorite	410±2 Ma	U-Pb titanite	Aydin, 1995	Aydin, 1995		
			420±2 Ma	U-Pb zircon	Aydin, 1995			
			408±0.8 Ma	U-Pb zircon	Aydin, 1995			
q	S Newfoundland	Fogo Island diorite complex	441±2 Ma	U-Pb baddeleyite	Greenough et al., 1993	Aydin, 1995; Currie, 2003		
r	NW Ireland	Cape St. Mary's sills	428±4 to ~400 Ma	U-Pb zircon	Archibald et al., 2021	Greenough, 1984		
		Donegal composite pluton	434.2±2.1 to 431±6 Ma	Ar/Ar hornblende	Murphy et al., 2019	Archibald & Murphy, 2019		
s	Midland Valley, Scotland	appinite & lamprophyre suite	453.6±8 & 415±3 Ma	Rb/Sr	Murphy et al., 2019	Murphy et al., 2019		
t	S Uplands, Scotland	xenoliths	408±1.5 Ma;	U-Pb zircon	Badenszki et al., 2019	Badenszki et al., 2019		
		Loch Doon pluton	410±1 & 406±2 Ma	U-Pb zircon	Piper, 2007	Tindle & Pearce, 1981		
u	S Ireland	Dunquin Gp	late Wenlock	biostrat. constraints	Holland, 1988	Sloan & Bennett, 1990		
v	SE Ireland	Leinster Batholith	405±2 Ma	U-Pb zircon	O'Connor et al., 1989	Sweetman, 1987		
w	S Wales	Skomer Volcanic Gp	Llandovery	biostrat. constraints	Ziegler et al., 1969	Thorpe et al., 1989		
x	S England	Tortworth volcanics	Lland. to Wenlock	biostrat. constraints	Reynolds, 1924;	van de Kamp, 1969;		
						Pharaoh et al., 1991		
y	NE England	igneous rocks in wells	449±13–442±3 Ma	U-Pb zircon & badd.	Noble et al., 1993	Pharaoh et al., 1993		
			452+8-5 Ma	U-Pb zircon	Pidgeon & Aftalion, 1978			
z	Brabant Massif, Belgium	NW province suite	Late Ord. to Wenlock	biostrat. constraints	Martin & Richards, 1979	André et al., 1986		

Abbreviations: badd.: baddeleyite; biostrat.: biostratigraphic; constr.: constraints; Ems.: Emsian; Fm: Formation; Gp: Group; Lland.: Llandovery; Loch.: Lochkovian; Mon.: monazite; Ord.: Ordovician; Settl.: Settlement; strat.: stratigraphic; tit.: titanium; zirc.: zircon.

Table 1.

Katian to early Emsian igneous rock units at the localities featuring in Figure 1.

Locality	Region	Unit	Age	Dating method	Age data	Geochemical data
a	Coastal Maine	Cranberry Island volcanics	424±1 Ma	U-Pb zircon	Seaman et al., 1995	Seaman et al., 1999
B	Coastal Maine	Eastport Fm	Pridoli?	biostrat. constraints	Gates & Moench, 1981	Llamas & Hepburn, 2013
		Leighton Fm	Pridoli?	biostrat. constraints	Gates & Moench, 1981	Llamas & Hepburn, 2013
		Edmunds Fm	Ludlow?	biostrat. constraints	Gates & Moench, 1981	Llamas & Hepburn, 2013
		Dennys Fm	late Lland. to Wenlock?	biostrat. constraints	Gates & Moench, 1981	Llamas & Hepburn, 2013
c	S New Brunswick	Passamaquoddy Bay volcanics	423±1 Ma	U-Pb zircon	van Wagoner et al., 2001	van Wagoner et al., 2002
d	S New Brunswick	Kingston terrane igneous suite	442±6 & 437±10 Ma	U-Pb zircon	Barr et al., 2002	Barr et al., 2002
e	W New Brunswick	Tobique Gp	435±1.5 Ma Pridoli to Lochkovian	U-Pb zircon biostrat. constraints	Doig et al., 1990 Dostal et al., 2021	Dostal et al., 2021
f	N New Brunswick	Miramichi plutons	~418 to ~402 Ma	U-Pb zircon tit. & mon.	Whalen et al., 1996	Whalen et al., 1996

Table 1 contd.

g	E Quebec	Lac Raymond Fm	late Llandovery	ostracods	David & Gariépy, 1990	David & Gariépy, 1990
h	NW New Brunswick	Pointe aux Trembles Fm	late Llandovery	ostracods	David & Gariépy, 1990	David & Gariépy, 1990
		Benjamin Fm	419.7±0.3 &	U-Pb zircon	Wilson & Kamo, 2012	Giggie, 1989;
		(Dickie Cove Gp)	420.8±0.4 Ma	U-Pb zircon	Wilson & Kamo, 2008	Wilson, 2017
		Bryant Point Fm	422.3±0.3 Ma	U-Pb zircon	Wilson & Kamo, 2012	Giggie, 1989;
i	NW New Brunswick	(Dickie Cove Gp)				Wilson, 2017
		Val d'Amour Fm	late Lochkovian to	Fossil assemblages,	Wilson et al., 2004, 2005	Wilson et al., 2005;
		(Dalhousie Gp)	early Emsian;	strat. constraints &		Wilson, 2017
			407.4±0.8 Ma	U-Pb zircon	Wilson et al., 2004	
		England Brook Fm	mid-Lochkovian	biostrat. constraints	Wilson, 2017	Murphy, 1989;
		(Dalhousie Gp)				Wilson, 2017
		Sunnyside Fm	early mid-Loch.	biostrat. constraints	Greiner, 1970;	Walker, 2010;
		(Dalhousie Gp)			Irrinki, 1990	Wilson, 2017
		Archibald Settlement Fm	415.6±0.4 Ma	U-Pb zircon	Wilson & Kamo, 2008	Walker, 2010;
		(Dalhousie Gp)				Wilson, 2017
	NW New Brunswick	Wildcat Brook Fm	417.5±0.4 Ma	U-Pb zircon	Wilson et al., 2017	Wilson, 2017
		(Dalhousie Gp)				Wilson, 2017

Table 1 contd.

		Mitchell Settlement Fm (Dalhousie Gp)	early Lochkovian	spores & strat. constraints	McGregor, 1992; Wilson, 2017	Wilson, 2017
j	NW New Brunswick	Weir Fm	429.2±0.5 Ma	U-Pb zircon	Wilson et al., 2008	Wilson et al., 2008
k	E Quebec	Baldwin & Lyall volcanics	Lochkovian to early Emsian?	biostrat. constraints	Doyon & Dalpé, 1993	Doyon & Dalpé, 1993
		Ristigouche	Wenlock to	biostrat. constraints	Bourque et al., 2000	Doyon & Dalpé, 1993
		Volcanics	Pridoli?			
l	NW Newfoundland	Burlington pluton	440±2 Ma	U-Pb monazite	Cawood & Dunning, 1993	Whalen et al., 2006
m	NW Newfoundland	Boogie Lake complex	435±6 Ma	U-Pb zircon	Dunning et al., 1990	Whalen et al., 2006
		Main Gut complex	431±2 Ma	U-Pb zircon	Dunning et al., 1990	Whalen et al., 2006
		Rainy Lake complex	435±1 Ma	U-Pb zircon	Whalen et al., 2006	Whalen et al., 2006
		Silver Pond complex	431.6±4 Ma	U-Pb zircon	Whalen et al., 2006	Whalen et al., 2006
		Puddle Pond complex	432.4±1 Ma	U-Pb zircon	Lissenberg et al., 2005	Whalen et al., 2006
		Taylor Brook complex	430.5±2 Ma	U-Pb zircon	Heaman et al., 2002	Whalen et al., 2006
n	NW Newfoundland	Topsails intrusive suite	427±1 Ma	U-Pb zircon	Whalen et al., 2006	Whalen, 1989
			425 ± 4 Ma	U-Pb zircon	van Staal et al., 2014	

Table 1 contd.

o	NW Newfoundland	Topsails volcanic gp	429±4 Ma	U-Pb zircon	Whalen et al., 1987	Whalen, 1989
		Springdale volcanic gp	430±5 Ma	U-Pb zircon	Chandler et al., 1987	Whalen et al., 2006
p	N Newfoundland	Mount Peyton Batholith	424±2 Ma	U-Pb zircon	Dunning, 1992	Strong & Dupuy, 1982
		Patch Valley rhyolite	423±3.5 Ma	U-Pb zircon	McNicoll et al., 2008	
		Stony Lake Volcanics	423+3-2 Ma	U-Pb zircon	Dunning et al., 1990	
		Port Albert dykes	422 ± 2 Ma	U-Pb zircon	Elliott et al., 1991	
		Lawrenceton Fm	421±4 Ma	U-Pb zircon	van Staal et al., 2014	
		Port Albert Fm	418.5±4 Ma	U-Pb zircon	van Staal et al., 2014	
		Fogo Island Batholith	410±2 &	U-Pb titanite	Aydin, 1995	Aydin, 1995
			420±2 Ma	U-Pb zircon		
		Fogo Island Batholith	408±0.8 Ma	U-Pb zircon	Aydin, 1995	Aydin, 1995;
						Currie, 2003
q	S Newfoundland	Cape St. Mary's sills	441±2 Ma	U-Pb baddeleyite	Greenough et al., 1993	Greenough, 1984
r	NW Ireland	Donegal composite pluton	428±4 to ~400 Ma	U-Pb zircon	Archibald et al., 2021	Archibald & Murphy, 2021
		appinite & lamprophyre	434.2±2.1 to	Ar/Ar hornblende	Murphy et al., 2019	Murphy et al., 2019
		suite	431±6 Ma			

Table 1 contd.

s	Midland Valley of	xenoliths	453.6±8 &	U-Pb zircon	Badenszki et al., 2019	Badenszki et al., 2019
	Scotland		415±3 Ma	U-Pb zircon	Badenszki et al., 2019	Badenszki et al., 2019
t	S Uplands of	Loch Doon pluton	408±1.5 Ma;	Rb/Sr	Piper, 2007	Tindle & Pearce, 1981
	Scotland		410±1 & 406±2 Ma	U-Pb zircon	Stone et al., 2012	
u	S Ireland	Dunquin Gp	late Wenlock	biostrat. constraints	Holland, 1988	Sloan and Bennett, 1990
v	SE Ireland	Leinster Batholith	405±2 Ma	U-Pb zircon	O'Connor et al., 1989	Sweetman, 1987
w	S Wales	Skomer Volcanic Gp	Llandovery	biostrat. constraints	Ziegler et al., 1969	Thorpe et al., 1989
x	S England	Tortworth volcs.	Llandovery to	biostrat. constraints	Reynolds, 1924;	van de Kamp, 1969;
			Wenlock			Pharaoh et al., 1991
y	NE England	igneous rocks in wells	449±13–442±3 Ma	U-Pb zircon & badd.	Noble et al., 1993	Pharaoh et al., 1993
			452+8-5 Ma	U-Pb zircon	Pidgeon & Aftalion, 1978	
z	Brabant Massif,	NW province suite	Late Ordovician to	biostrat. constraints	Martin & Richards, 1979	André et al., 1986
	Belgium		Wenlock			

Abbreviations: badd.: baddeleyite; biostrat.: biostratigraphic; Fm: Formation; Gp: Group; Lland.: Llandovery; mon.: monazite; strat.: stratigraphic; tit.: titanium.